

Spring 3-16-2022

DELINEATING THE EXOCYTIC FUSION MACHINERY REQUIRED FOR MAST CELL EXOCYTOSIS

Pratikshya Adhikari
University of Southern Mississippi

Follow this and additional works at: <https://aquila.usm.edu/dissertations>



Part of the [Cell Biology Commons](#), and the [Molecular Biology Commons](#)

Recommended Citation

Adhikari, Pratikshya, "DELINEATING THE EXOCYTIC FUSION MACHINERY REQUIRED FOR MAST CELL EXOCYTOSIS" (2022). *Dissertations*. 2001.
<https://aquila.usm.edu/dissertations/2001>

This Dissertation is brought to you for free and open access by The Aquila Digital Community. It has been accepted for inclusion in Dissertations by an authorized administrator of The Aquila Digital Community. For more information, please contact aquilastaff@usm.edu.

DELINEATING THE EXOCYTIC FUSION MACHINERY REQUIRED FOR MAST
CELL EXOCYTOSIS

by

Pratikshya Adhikari

A Dissertation
Submitted to the Graduate School,
the College of Arts and Sciences
and the School of Biological, Environmental, and Earth Sciences
at The University of Southern Mississippi
in Partial Fulfillment of the Requirements
for the Degree of Doctor of Philosophy

Approved by:

Dr. Hao Xu, Committee Chair

Dr. Alex Flynt

Dr. Shahid Karim

Dr. Vijay Rangachari

Dr. Yanlin Guo

May 2022

COPYRIGHT BY

Pratikshya Adhikari

2022

Published by the Graduate School



ABSTRACT

Mast cells undergo exocytosis to release a wide array of inflammatory mediators by utilizing membrane fusion proteins-SNAREs (soluble-N-ethyl-maleimide sensitive factor attachment protein receptor) along with essential regulatory Munc18 and Munc13 proteins. Accumulating evidence in mast cell biology suggests the existence of distinct pools of mast cell mediators. However, the precise mechanism underlying the release of each mast cell mediator is not clear. To determine whether different exocytic machineries are required for differential mediator release, I used reconstitution to investigate the differential role of Munc18s in fusion machinery regulation. Munc18a and Munc18c stimulated VAMP2 and VAMP3-mediated lipid mixing, whereas Munc18b only stimulated VAMP8/Stx3/SNAP23-mediated fusion. I then investigated the role of Munc18 post-translational modification in mast cell exocytosis. In reconstitution assays, phosphomimetic mutants- Munc18a^{S306E/S313E} and Munc18a^{T574E} did not alter the activity or specificity of wild-type Munc18a. Munc18b^{T572D}, on the other hand, abolished Munc18b's ability to stimulate VAMP8-dependent degranulation. I further showed that Munc18a undergo PKC-dependent phosphorylation at Ser313 in activated Rat Basophilic Leukemia (RBL-2H3) mast cells (Adhikari and Xu, 2018). These findings suggest site-specific phosphorylation regulates the interaction between Munc18 proteins and their cognate VAMPs. Furthermore, I investigated the differential requirement of vesicular SNAREs in the release of a selection of proinflammatory mediators. Using RNAi, I showed that the knockdown of VAMP8 inhibited IgE/antigen-induced release of β -hexosaminidase, histamine, and serotonin but not TNF. Knocking out VAMP3, which mediates TNF release from human synovial cells and phagocytosing macrophages, did

not display any defect in the TNF exocytosis in RBL-2H3 mast cells; however, the release of β -hexosaminidase was enhanced (manuscript in preparation). Finally, I used the knockout approach to address the roles of Munc13 proteins in mast cell exocytosis. The regulated release of β -hexosaminidase, histamine, and serotonin is virtually eliminated in Munc13-4 knockout RBL-2H3 cells, but TNF release is only partially inhibited (Ayo, Adhikari, et al, 2020). Knocking out Munc13-4 homolog BAIAP3 seems to affect TNF release, although not in a statistically significant fashion. My investigation has set the stage for further dissection of the different molecular mechanisms underlying the exocytosis of distinct mast cell mediators.

ACKNOWLEDGMENTS

I would like to extend my heartfelt gratitude to my advisor Dr. Hao Xu for this incredible opportunity to conduct my research in his lab. I am extremely grateful for his excellent advisement, guidance, patience, generous support, encouragement, constructive criticism, and valuable time throughout my studies. I am fortunate to be able to grow, learn, think critically, ask questions, and tackle research problems under his supervision.

I am grateful to my committee members Dr. Alex Flynt, Dr. Shahid Karim, Dr. Vijay Rangachari, and Dr. Yanlin Guo, for their valuable time, scientific insights, and assistance throughout this study.

I would like to thank my lab mate Tolulope Ayo for being such a wonderful person to work with and providing insights into my work every time I reach out to her. I would like to thank the current and past Xu lab members, including undergrads, and MS-INBRE summer interns, who have directly or indirectly helped me in my study. It was a wonderful opportunity to teach them, and equally, I learned a lot.

I am thankful to our collaborator Dr. Shuzo Sugita (University of Toronto), for providing the cell lines and the plasmids. I would also like to thank the Mississippi IDEa Network of Biomedical Research Excellence (MS-INBRE) for providing excellent research facilities. I am grateful to Dr. Jonathan Lindner for his valuable suggestions and assistance when needed. I am thankful to all of my friends at and outside of USM who have been a constant source of encouragement.

DEDICATION

I dedicate this dissertation to my parents, Ramesh Kumar Adhikari and Sushila Adhikari, who have always believed in and supported me in all my endeavors. They have taught me to work hard, and their blessings have enabled me to achieve my goals. This work is dedicated to two gentlemen in my life: my husband, Surendra Raj Sharma, and my son Samipya Sharma. I am grateful for Surendra's unending love and support; from being the biggest critic to the most ardent admirer, I thank him for everything. My son Samipya has been the greatest blessing in my life and my greatest joy and motivation. He has sacrificed a lot of mama times, and I am eternally grateful to him. This dissertation would not have been possible without the love and support of these four pillars of my life.

TABLE OF CONTENTS

ABSTRACT	ii
ACKNOWLEDGMENTS	iv
DEDICATION	v
LIST OF TABLES	xi
LIST OF ABBREVIATIONS	xiv
CHAPTER I – INTRODUCTION	1
1.1 History and Origin of Mast cells.....	1
1.2 Subtypes of Mast cells	2
1.3 Mast cells in immunity and health	3
1.4 Mast cells in allergic reactions.....	5
1.5 Mast cell mediators	7
1.5.1 β -hexosaminidase.....	9
1.5.2 Histamine	9
1.5.3 Serotonin	10
1.5.4 TNF	10
1.6 Mast cell receptors	11
1.6.1 Toll-like receptors	13
1.6.2 IgE (Fc ϵ RI) receptor	14
1.7 Eukaryotic membrane fusion	16

1.7.1 The SNARE core complex.....	18
1.7.2 The SNARE complex assembly and disassembly	20
1.8 Regulation of SNARE-mediated membrane fusion.....	20
1.8.1 SM proteins	21
1.8.2 Munc13 proteins	22
1.8.3 Rabs and tethering complexes	23
1.8.4 Synaptotagmins and Complexins.....	24
1.9 Mast cell exocytosis.....	25
1.9.1 SNAREs mediated mast cell exocytosis	27
1.9.2 Heterogeneity in exocytic pathways in mast cells	27
1.9.3 Regulation of mast cell exocytosis by Munc18 proteins	30
1.9.4 Regulation of mast cell exocytosis by Munc13 proteins	32
1.10 Regulation of exocytosis by post-translational modification.....	32
1.11 Experimental models to study mast cell exocytosis	35
1.12 Rationale and Hypothesis	38
CHAPTER II – MATERIALS AND METHODS.....	40
2.1 General materials	40
2.1.1 Antibodies	40
2.1.2 Plasmids	40
2.2 Protein expression and purification	41

2.3 Preparation of Proteoliposome.....	44
2.4 Lipid-mixing assay.....	45
2.5 Proteoliposome clustering assay	45
2.6 Cell culture.....	45
2.7 RBL-2H3 mast cell activation	46
2.8 Secretion assay.....	46
2.8.1 β -hexosaminidase release assay	47
2.8.2 TNF assay	47
2.8.3 Histamine assay	47
2.8.4 Serotonin assay	48
2.9 Phosphoprotein isolation and detection	48
2.10 siRNA knockdown.....	49
2.10.1 siRNA transfections.....	49
2.10.2 Reverse transcription and Quantitative Real-time PCR.....	50
2.11 Cell lysate harvest and Immunoblotting	50
2.12 Densitometry and band quantification	51
2.13 Generation of CRISPR/Cas9 mediated VAMP3 KO RBL-2H3 cells	51
2.13.1 Digestion of vector.....	51
2.13.2 gRNA selection.....	52
2.13.3 Ligation of gRNA into the CRISPR vector	53

2.13.4 Homologous Recombination (HR) vector design.....	53
2.13.5 Transfection of CRISPR plasmids and screening of clones	54
2.14 Generation of stable VAMP3 rescue cells	55
2.15 Generation of CRISPR based Base-edited BAIAP3 KO RBL-2H3 cells.....	56
2.16 Isolation of primary mast cells.....	58
2.16.1 Secretion of primary mast cells.....	59
2.17 Data analysis	59
CHAPTER III – MUNC18 DEPENDENT MAST CELL EXOCYTOSIS.....	62
3.1 Characterizing wild-type and phosphomimetic mutant Munc18s in reconstituted degranulation assays	62
3.2 PKC-dependent phosphorylation of Munc18a at Ser313 in activated RBL-2H3 cells	70
3.3 Munc18a clusters SNARE-bearing liposomes prior to trans-SNARE zippering ...	73
CHAPTER IV – DELINEATING THE EXOCYTIC PATHWAYS OF MAST CELL MEDIATORS	78
4.1 Differential release of RBL-2H3 mast cell mediators via VAMP homologs	78
4.2 Deciphering the role of VAMP3 in RBL-2H3 mast cell exocytosis	83
CHAPTER V – CHARACTERIZING BAIAP3 IN MAST CELL EXOCYTOSIS	93
CHAPTER VI – DISCUSSION.....	103
6.1 Munc18s in mast cell exocytosis	103

6.2 PKC dependent Munc18a phosphorylation	107
6.3 Munc18a in clustering.....	109
6.4 Differential release of mast cell mediators via VAMPs	111
6.5 BAIAP3 in mast cell exocytosis	118
6.6 CRISPR based modifications of RBL-2H3 cells	119
6.7 Primary mast cells secretion	123
CHAPTER VII – CONCLUSION	127
REFERENCES	129

LIST OF TABLES

Table 1.1 Activities of mast cell mediators	7
Table 1.2 Molecules involved in mast cell exocytosis	25
Table 2.1 List of primers used	60

LIST OF ILLUSTRATIONS

Figure 1.1 Developmental pathways of mast cells in mice.	2
Figure 1.2 Schematic representation of mast cell receptors.	13
Figure 1.3 Simplified diagram of FcεRI-IgE signaling pathway in activated mast cells.	15
Figure 1.4 Simplified model of SNARE-mediated membrane fusion and schematic representation of the trans-SNARE complex.....	19
Figure 1.5 Known or predicted phosphorylation sites in Munc18s.....	34
Figure 3.1 Munc18b based lipid mixing.	64
Figure 3.2 Munc18c based lipid mixing.	66
Figure 3.3 Munc18a based lipid mixing.	69
Figure 3.4 PKC inhibitor prevents mast cell degranulation and Munc18a phosphorylation at Ser313.	72
Figure 3.5 Munc18a selectively promotes the clustering of SNARE-bearing proteoliposomes.	77
Figure 4.1 Sequence alignment of rat VAMPs.	78
Figure 4.2 Characterization of VAMPs in RBL-2H3 cell lysates using VAMP-specific antibodies.	80
Figure 4.3 Assessing the involvement of VAMPs in the differential release of mediators.	82
Figure 4.4 HDR-based CRISPR/Cas9 mediated VAMP3 genome editing.	84
Figure 4.5 Fluorescence microscopy of transfected cells.	85
Figure 4.6 PCR-based screening of CRISPR/Cas9 edited clones.....	86
Figure 4.7 Immunoblotting of WT and VAMP3 KO RBL-2H3 clones.	87

Figure 4.8 Sequence analysis of edited clone.	88
Figure 4.9 Analyzing VAMP3 KO clone in secretion assays.....	89
Figure 4.10 Expression of R-SNAREs in VAMP3 KO RBL-2H3 cells.	91
Figure 4.11 Lentiviral mediated rescue of VAMP3 KO.....	92
Figure 5.1 Phylogeny of Munc13 proteins and expression of BAIAP3 in RBL-2H3 cells.	94
Figure 5.2 Gene structure and target sequence location of BAIAP3.....	95
Figure 5.3 Schematic representation of genotype determination of base edited clones by RFLP.....	96
Figure 5.4 Target amplification and RFLP analysis of base edited clones.....	99
Figure 5.5 Sequence analysis of base edited clones.	100
Figure 5.6 Analyzing BAIAP3 base edited clone in secretion assays.....	101
Figure 5.7 Expression of Munc13-1 in BAIAP3 base edited clone.....	102
Figure 6.1 Model for Munc18a action in membrane fusion.	110
Figure 6.2 Successful isolation and cultivation of primary mast cells.	124
Figure 6.3 Secretion from primary mast cells.....	126

LIST OF ABBREVIATIONS

<i>°C</i>	Degree Celsius
<i>ADAM17</i>	A disintegrin and metalloprotease17
<i>ATCC</i>	The American Type Culture Collection
<i>ATP</i>	Adenosine Tri Phosphate
<i>BAIAP3</i>	Brain-Specific Angiogenesis Inhibitor 1-Associated Protein 3
<i>BE</i>	Base Edited
<i>BMMCs</i>	Bone Marrow-Derived Mast Cells
<i>BSA</i>	Bovine Serum Albumin
<i>Ca⁺⁺</i>	Calcium
<i>Cas9</i>	CRISPR Associated Protein 9
<i>CDK</i>	Cyclin Dependent Kinase
<i>cDNA</i>	Complementary Deoxyribonucleic Acid
<i>CHAPS</i>	3-[(3-Cholamidopropyl) dimethylammonium]-1- Propanesulfonate
<i>CO₂</i>	Carbon dioxide
<i>CRISPR</i>	Clustered Regularly Interspaced Short Palindromic Repeats
<i>CTMCs</i>	Connective Tissue-Type Mast Cells
<i>DAG</i>	Diacylglycerol
<i>DMEM</i>	Dulbecco's Modified Eagle Medium
<i>DMSO</i>	Dimethyl Sulfoxide

<i>DNA</i>	Deoxyribonucleic Acid
<i>DSB</i>	Double Strand Break
<i>DTT</i>	Dithiothreitol
<i>EDTA</i>	Ethylenediamine Tetraacetic Acid
<i>ELISA</i>	Enzyme-Linked Immunosorbent Assay
<i>ER</i>	Endoplasmic Reticulum
<i>FBS</i>	Fetal Bovine Serum
<i>FcεRI</i>	Fc Epsilon RI
<i>FDA</i>	Food and Drug Administration
<i>FT</i>	Flow Through
<i>FRET</i>	Fluorescence Resonance Energy Transfer
<i>g</i>	Gram
<i>GFP</i>	Green Fluorescent Protein
<i>GLUT4</i>	Glucose Transporter Type 4
<i>gRNA</i>	Guide RNA
<i>h</i>	hour
<i>HA</i>	Homologous Arms
<i>HCl</i>	Hydrochloric Acid
<i>HDR</i>	Homology-Directed Repair
<i>HEK</i>	Human Embryonic Kidney
<i>HEPES</i>	N-2-Hydroxyethylpiperazine-N'-2-Ethanesulfonic Acid
<i>HOPS</i>	Homotypic Fusion and Vacuolar Protein Sorting

<i>HR</i>	Histamine Receptor
<i>IDT</i>	Integrated DNA Technology
<i>Ig</i>	Immunoglobulin
<i>IL</i>	Interleukin
<i>InsP3</i>	Inositol Triphosphate
<i>ITAM</i>	Immunoreceptor Tyrosine-Based Activation Motif
<i>KCl</i>	Potassium Chloride
<i>KD</i>	Knock Down
<i>KO</i>	Knock Out
<i>KOH</i>	Potassium Hydroxide
<i>l</i>	Liter
<i>LAMP</i>	Lysosomal-Associated Membrane protein
<i>LB</i>	Luria-Bertani Medium
<i>LPS</i>	Lipopolysaccharide
<i>MAPK</i>	Mitogen-Activated Protein Kinase
<i>MBP</i>	Maltose Binding protein
<i>MCS</i>	Multiple Cloning Site
<i>mg</i>	Milligram
<i>MHC</i>	Major Histocompatibility Complex
<i>ml</i>	Milliliter
<i>M</i>	Molar
<i>mM</i>	Millimolar
<i>mRNA</i>	Messenger Ribonucleic Acid

<i>MTC</i>	Multisubunit Tethering Complexes
<i>MTMCs</i>	Mucosal-Type Mast Cells
<i>Munc</i>	Mammalian Uncoordinated
<i>MVB</i>	Multi Vesicular Bodies
<i>MWCO</i>	Molecular Weight Cut Off
<i>MYD88</i>	Myeloid Differentiation Primary Response 88
<i>N₂</i>	Nitrogen
<i>NaCl</i>	Sodium Chloride
<i>NaOH</i>	Sodium Hydroxide
<i>NEB</i>	New England Biolab
<i>NF-κB</i>	Nuclear Factor Kappa Light Chain Enhancer of Activated B cells
<i>ng</i>	Nanogram
<i>NGF</i>	Nerve Growth Factor
<i>NHEJ</i>	Non-Homologous End Joining
<i>Ni-NTA</i>	Nickel-Nitrilotriacetic Acid
<i>NK</i>	Natural Killer
<i>NLR</i>	Nucleotide-binding oligomerization domain (NOD)-Like Receptor
<i>NSF</i>	N-ethylmaleimide-Sensitive Factor
<i>PAM</i>	Protospacer Adjacent Motif
<i>PAMPs</i>	Pathogen-Associates Molecular Patterns
<i>PBS</i>	Phosphate Buffered Saline

<i>PCMCs</i>	Peritoneal Cell-Derived Culture Mast Cells
<i>PCR</i>	Polymerase Chain Reaction
<i>PF</i>	Protein-Free
<i>PGN</i>	Peptidoglycan
<i>PIC</i>	Protease Inhibitor Cocktail
<i>PKC</i>	Protein Kinase C
<i>PLC</i>	Phospholipase C
<i>PMA</i>	Phorbol Myristate Acetate
<i>PMSF</i>	Phenylmethylsulfonyl Fluoride
<i>Poly:IC</i>	Polyinosinic:Polycytidic Acid
<i>PRR</i>	Pattern Recognition Receptors
<i>qPCR</i>	Quantitative Real Time PCR
<i>RB</i>	Reconstitution Buffer
<i>RBL</i>	Rat Basophilic Leukemia
<i>RFP</i>	Red Fluorescent Protein
<i>RFLP</i>	Restriction Fragment Length Polymorphism
<i>RIPA</i>	Radio Immunoprecipitation Assay
<i>RNA</i>	Ribonucleic Acid
<i>RNAi</i>	RNA interference
<i>rpm</i>	Rotation Per Minute
<i>RPMI</i>	Roswell Park Memorial Institute Medium
<i>RT</i>	Room Temperature
<i>SCF</i>	Stem Cell Factor

<i>SDS-PAGE</i>	Sodium Dodecyl-Sulfate Polyacrylamide Gel Electrophoresis
<i>SD</i>	Standard Deviation
<i>siRNA</i>	Short Interfering RNA
<i>SNAP</i>	Synaptosome-Associated Protein
<i>SNAREs</i>	Soluble-N-ethyl-Maleimide Sensitive Factor Attachment Protein Receptor
<i>TACE</i>	Tumor Necrosis Factor-Alpha Converting Enzyme
<i>TCS</i>	TEV Cleavable Site
<i>TEV</i>	Tobacco Etch Virus
<i>TGF</i>	Transforming Growth factor
<i>TLR</i>	Toll-Like Receptors
<i>TNF</i>	Tumor Necrosis Factor
<i>TNFR</i>	Tumor Necrosis Factor Receptor
<i>TNP</i>	Trinitrophenyl
μg	Microgram
μl	Microliter
μm	Micrometer
<i>VAMP</i>	Vesicle Associated Membrane Protein
<i>VEGF</i>	Vascular Endothelial Growth Factor
<i>WT</i>	Wild Type

CHAPTER I – INTRODUCTION

Mast cells are conserved immune cells present in all vertebrates. Mast cells- like cells have been identified in ancestors of vertebrates (like tunicates), indicating that mast cells are evolutionarily old (Cavalcante et al., 2002). Moreover, humans with an absolute lack of mast cells have never been identified, suggesting mast cells are crucial to organismal functioning (Galli et al., 2020). As sentinel cells, mast cells act as the first line of defense for host protection. However, their misregulation is eminently linked to immunoglobulin E (IgE) mediated allergies and other inflammatory diseases. The sections below briefly describe the origin of mast cells, various functions (in health and disease), and molecular mechanisms governing mast cell function.

1.1 History and Origin of Mast cells

German scientist Paul Ehrlich first described mast cells in his doctoral thesis in the late nineteenth century as “mastung” (well-fed in German) because their cytoplasm is filled with granular contents (which he thought provided nourishment) that is stained strongly with histological dyes. Ehrlich identified mast cells as granular cells of the connective tissue and proposed those cells differentiate from fibroblasts (Crivellato et al., 2003). However, we now know that mast cells are unique immune cells of multipotent hematopoietic lineage and originate from bone marrow. Unlike other hematopoietic pedigrees, which circulate as mature cells, mast cells are released into the blood as immature progenitors (Fig.1.1). They then differentiate into matured cells in diverse tissues in the presence of growth factors like stem cell factor (SCF) and cytokines like Interleukin-3 (IL-3) (Gurish & Austen, 2012). Receptor tyrosine kinase c-kit, whose ligand is SCF, is vital to mast cell development, survival and maturation as c-kit

mutation-based mouse models exhibited profound mast cell deficiency (Reber et al., 2012).

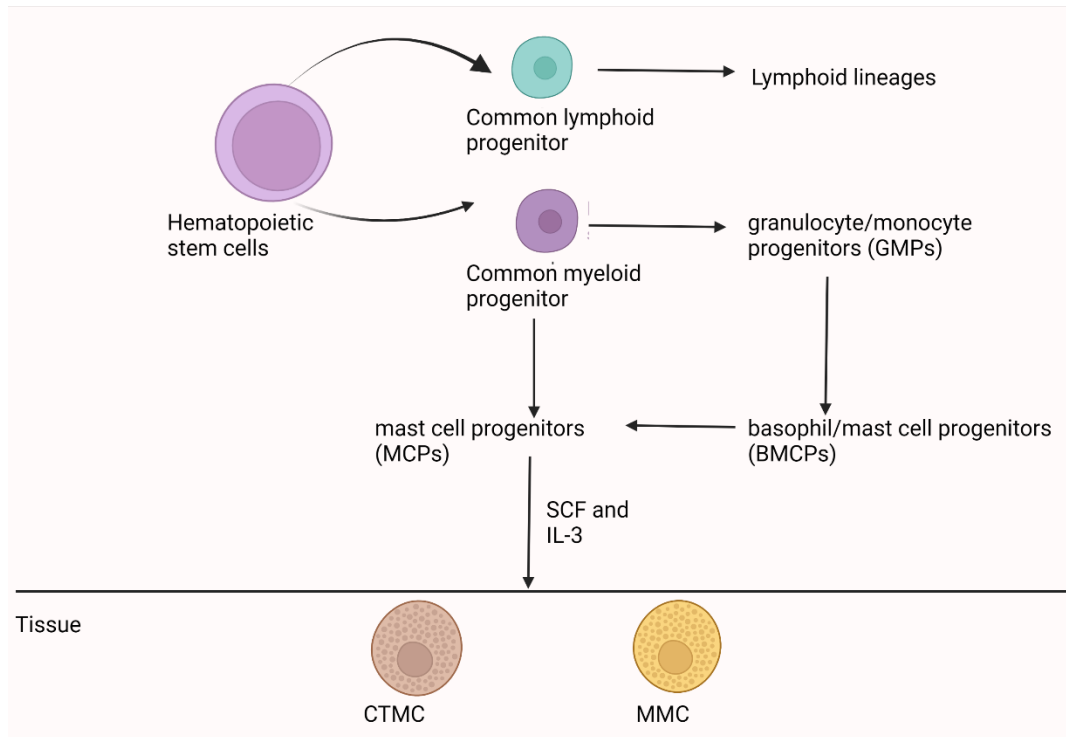


Figure 1.1 *Developmental pathways of mast cells in mice.*

Mast cells originate from the common myeloid progenitors (CMPs) derived from hematopoietic stem cells (HSC). Mast cell progenitors (MCPs) differentiate from CMPs or intermediate basophil/mast cell progenitors (BMCPs) derived from granulocyte/monocyte progenitors (GMPs). Immature mast cells (MCPs) enter tissues and mature in response to signals in the tissues they localize, i.e., connective tissue mast cells (CTMCs) or mucosal mast cells (MMCs). Adapted from (Voehringer, 2013). Created with BioRender.com

1.2 Subtypes of Mast cells

Based on their tissue localization and the proteases they express; the murine mast cells can be differentiated into two subsets: mucosal-type mast cells (MTMCs) and connective tissue-type mast cells (CTMCs). MTMCs contain chymase protease 1 and 2 and are found in the intestine and epithelial cells of lung mucosal tissues, whereas CTMCs express chymase protease 4 and 5, tryptase protease 6, and carboxypeptidase and are in the skin, peritoneal cavity, and submucosa of the intestine vascularized tissues

(Gurish & Austen, 2012). Human mast cells, on the other hand, are subtyped based on their serine protease contents as i) tryptase only containing mast cells (MC_T), ii) chymase only mast cells (MC_C), and iii) both tryptase and chymase positive mast cells (MC_{TC}) (Moon et al., 2010). MC_T resembles murine MTMCs distributed in the nasal and small intestinal mucosa, while MC_{TC} share characteristics with CTMCs and are abundant in human skin and small intestinal submucosa (Jiménez et al., 2021). However, mast cells are much more diverse and heterogenous than what was suggested by the number of subtypes. The different anatomical locations and different organs, such as skin, intestine, lungs, pancreas, etc., have specialized factors that shape the tissue-specific functions of mast cells (Frossi et al., 2018). Thus, mast cells are versatile cells that differentiate into many phenotypes. This heterogeneity enables them to respond to various stimuli at different locations to generate a distinct secretory response to carry out multiple functions.

1.3 Mast cells in immunity and health

Strategically placed at the host-environment interface, such as skin and mucosa, mast cells act as the first line of defense against invading pathogens. Pathogens such as bacteria, pathogen products, viruses, and parasites have unique pathogen-associated molecular patterns (PAMPs) recognized via specific pattern recognition receptors (PRRs) on mast cells. Toll-like receptors (TLR) are members of PRRs that recognize different PAMPs. Their differential activation leads to the synthesis and release of various secretory molecules that aid in pathogen clearance (Sandig & Bulfone-Paus, 2012). Along with other innate immune cells, including macrophages and dendritic cells, mast cells act as starters of the host innate response (John & Abraham, 2013).

Mast cells protect against invading pathogens via several mechanisms. The direct defense in bacterial, viral, and parasitic infections occurs by directly killing pathogens via phagocytosis, producing reactive oxygen species, and releasing antimicrobial agents (e.g., cathelicidin and β -defensins) (Urb & Sheppard, 2012). The indirect antimicrobial response is initiated by releasing chemotactic factors that enhance the recruitment of multiple innate effector inflammatory cells such as neutrophils, eosinophils, Natural killer (NK) cells, and dendritic cells and effector T-cells to target the pathogens (John & Abraham, 2013). The release of vasoactive mediators like histamine as well as proteases and leukotrienes cause vasodilation and increased vascular permeability that induces smooth muscles to increase the expulsion of mucosal parasites. In epithelial cells, enhanced mucus secretion aids in pathogen clearance (Urb & Sheppard, 2012). In addition, mast cells can form extracellular traps composed of DNA, histones, antimicrobial peptide (cathelicidin LL-37), and tryptase to trap and immobilize invading bacteria, thereby contributing to bacterial clearance (Komi & Kuebler, 2021).

Mast cells also induce the host's adaptive immune response. The release of inflammatory cytokines such as tumor necrosis factor (TNF) facilitates the recruitment of dendritic cells, naïve T cells, and antigen-presenting cells (APCs) to the draining lymph nodes, inducing antigen-specific adaptive immunity (Shelburne & Abraham, 2011). Mast cells also express major histocompatibility complex (MHC) molecules, acting as antigen-presenting cells that induce antigen-specific T cell stimulation (Paus & Bahri, 2015). Moreover, mast cells can form immunological synapses with the dendritic cells to facilitate intracellular antigen transfer and subsequent T cell activation (Portillo et al., 2015).

Lastly, mast cells regulate homeostasis and contribute to wound healing as well as tissue remodeling through the release of numerous growth factors (Noli & Miolo, 2001). However, uncontrolled secretory responses of mast cells can cause a variety of pathological conditions other than well-known allergic reactions, such as peritonitis, worsening of inflammatory conditions, and have been linked to damaging responses, cardiovascular diseases, cancer, and autoimmune diseases (Rao & Brown, 2008). The secretion of inflammatory mediators from mast cells enhances the recruitment of immune cells to the inflammation site, promotes vascularization and vascular permeability that are known to cause chronic inflammation and progression of autoimmune diseases (e.g., rheumatoid arthritis, multiple sclerosis, etc.), facilitating cancer development (Noto et al., 2021). Hence, mast cells are essential components of the host's innate and adaptive immune system and are multitasking cells exhibiting protective roles, physiologic homeostasis, and contributing to diseases. Mast cells thus contribute to physiologic and pathologic functions that go well beyond their accepted role in allergic disease.

1.4 Mast cells in allergic reactions

Mainly recognized as effector cells in allergy, inordinate mast cell activation leads to the pathogenesis of IgE-linked allergy (also called type 1 hypersensitivity reaction), allergic asthma, rhinitis, atopic dermatitis, food allergies, and catastrophic anaphylaxis. IgE-mediated allergic reactions occur due to mature B cells' production of allergen-specific IgE antibodies. The allergic immune response starts with exposure to an allergen, i.e., low molecular weight proteins that are taken up by the dendritic cells to process into peptides (12-18 amino acid long) (Hellman et al., 2017). These peptides are then presented to the MHC Class II molecules on naïve T cells. Upon peptide recognition, T

helper 2 cells (Th2) immune cells proliferate and release inflammatory cytokines such as IL-4 and IL-13. In response to these cytokines, B cells are activated, causing class switching (the process by which B cells produce specific antibodies based on functional requirements) from IgM to IgE producing cells, allowing IgE antibodies to be secreted (González-Deolano & Álvarez-Twose, 2018). IgE binds to the FcεRI (IgE receptor) present on the mast cell surface. This process of first antigen exposure, production of IgE against it, and binding of IgE to FcεRI on mast cells is called to be a sensitized state (Hellman et al., 2017). When exposed to the same antigen again, the antigen crosslinks the IgE bound FcεRI receptors to trigger mast cell degranulation, which leads to the onset the allergy symptoms like vasodilation, bronchoconstriction, smooth muscle contraction, mucous production, etc. (Galli & Tsai, 2010; Hellman et al., 2017). The typical body sites constantly exposed to antigens include the respiratory tract and gastrointestinal tract. The lower respiratory tract inflammation (i.e., allergic asthma) is characterized by airway obstruction due to enhanced vascular permeability, bronchoconstriction, mucus production, cough, and accumulation of fluids and edema (Whittemore et al., 2016). Food allergens trigger the degranulation of mucosal mast cells in the gastrointestinal tract to release various inflammatory mediators that cause increased fluid secretion, smooth muscle contraction, increased peristalsis, vascular permeability, and edema of gut epithelium, giving rise to diarrhea and vomiting (Whittemore et al., 2016). Antigens bound to connective tissue mast cells in the skin cause skin reactions like urticaria, angioedema, and prolonged response, including atopic dermatitis or eczema (chronic itching). Thus, mast cells are the well-ascribed effector cells in IgE-associated allergic reactions.

1.5 Mast cell mediators

The mast cell mediators are vital players in various physiological and pathological settings and understanding their mode of action and molecular pathways is of prime interest. Mast cells consist of 50-200 granules that contain numerous biologically active compounds such as histamine, heparin, number of proteases, and various cytokines and growth factors (Whittemore et al., 2016; Wernersson & Pejler, 2014). Mast cell mediators are classified as pre-formed mediators (e.g., biogenic amines, proteases, and enzymes) that are stored in secretory granules, as well as neosynthesized mediators that are produced upon mast cell activation (e.g., lipid-derived mediators, chemokines, and cytokines) (da Silva et al., 2014; Whittemore et al., 2016). Pre-formed mediators are immediately released following mast cell activation (also known as anaphylactic degranulation) and orchestrate the early phase responses. The release of a neosynthesized large panel of cytokines and lipid-derived compounds contributes to delayed response and chronic inflammation. The implications of various bioactive mediators are summarized in Table 1.1.

Table 1.1 *Activities of mast cell mediators*

Granule compounds	Essential features	Biological effects	References
Lysosomal enzymes- β -hexosaminidase β -D-galactosidase, β -glucuronidase	May be present in all mast cell granular subsets and β -hexosaminidase widely used as a marker of mast cell degranulation	Involved in turnover of gangliosides and carbohydrates. Role in normal lysosomal degradation process and homeostasis maintenance. Act along with tryptases and chymases for degrading extracellular matrix	(Fukuishi et al., 2014; Wernersson & Pejler, 2014)

Table 1.1 (continued).

Proteases	Chymases (chymotrypsin-like), tryptase (trypsin-like), carboxypeptidase	Effect on extracellular matrix; granule homeostasis; regulate coagulation; inactivation of toxins, inflammation control by cleavage of selective cytokines	(Akula et al., 2020; Wernersson & Pejler, 2014)
Proteoglycans- Heparin and chondroitin sulfate	Glycosaminoglycan (GAG) chains	Interact and form stable complexes with other granule compounds facilitating their storage.	(Wernersson & Pejler, 2014)
Biogenic amines- Histamine	Best recognized amine present in mast cell subtypes.	Vascular, permeability, bronchoconstriction; vasodilation; angiogenesis; mucus secretion	(Thangam et al., 2018)
Serotonin	Abundant in rodent mast cells, less in human mast cells	Neurotransmitter; mediate signaling to the nerve endings	(Kritas et al., 2014)
Cytokines	TNF, an only cytokine that is prestored as well as newly synthesized	Acute and chronic inflammation Pleiotropic cytokine exhibiting beneficial (recruitment of cells and defense against pathogen) and detrimental (tissue damage) effects.	(Mukai et al., 2018)
Growth factors-	Preformed VEGF, TGF- β , NGF	Angiogenesis, regulation of inflammation	(Lundequist & Pejler, 2011)
Chemokines	Neosynthesized along with other numerous cytokines	Chemoattractants enhance the recruitment of immune cells to the inflammation site	(Katsanos et al., 2008)
Lipid mediators- Leukotriene; Prostaglandin D2	Derived from arachidonic acid (membrane phospholipids)	Leucocyte chemotaxis, vasodilation, bronchoconstriction, platelet activation, mucus secretion	(Deolano & Twose, 2018; Moon et al., 2014)

Mast cells produce a plethora of active mediators. β -hexosaminidase is widely used as a degranulation marker. Histamine and serotonin are released immediately upon mast cell activation and are considered pre-formed mediators. TNF is prestored but also rapidly synthesized in activated cells. Several mast cell studies have analyzed the release

of mediators described below. In my research, I will be monitoring the secretion of these four significant mediators in cell-based assays.

1.5.1 β -hexosaminidase

Mast cell granules have lysozyme-like properties, thus also called secretory lysosomes. They contain many lysosomal hydrolases, the most common being β -hexosaminidase. It is predominantly released upon mast cell activation and used routinely to monitor mast cell degranulation (Puri & Roche, 2008; Tiwari et al., 2008). Essential as a lysosomal enzyme in glycoprotein metabolism and cell homeostasis, β -hexosaminidase is found abundantly in mast cell granules. Physiologically, the granule-borne β -hexosaminidase in BMDCs was crucial to host defense against bacterial infections but was not involved in allergic reactions (Fukuishi et al., 2014).

1.5.2 Histamine

An essential contributor to allergic conditions and anaphylaxis is histamine. Histamine is the best-known prominent biogenic amine stored in mast cell granules and accompanies all mast cell degranulation events (Lundequist & Pejler, 2011). Decarboxylation of amino acid histidine by histidine decarboxylase leads to the production of histamine, which exerts its effect by binding to histamine 1 receptor to histamine 4 receptors (H1R-H4R). Mast cells express H1R and H4R and are mainly involved in the progression of allergic diseases mediated by histamine (Thangam et al., 2018). Histamine-mediated activation of H4 receptors induces the production of other proinflammatory cytokines such as IL-4 and TNF in various mast cells, accelerating the inflammation (Jemima et al., 2014; Zhang et al., 2011). Histamine elicits immediate hypersensitivity responses characterized by bronchoconstriction, vasodilation, increased

vascular permeability, smooth muscle contraction etc. (Galli & Tsai, 2010). The increased permeability allows other leucocytes and proteins to act on invading pathogens, constituting a protective role.

1.5.3 Serotonin

Serotonin (5-hydroxytryptamine(5-HT) is a neurotransmitter regulating various brain functions like sleep, mood, etc. Identified as a vasoconstrictor, it has a role in inflammation, atopic dermatitis, chronic stress, migraine, etc.(Kritas et al., 2014). It is also involved in producing chemotactic factors, activation of T-cells and NK cells (Mossner and Lesch, 1998). Serotonin is present in a high amount in rodent mast cells while in a very minimal amount in human mast cells (Sukhov et al., 2007). Like histamine, serotonin is sorted into the granules via a vesicular monoamine transporter 2 (VMAT2) (Travis et al., 2000); however, there is evidence suggesting that histamine and serotonin are localized in two separate granule subpopulations (Puri & Roche, 2008), and their release seems to be differentially regulated in rat mast cells (Theoharides et al., 1982).

1.5.4 TNF

Tumor Necrosis Factor (TNF) is a unique cytokine that is prestored and produced after mast cell activation. TNF is a cytokine with multiple functions, having role in immunity, allergy, autoimmune diseases, cancer, acute and chronic inflammation, etc. (Saggini et al., 2011). TNF binds to two different cell surface receptors- tumor necrosis factor receptor 1 (TNFR1) and TNFR2. TNF exists in soluble form (sTNF), and membrane-bound form (also called mTNF). mTNF (26 Kda) is processed by a transmembrane protease called TNF converting enzyme (disintegrin metalloproteinase

TNF converting enzyme (TACE: ADAM17) at the cell surface to produce sTNF (17 kda) (Black et al., 1997). sTNF binds to the TNFR1 and initiates a signaling cascade that leads to various biological effects such as pro-inflammatory responses, host defense against pathogens, cell survival, and cell proliferation (Yang et al., 2018). mTNF binds to TNFR2 and initiates immune modulation, cell homeostasis, proliferation, and survival (Jang et al., 2021). TNF is a crucial component of innate immunity conferring protection against infections. For example, studies involving mast cell-deficient mice infected with bacteria demonstrated that the release of TNF from mast cells was essential for recruiting neutrophils to control the infection (Bradding & Arthur, 2016). In addition to the recruitment of neutrophils, lymphocytes, and monocytes to the inflammatory site, TNF increases these cells' response, causing acute and chronic inflammatory reactions (Yang et al., 2018). TNF stimulates the synthesis of proinflammatory cytokines and chemokines (Jang et al., 2021). Uncontrolled TNF production causes an enhanced inflammatory response and leads to chronic autoimmune disease such as rheumatoid arthritis via various effector cells such as macrophages, type 1 helper T cells (Th1), B cells, and plasma cells (Jang et al., 2021). Understanding TNF signaling and its release mechanism will help develop effective therapeutics in controlling numerous TNF-mediated diseases.

1.6 Mast cell receptors

The regulated release of mast cell mediators discussed above is initiated by environmental stimuli that are recognized by various immune receptors on the mast cell surface (Fig.1.2). The most recognized and well-studied is FcεRI, a high-affinity IgE receptor that binds to IgE (for type I hypersensitive response and various mast cell disorders) (Blank & Rivera, 2004). Mast cells also express other receptors such as Toll-

like receptors (TLRs), nucleotide-binding oligomerization domain (NOD)-like receptor (NLRs) [for pathogen recognition], Fc receptors for IgG (Fc γ RI) and IgA, G-protein-coupled receptors, complement receptors, chemokine and cytokine receptors (Gilfillan & Beaven, 2011). Mas-related G-protein coupled receptors (MRGPCRs) are newly discovered receptors that respond to cationic compounds, FDA-approved drugs, toxins, and other substances by readily releasing granular contents to cause allergic reactions. (Hagenbach et al., 2021). The expression of these different receptors is responsible for various modes of activation and differential release of mast cell mediators. TLRs and Fc ϵ RI are widely known for their respective roles in native immunity and allergic response.

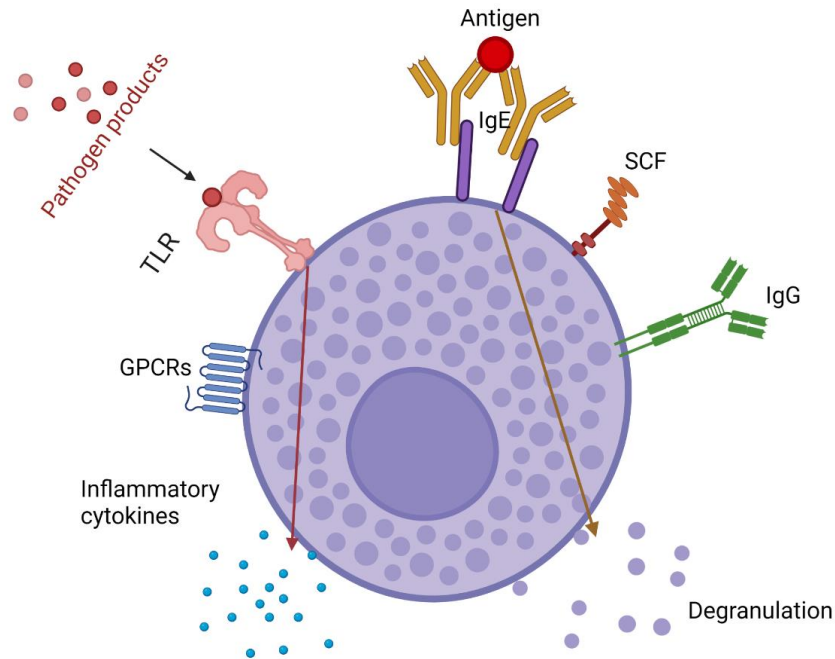


Figure 1.2 *Schematic representation of mast cell receptors.*

Mast cells express various cell surface receptors that bind to many immunological and non-immunological ligands inducing mast cell degranulation (via IgE activation) or synthesis of cytokines via TLR. Created with BioRender.com.

1.6.1 Toll-like receptors

TLRs belong to the membrane receptors of the pathogen recognition receptors (PRR) family that recognize the invading pathogens via PAMPs. Multiple TLRs (TLR1-TLR10) in humans and (TLR1-TLR9 and TLR11-TLR13) in murine are differentially expressed in various mast cell subtypes and recognize specific PAMPs (Kawasaki & Kawai, 2014; Shelburne & Abraham, 2011). Mast cell signaling in response to the stimulation of TLR2, TLR3, and TLR4 has been studied. TLR2 is activated via bacterial peptidoglycan (PGN), and TLR4 is activated by lipopolysaccharide (LPS). TLR3 is activated by dsRNA viruses and poly I: C (Sandig & Bulfone-Paus, 2012). The canonical TLR signaling pathway occurs via the MyD88 pathway, which requires NF- κ B and MAPK that cause transcriptional activation of inflammatory cytokine genes. In response

to multiple TLR ligands, mast cells secrete cytokines (such as TNF), chemokines, and lipid mediators integral for host defense (Kawasaki & Kawai, 2014). However, the involvement of TLR in mast cell degranulation (release of granular contents such as β -hexosaminidase and histamine) is contentious. In one study, stimulation of BMDCs by PGN (via TLR2) increased vascular permeability, while LPS did not (Supajatura et al., 2002). In a separate study with human mast cells, PGN, but not LPS, stimulated histamine secretion (Varadaradjalou et al., 2003). Other studies have found that mast cell degranulation is not induced by PGN, polyI:C, and LPS suggesting that mast cells do not degranulate via TLRs 2, 3, and 4 (Ikeda & Funaba, 2003; Matsushima et al., 2004; Wierzbicki & Brzezińska-Błaszczyk, 2009). Mast cells, hence, readily respond to many TLR ligands and widely secrete TNF without undergoing degranulation, providing an essential innate immune response in microbial infections. TLR can work together with Fc ϵ RI, heightening the cell's response to antigen/allergen by increased cytokine release in the absence of degranulation (Qiao & Beaven, 2006).

1.6.2 IgE (Fc ϵ RI) receptor

All mast cells express Fc ϵ RI, a high-affinity IgE receptor. The IgE- Fc ϵ RI signaling pathway (Fig.1.3) pass on the initial signal in an organized manner with activation of multiple enzymes, generation of second messengers, reorganization of the cytoskeleton, and movement of the granules from the inner side towards the plasma membrane and final fusion of the two membranes (Blank et al., 2021). This sophisticated process is regulated by protein kinases, phosphatases, calcium via calcium sensors that ultimately promote membrane fusion and release of granular contents (Blank & Rivera, 2004).

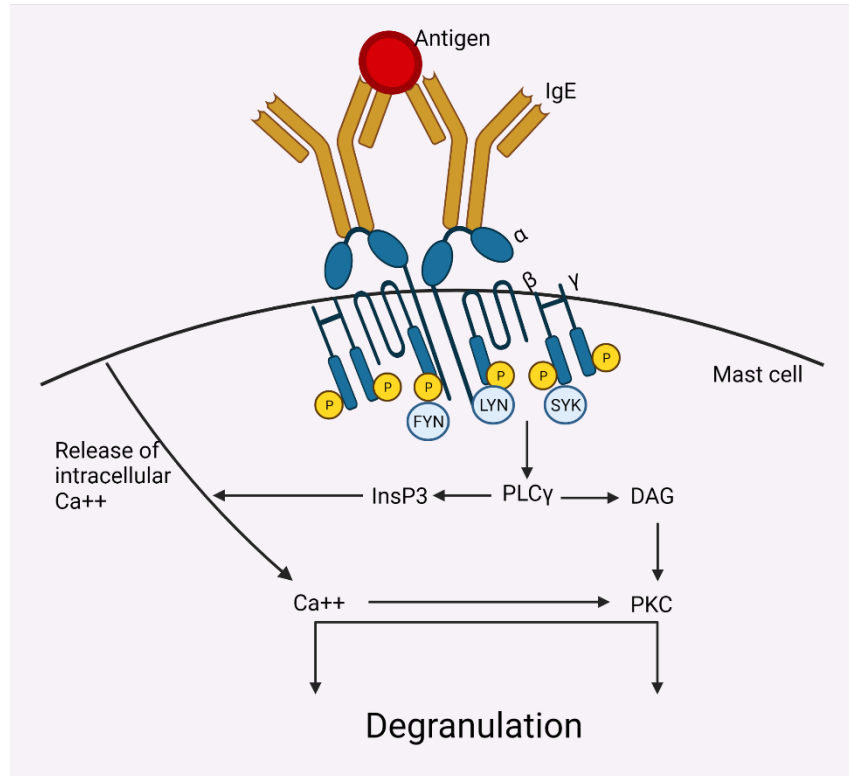


Figure 1.3 *Simplified diagram of FcεRI-IgE signaling pathway in activated mast cells.*

IgE-mediated mast cell signaling events starts with binding of a multivalent antigen (allergen) with its specific IgE bound to FcεRI receptor causing crosslinking of receptors and signal transduction via phosphorylation of intermediate signal transducers that lead to PKC activation and increase in intracellular Ca⁺⁺ which activates the degranulation machinery to release out the granular contents. The signaling cascade is sophisticated and shown here is a very simplified version. Created with Biorender.com.

FcεRI receptor on mast cells is a heterotetrameric transmembrane protein consisting of α, β, and γ subunits. The Fc portion of IgE binds to α chain at 1:1 ratio; β chain consists of four transmembrane domains and acts as a signal amplifier, and dimeric γ chains act as signal triggering subunits (Blank et al., 2021). Upon binding of multivalent antigen, IgE causes crosslinking of FcεRI receptors. The cross-linking causes the immunoreceptor tyrosine-based activation motif (ITAMs) present on β and γ chains to be phosphorylated by Src family tyrosine kinase Lyn kinase (LYN). Phosphorylated ITAMs can bind to number of proteins and amplify the signal. The tyrosine kinase Syk

kinase (SYK) and Fyn kinase (FYN) are activated to amplify signal further via the adaptor proteins -linker for activation of T cells (LAT) and GRB2-associated binding protein2 (GAB2) (Gilfillan & Rivera, 2009). The phosphorylated adaptor proteins bind to many signaling proteins such as Phospholipase C γ (PLC γ) and Phosphoinositide 3-kinase. This results in the production of second messenger molecules- Inositol-1,4,5 triphosphate (IP3). IP3 is critical in releasing Ca⁺⁺ from the Endoplasmic reticulum (ER) (Blank & Rivera, 2004). This increased Ca⁺⁺ and PKC activation activate the degranulation machinery, causing the granules to move towards the plasma membrane from the cell's interior in a microtubule-dependent manner (Wernersson & Pejler, 2014). Actin depolymerization facilitates the docking of secretory granules to the plasma membrane. The ultimate step, i.e., the fusion of docked secretory granules to the plasma membrane, is mediated by a unique set of membrane fusion proteins described below.

1.7 Eukaryotic membrane fusion

Membrane fusion is the fundamental process occurring in all eukaryotic cells and occurs via merging two separate lipid membranes. The exocytosis process begins with the formation of vesicles from the precursor membrane, which then fuses with the plasma membrane and allows the vesicular content to be released to the target area (Jahn & Scheller, 2006). Membrane fusion is the final step in cellular transport and is mediated by SNARE (soluble N-ethyl-maleimide sensitive factor attachment protein receptor) proteins anchored to opposing biological membranes.

SNARE are conserved from yeast to humans. There are 38 mammalian SNAREs known so far (Stow et al., 2006). Based on their location, SNAREs on the vesicular membrane are called v-SNAREs, and on the target membrane are called t-SNAREs. v-

SNAREs include vesicle-associated membrane proteins (VAMPs), and t-SNAREs include syntaxin and SNAP23/25 (synaptosome-associated protein)(Jahn et al., 2003). Most SNARE proteins have a C-terminal membrane-spanning domain, except SNAP23/25-like proteins which are independently attached to the membrane by multiple palmitoylated cysteine residues (Chen & Scheller, 2001).

The key feature of SNAREs is the presence of a conserved coiled-coil SNARE motif. It consists of heptads repeats of approximately 60-70 amino acids which are critical for SNARE complex formation. A short linker connects the SNARE motif with its N-terminal and C-terminal domains (Jahn & Scheller, 2006). Unlike the conserved SNARE motifs, the N-terminal domain differs between various subgroups of SNAREs which is crucial in SNARE protein activation and SNARE complex assembly. In most syntaxins, there is three α -helical bundle consisting of H-a,b,c domain preceded by N-terminal peptide. A C-terminal H3 or SNARE domain participates in the SNARE complex formation (Hong, 2005). The Habc-domain and H3 SNARE domain form a closed, inhibitory conformation (Dulubova et al., 1999). The opening of the Habc domain allows the SNARE motif to be accessible to other SNARE domains from the interacting partners, in a process that is regulated by SM proteins (discussed in section 1.8.1).

The v-SNAREs also differ in their N-terminal extensions. Some such as VAMP7 and Ykt6 have longin domains that could fold back to bind the SNARE domain, adopting an autoinhibitory conformation (Hong, 2005) that arrests trans-SNARE complex formation and membrane fusion. Phosphorylation on tyrosine 45 of longin domain of VAMP7 by c-Src kinase activates the VAMP7 function and allows it to interact with the cognate t-SNAREs (Burgo et al., 2013). Ykt6 bears a profilin-like hydrophobic N-

terminal domain which adopts a closed conformation by interacting with the SNARE motif (Hong, 2005). Human YKT6 N-terminal domain is shown to mediate palmitoylation of itself and other fusion proteins essential for vacuole fusion (Veit, 2004). Hence, the N-terminal domains of SNAREs are involved in regulating SNARE functions.

1.7.1 The SNARE core complex

The basis of SNARE-mediated membrane fusion (Fig.1.4 A) is the formation of SNARE complex via the interaction of SNARE motifs (Fig.1.4 B). It is an intermolecular coiled coil, intertwined four-alpha helical bundle where each distinct SNARE motif contributes a helix. The bundle is a 16 stacked layer characterized by a zero layer at its longitudinal midpoint. Based on the presence of hydrophilic residues such as Arginine or Glutamine at the zero ionic layers of the four helical bundles, SNAREs are classified into R-SNAREs (arginine- containing SNAREs) or Q-SNAREs (glutamine- containing SNAREs) (Fasshauer et al., 1998). In the typical SNARE complex, one of the helices is contributed by vesicle bound R-SNARE or VAMPs, while two target organelle Q-SNARE proteins contribute the other three: SNAP23/25 like proteins (Qb, Qc contributing two helices) and syntaxin (Qa contributing one helix) (Fasshauer et al., 1998). Each type of transport vesicle with a distinct R-SNARE only pair with cognate Q-SNARE at the correct target to form the trans-SNARE complex, a twisted four helical bundle comprising Qa, Qb, Qc, and R-SNARE motifs.

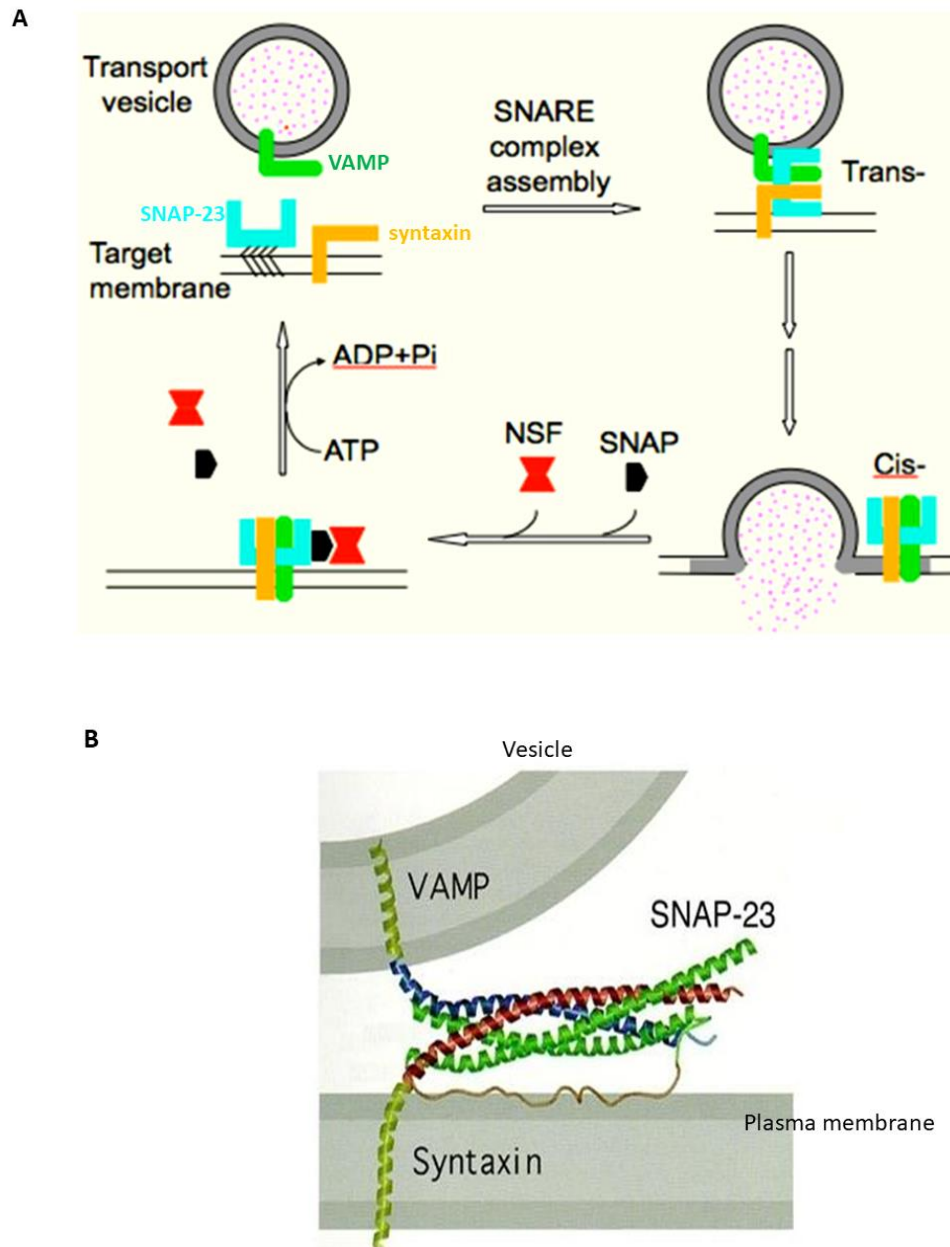


Figure 1.4 *Simplified model of SNARE-mediated membrane fusion and schematic representation of the trans-SNARE complex.*

(A) The R-SNARE (VAMP) on the vesicle and three Q-SNAREs (syntaxin and SNAP-23) on the acceptor membrane assemble in the acceptor complex. The acceptor complex then interacts with R-SNAREs on vesicles via their SNARE motifs to form a trans-SNARE complex characterized by a four helical bundle which are coiled-coil structures (B). The trans-SNARE complex then proceeds to cis complex that mediates complete fusion and release of vesicular contents. NSF and SNAPs then disassemble the cis complex to separate R and Q SNAREs. (B) Adapted and modified from (Chen et al., 1999).

1.7.2 The SNARE complex assembly and disassembly

The opposing membranes destined to fuse are first bridged via the formation of a partial trans-SNARE complex by the interaction of specific Q-SNAREs and R-SNAREs (Ma et al., 2015). The SNARE complex assembly starts from the N-terminus (distal from the fusion site) and progresses towards the C-terminus (proximal to the fusion site) of SNAREs (Rizo & Xu, 2015). It releases free energy so the two opposing membranes can overcome the electrostatic repulsive forces and merge into one (Lou & Shin, 2016). The first step, which is also a rate-limiting step in the SNARE assembly, is forming a Q-SNARE complex on the target plasma membrane. This then serves as a template to recruit R-SNARE to form a four helical bundle in a fashion that is regulated by accessory proteins (Zhang et al., 2016). Once membrane fusion has occurred, trans-SNARE complex transitions into cis-SNARE complex, and for further rounds of fusion, the cis-SNARE complex has to be disassembled and recycled by ATPase NSF (N-ethylmaleimide-sensitive factor) and its cofactor α -SNAP (soluble N-ethylmaleimide-sensitive factor attachment protein) (Jahn & Scheller, 2006; Yoon & Munson, 2018).

1.8 Regulation of SNARE-mediated membrane fusion

To ensure the membrane fusion occurs correctly, SNARE cooperates with the regulatory proteins that have evolved along with the SNAREs (Sauvola & Littleton, 2021). These regulatory proteins consist of Sec/Munc (SM) protein family members, Munc-13 group of proteins, Rab family of GTP binding proteins, tethering factors, synaptotagmins, and complexins (McNew, 2008). Though designated as the SNARE regulators, SM and Munc13 are central to the fusion process in vivo and the focus of my study.

1.8.1 SM proteins

In eukaryotes, four subfamilies of SM (Sec1/Munc like) proteins- Sec1p/Munc18 (at plasma membrane/ exocytosis), Sly1p (Endoplasmic reticulum to Golgi transport/protein biosynthesis), Vps45 (Trans Golgi Network-endosomal complex/ endocytosis) and Vps33 (vacuolar traffic/ degradation) have been identified (Carr & Rizo, 2010; McNew, 2008) each participating in a distinct trafficking pathway. Munc18 (Mammalian uncoordinated `unc-18) are the founding members of the conserved Sec-1 Munc18 (SM) protein family and consists of 3 isoforms: Munc18-1, Munc18-2, and Munc18-3 (also called Munc18a, Munc18b, and Munc18c, respectively). Munc18a is a neuronal isoform and binds to syntaxin1(Hata et al., 1993). The critical roles of Munc18a have been demonstrated in neurotransmitter release as it was severely impaired in the Munc18a knockout mice (Verhage et al., 2000).

Munc18 proteins are dynamic in nature and can undergo conformational changes. They have demonstrated different binding modes with exocytic SNAREs, and their multiple binding sites make them highly complex and complicated machinery in regulating SNARE-mediated membrane fusion (Carr & Rizo, 2010). A vesicle fusion event likely starts with the binding of Munc18 protein to the closed conformation of syntaxin, which stabilizes the syntaxin structure and prevents premature SNARE assembly (Carr & Rizo, 2010; Dulubova et al., 1999). According to a recent study, Munc18a actually induces the closed confirmation of syntaxin1 in free syntaxin1 and syntaxin1/SNAP25 complexes, thereby gating the formation of binary and ternary SNARE complexes (Lee et al., 2020). Munc18 proteins also act as chaperones of syntaxins for trafficking to the target membrane. Some Munc18 proteins can also bind to

open syntaxin. This interaction occurs between the hydrophobic pocket (N-pocket) on the D1 domain of Munc18 protein and the N-peptide motif at the N-terminus of syntaxins (Carr & Rizo, 2010). Additionally, Munc18 proteins can directly bind to the four helical SNARE bundles, potentially playing a direct role in membrane fusion (McNew, 2008).

A structure-based mechanism for SNARE complex assembly mediated by SM protein has been described by Baker & Hughson (2016). Munc18 makes initial contact with almost the entire length of the cytosolic domain of closed syntaxins, which acts as a clamp to prevent premature syntaxin binding to other SNAREs. Opening of Munc18 bound syntaxin by other regulatory factors (e.g., Munc13) enables the exposure of the R-SNARE binding site in Munc18 protein. The R-SNARE/ VAMP in apposing membrane can bind to individual R- and Q-SNAREs, thus catalyzing the trans-SNARE complex formation (Baker and Hughson, 2016). The structural studies show that Munc18 proteins act as catalysts for the formation of trans-SNARE complexes during membrane fusion events.

1.8.2 Munc13 proteins

The mammalian uncoordinated gene 13 (Munc13) group consists of Munc13-1, -2, -3, and -4 and the recently identified brain-specific angiogenesis inhibitor 1-associated protein (BAIAP3). Munc13-1, -2, and -3 play a role in neuronal cells, while Munc13-4 is expressed in non-neuronal cells. Munc13-1 played a critical role in neurotransmitter release as complete loss of release was observed in the absence of Munc13 (Richmond et al., 1999). Structurally, Munc13 proteins bear an N-terminal Calcium-binding C2A, C1, and C2B domain, a central Munc Homology domain (MUN), and the C-terminal C2C domain, (Rizo & Xu, 2015). Munc13-4 and BAIAP3 differ from other Munc13 homologs

lacking C1 and C2C domains, yet they share MUN and C2 domains. C2A domain is involved in binding to Rab3-interacting molecule (RIM), C2B, and C2C in bridging vesicle and target membrane. The C1 and C2 domains are involved in DAG, and membrane binding in calcium triggered secretion, while the MUN domain helps in tethering of vesicles to the target membrane, acting as the binding site for final SNARE complex assembly (Jahn & Fasshauer, 2012).

MUN domain is the key domain for the Munc13 priming function similar to tethering factors (Li et al., 2011). The MUN domain of Munc13-1 has been shown to facilitate the opening of the closed conformation of syntaxin1, dissociation of the Munc18a/syntaxin1 complex, and formation of the trans-SNARE complex in synaptic vesicle fusion studies (Baker & Hughson, 2016). It was recently shown that Munc13-1 and Munc18a work cooperatively to chaperone SNARE assembly. Munc18a catalyzes a complex formation between syntaxin1 and VAMP2. The MUN domain in Munc13-1 stabilizes this complex as well enhances the binding of SNAP25 to the template complex. This MUN bound SNARE complex is essential for synaptic vesicle fusion (Shu et al., 2020).

1.8.3 Rabs and tethering complexes

The fusion of vesicles with plasma membrane occurs in 3 distinct and consecutive steps-docking (retention of vesicles to the plasma membrane), priming (docked vesicles ready for Ca^{++} dependent exocytosis), and fusion (merging of lipid bilayers) (Jahn & Fasshauer, 2012). Membrane tethering factors which include coiled-coil homodimers and multisubunit tethering complexes (MTCs) heterooligomers, facilitate the tethering of two different membranes. The best characterized MTC, i.e., homotypic fusion and vacuolar

protein sorting (HOPS), play an essential role in tethering by binding to the membrane-associated Rab proteins and acting as chaperones for SNARE assembly (Baker & Hughson, 2016). Rab proteins belonging to the Ras-like GTPases family are present in GTP bound active form or GDP bound inactive form linked to membrane association/disassociation. They act as an essential communication between the vesicle tethering and SNARE complex as MTC recruiters of MTCs to ensure the vesicle and target membrane associate properly. Rabs are also known to directly interact with SNAREs or direct SNARE regulators such as SM proteins to regulate the fusion (Hutagalung & Novick, 2011). Rab3A binding to the Munc18a-closed syntaxin1 complex facilitates docking and can also form a tripartite complex with Munc13 through the RIM (Rizo & Xu, 2015).

1.8.4 Synaptotagmins and Complexins

Exocytic fusion is ultimately triggered by increased calcium concentration, which is detected by calcium sensors that include synaptotagmins. Sixteen members are in the synaptotagmin family and structurally consist of N-terminal luminal/extracellular domain, a transmembrane α -helix, and two calcium-binding domains (C2)-C2A and C2B (Sutton et al., 1995). In the presence of calcium, C2 domains bind to acidic phospholipids containing membranes, enhance lipid binding, and trigger fusion (Jahn & Fasshauer, 2012; McNew, 2008). SynaptotagminI is the primary neuronal calcium sensor for fast synchronous synaptic vesicle release. The binding of synaptotagmin to the SNARE complex in response to Ca^{++} stimulation is thought to alleviate the inhibitory effect of another SNARE interacting proteins, i.e., complexins (Xu et al., 2013).

Complexins include small (14-20Kda) cytoplasmic proteins known to bind to the groove on the SNARE complex via a central helix. Complexins, are known to function in partially assembled SNAREs which may help to stabilize partially zipped SNARE complex and also act as a clamp to inhibit the progression of SNARE zippering. The clamp is released via synaptotagmins upon calcium triggering, facilitating the fusion (Jahn & Fasshauer, 2012).

1.9 Mast cell exocytosis

Section 1.7 and 1.8 reviewed the membrane fusion and regulatory mechanisms based on the studies on synaptic vesicle fusion. This section focuses on mast cell exocytosis and the mechanisms regulating the release of granular contents from mast cells. Signaling triggered mast cell exocytosis leads to the regulated secretion of various pharmacologically active mediators to the extracellular environment via the fusion of granule membrane with the plasma membrane. The fusion machinery is made up of unique SNAREs and regulatory proteins such as Munc18, Munc13, Rab GTPases, and others that determine the specificity of fusion events (Table 1.2). This section summarizes the SNAREs expressed in mast cells, the SNARE regulators, and the current understanding of their function mode.

Table 1.2 *Molecules involved in mast cell exocytosis*

Protein	Effects	Cell type	Ref
VAMP2	N-terminal mimicking peptide inhibited histamine release	RBL-2H3	(Yang et al., 2018)
VAMP3	No effect on IgE induced degranulation	BMMCs	(Puri & Roche, 2008)
VAMP7	Impaired β -hexosaminidase and histamine release	RBL-2H3, human MCs	(Sander et al., 2008; Woska & Gillespie, 2011)

Table 1.2 (continued).

VAMP8	Major VAMP studied, affects β -hexosaminidase, serotonin release; controversial in histamine secretion	RBL-2H3, BMBCs, human MCs	(Yang et al., 2018)(Puri & Roche, 2008)(Tiwari et al., 2008)
syntaxin3	Essential in granule to granule and granule to plasma membrane fusion, crucial for chemokine/cytokine release	PCMCs, RBL-2H3, human MCs	(Sanchez et al., 2019)(Frank et al., 2011)(Tadokoro et al., 2007)
syntaxin4	Overexpression inhibited exocytosis, do not mediate compound exocytosis	PCMCs, RBL-2H3	(Sanchez et al., 2019)(Paumet et al., 2000)
SNAP23	Plasma membrane-localized; forms complex with Syntaxin4 and VAMP8; affects IgE induced degranulation; also required for cytokine and chemokine secretion	RBL-2H3, human and murine mast cells,	(Frank et al., 2011; Sander et al., 2008; Vaidyanathan et al., 2001)
Munc18a	Required for β -hexosaminidase release	RBL-2H3	(Bin et al., 2013)
Munc18b	Essential in compound exocytosis	RBL-2H3, PCMCs	(Gutierrez et al., 2018)(Tadokoro et al., 2007)
Munc18c	Overexpression does not affect exocytosis, not required for degranulation	PCMCs	(Gutierrez et al., 2018)
Munc13-1	Overexpression inhibited exocytosis	RBL-2H3	(Higashio et al., 2017)
Munc13-4	Essential for mast cell exocytosis	RBL-2H3, PCMCs	(Ayo et al., 2020)(Rodarte et al., 2018)
Rabs	Differential requirement in secretory granule exocytosis- Rab27a negatively regulates exocytosis; Rab27b positively regulates exocytosis via Munc13-4 interaction	BMBCs	(Singh et al., 2013)
Complexin II	Facilitates exocytosis by binding to the SNARE complex formed by syntaxin3, SNAP 23, and VAMP8 but not syntaxin4	RBL-2H3	(Tadokoro et al., 2010)
Synaptotagmin II	Essential for mast cell degranulation	BMBCs	(Melicoff et al., 2009)

1.9.1 SNAREs mediated mast cell exocytosis

Mast cells express several exocytic SNAREs. The reported SNARE proteins in mast cells degranulation include Q-SNAREs SNAP23 and syntaxins 2,3, 4, and 6 and R-SNAREs VAMP 2, 3, 7, and 8 (Blank, 2011; Lorentz et al., 2012). It is unclear why so many exocytic SNAREs are required for mast cell exocytosis. According to 3Q and 1R rule (Fasshauer et al., 1998), a set of 3Q- and 1R- SNAREs are sufficient for a specific fusion event. The widely studied neurotransmitter release is orchestrated by well-defined interaction of VAMP2, Syntaxin1, and SNAP25 along with Munc18a and Munc13-1 and calcium sensors Synaptotagmin1 and Complexin1 (Rizo et al., 2008). Unlike the synaptic vesicle fusion, mast cells have multiple sets of SNAREs and Munc18 as well as Munc13 proteins, and we do not have a full understanding of their functional roles in mast cell exocytosis. In our lab, intensive testing of the association of two Q-SNARE sub complexes (syntaxin3/SNAP23 and syntaxin4/SNAP23) with four granular R-SNAREs (VAMP2,3,7 and 8) led to form potentially eight distinct trans-SNARE complexes (Xu et al., 2015), suggesting multiple SNARE sets carry out various exocytic events in mast cells. The presence of multiple sets of SNAREs suggests that diverse exocytic events are occurring in activated mast cells.

1.9.2 Heterogeneity in exocytic pathways in mast cells

Mast cells are undergoing a variety of exocytic pathways. Mast cells are known to undergo constitutive exocytosis and regulated exocytosis. Newly synthesized cytokines and chemokines are packaged into secretory vesicles and released constitutively while the prestored granular mediators are released via regulated exocytosis from activated mast cells (Blank et al., 2014). Different modes of the regulated exocytosis occur in activated

mast cells, such as i) full exocytosis where the secretory granule fuses with the plasma membrane to fully discharge all of the contents; ii) kiss and run exocytosis where secretory granule fuses with plasma membrane but does not collapse and the granule is recovered; iii) piecemeal degranulation where there is gradual loss of vesicular contents without shreds of evidence of complete fusion and; iv) multi granular compound exocytosis where there is a homotypic fusion of granules to form giant secretory granules followed by heterotypic fusion of large secretory granules with the plasma membrane; and v) sequential compound exocytosis where a single secretory granule fuses with plasma membrane first to release its content followed by secondary fusion of vesicles to the fused granule acting as a channel for secretion of all cargo contents (Klein & Eisenberg, 2019). These unique exocytic events may occur in the same mast cells, with compound exocytosis being the primary exocytic pathway (Blank, 2011).

Another critical but often neglected factor attributing to multiple exocytic SNAREs in mast cells is the heterogeneity in mast cell granules. Mast cells are functionally as well as phenotypically diverse (described as different subsets). Based on the development of progenitor cells in tissue-specific microenvironments such as cytokines, growth factors and hormones, genetic and epigenetic regulation, and pathological conditions, differentiation into heterogenous mast cell phenotype occurs (Moon et al., 2010). At the ultrastructural level, human mast cells have a mixture of crystalline and amorphous structures where the proteases like tryptase and chymase localize, respectively (Lundequist & Pejler, 2011). Based on the composition of β -hexosaminidase (a lysosomal marker) and MHC Class II, bone marrow-derived mast cells (BMMCs) are proposed to be of 3 subtypes. i) Subtype I granules represent a

classical lysosome and consist of MHC Class II, β -hexosaminidase, lysosomal membrane protein (LAMP)-1,-2 but no serotonin; ii) subtype II granules represent a classical lysosome and consist all as type I along with serotonin; while iii) subtype III granules contain β -hexosaminidase and serotonin but not MHC class II (Baram et al., 1999; Moon et al., 2014; Raposo et al., 1997). The homotypic fusion of immature progranule form subtype III granules, which upon merging with subtype I (lysosome/endosomes) generates a subtype II secretory lysosome. The release of these various heterogenous contents such as β -hexosaminidase (present in all granules), serotonin and histamine (in subtype II granules), and TNF (in subtype III and may be in subtype II as well) may require different protein machinery (Moon et al., 2014).

Localization and functional studies have lent support to the notion of a distinct subset of secretory granules. Serotonin and histamine appear to localize to specific granule populations (Puri & Roche, 2008). VAMP8 deficient mast cells showed defects in Fc ϵ RI regulated release of β -hexosaminidase, serotonin, and cathepsin D while histamine and TNF release was normal (Puri & Roche, 2008). The differential requirement for VAMP8 in β -hexosaminidase and TNF release from BMDC has been corroborated by independent studies (Puri & Roche, 2008; Tiwari et al., 2008), but the requirement for VAMP8 in histamine release is still controversial. The mast cells derived from bone marrow showed that VAMP8 affected the release of β -hexosaminidase and histamine (Tiwari et al., 2008). The subsequent studies including siRNA and N-peptides directed against VAMPs showed VAMP8 to be involved in release of β -hexosaminidase and histamine (Woska & Gillespie, 2011; Yang et al., 2018). Studies of human mast cells showed that inhibition of VAMP7 reduced histamine release while VAMP2 or VAMP3

inhibition did not affect histamine release (Sander et al., 2008). Colocalization studies suggest that TNF colocalized with the VAMP3 positive compartment at the plasma membrane in BMMCs (Tiwari et al., 2008). The specific granule content utilizes unique exocytic machinery for its release.

Finally, different secretion profiles have been observed in mast cells activated via various modes. Upon activation of the corticotropin-releasing hormone (CRH) receptors, human mast cells selectively secreted VEGF without other granular contents like tryptase, histamine, and pro-inflammatory cytokines such as TNF, IL-6, IL-8 (Cao et al., 2005). This suggests mast cells could participate in inflammatory response without causing an allergic reaction. Various pathogens are known to trigger the selective release of the mediators by binding to different TLRs. In murine BMMCs, PGN from *Staphylococcus aureus* stimulated TLR2 and released cytokines such as TNF, IL-4, IL-5, IL-6, IL-13, while TLR4 was responsive to LPS from *Escherichia coli* and secreted TNF, IL-1 β , IL-6, and IL-13. Moreover, PGN but not LPS induced mast cell degranulation via TLR2 (Supajatura et al., 2002). In another study, none of these stimuli were found to cause anaphylactic degranulation (release of preformed granular contents such as histamine) (Ikeda & Funaba, 2003). These observations suggest different pool of mediators are differentially released in a highly sensitive fashion to the extracellular cues.

1.9.3 Regulation of mast cell exocytosis by Munc18 proteins

In line with the presence of multiple exocytic SNAREs, mast cell expresses all three known isoforms of Munc18 (Nigam et al., 2005); however, their exact roles is not clearly understood. Mainly known as syntaxin1 binding partner, Munc18a, a neuronal Munc18 isoform, has been essential in mast cell exocytosis. A Munc18a and Munc18b

double knock down RBL cells abolished β -hexosaminidase release, while the reintroduction of Munc18a alone rescued the secretion defects (Bin et al., 2013). This implies Munc18a is indeed involved in the β -hexosaminidase release. A recent study showed that Munc18b, but not Munc18a or Munc18c, is required for compound exocytosis in matured mast cells (Gutierrez et al., 2018). Published data from our lab (Xu et al., 2015) showed Munc18a stimulated VAMP2 and VAMP3 but not VAMP7 or VAMP8-based lipid mixing, suggesting that in the events where VAMP8-dependent degranulation is compromised, VAMP2 and VAMP3 based trans-SNARE complexes might play compensatory roles.

Munc18b has been found to regulate mast cell exocytosis (Gutierrez et al., 2018; Tadokoro et al., 2007). siRNA mediated knockdown of Munc18b in RBL cells remarkably inhibited β -hexosaminidase release (Tadokoro et al., 2007) and showed that Munc18b interacted with syntaxin3 but not with syntaxin4. The Munc18b-syntaxin3 interaction was found on the plasma membrane as well as on secretory granules, suggesting that Munc18b might be involved in homotypic granule-granule fusion as well as heterotypic granule-plasma membrane fusion (Tadokoro et al., 2007).

Munc18c is ubiquitously expressed Munc18 member in mammalian tissues and is primarily present in the plasma membrane and associates with syntaxin4 in secretory cells such as mast cells (Blank, 2011). Munc18c has been shown to have positive (stimulation) and negative (inhibition) in the regulated exocytosis of glucose transporter GLUT4 (Kioumourtzoglou et al., 2014; Brandie et al., 2008). The role of Munc18c in mast cells has not been extensively studied. A study led by (Gutierrez et al., 2018) found that exocytosis from matured mast cells was not dependent on Munc18c.

1.9.4 Regulation of mast cell exocytosis by Munc13 proteins

An essential feature in regulated mast cell exocytosis is the Ca^{++} influx and subsequent fusion of membranes. The C2 domain as in Munc13 proteins containing Ca^{++} binding proteins act as essential proteins in docking and priming and are indispensable regulators of all exocytic events including regulated mast cell exocytosis. One study showed that matured mouse peritoneal mast cells express Munc13-2 and Munc13-4 (Rodarte et al., 2018), while RBL-2H3 mast cells were shown to express Munc13-1 and Munc13-4 isoforms (Higashio et al., 2017; Woo et al., 2017). Munc13-1 was shown to inhibit antigen-induced RBL-2H3 mast cell degranulation (Higashio et al., 2017), and Munc13-4 was the essential Munc13 protein involved in homotypic secretory granules fusion in various mast cells (Rodarte et al., 2018; Woo et al., 2017). Munc13-4 was identified as an effector of Rab27 (a Rab GTPases), where the Munc13-4 binding to Rab27 was essential for secretory lysosome exocytosis (Elstak et al., 2011). Our lab has shown that when Munc13-4 is knocked out from RBL-2H3 cells, it affects the release of preformed mediators and partial inhibition of TNF release (Ayo et al., 2020). BAIAP3 is a Munc13-4 homolog whose role has been investigated in dense-core vesicle fusion (Zhang et al., 2017), but the function is unknown in mast cells.

1.10 Regulation of exocytosis by post-translational modification

In addition to accessory regulator proteins like Munc18 and Munc13, another essential but under-investigated factor in regulating SNARE complex formation is post-translational modifications such as protein phosphorylation (Snyder et al., 2006). Protein kinases are an integral part of the signal transduction pathway. These kinases are known to phosphorylate SNAREs and SNARE regulators. In mast cells, Thr14 of syntaxin3 was

phosphorylated by Ca^{++} /calmodulin-dependent protein kinaseII (CamKII) that impaired its interaction with Munc18b, inhibiting RBL mast cell exocytosis (Tadokoro et al., 2016). SNAP23 was phosphorylated at Ser95 and Ser120 in stimulated RBL-2H3 cells and bone marrow-derived mast cells to maximize exocytosis (Hepp et al., 2005) in an I κ B Kinase (IKK2) dependent fashion (Suzuki & Verma, 2008). In addition, a recent study showed that Protein Kinase C (PKC) dependent phosphorylation of residues within the VAMP8 SNARE domain reduced the kinetics of exocytosis invitro and in vivo by impairing SNARE complex formation (Malmersjö et al., 2016).

Phosphorylation of Munc18 has been shown to regulate the exocytosis process in various secretory events. In adrenal chromaffin cells, PKC phosphorylated Munc18a at serine residues 306 and 313. This site-specific phosphorylation reduced its affinity for syntaxin and led to short-term enhancement of transmitter release during post-tetanic potentiation (Genç et al., 2014). In neuronal cells, phosphorylation of Munc18a at threonine 574 residue by CDK5 decreased its affinity for syntaxin1a and enhanced secretion from neuroendocrine cells (Fletcher et al., 1999). In embryonic kidney cells, Dyrk 1A mediated phosphorylation of Munc18a at T479 enhanced Munc18a and syntaxin1 binding, thus regulating their interaction (Park et al., 2012). In epithelial cells, CDK5 mediated Munc18b phosphorylation at threonine 572 promoted the assembly of functional VAMP2/syntaxin3/SNAP-25/ Munc18b fusion complex that stimulated the gastric acid secretion from parietal cells (Liu et al., 2007). Study in adipocytes and muscle cells, insulin-dependent phosphorylation of Munc18c at tyrosine 521 residue showed an enhancement of SNARE complex formation between VAMP2/syntaxin4 and SNAP23, thus facilitating the delivery of GLUT4 to the cell surface (Kioumourtzoglou et

al., 2014). In contrast, wild-type (unmodified) Munc18c inhibited exocytosis by binding to the syntaxin4 in its auto-inhibitory state (Brandie et al., 2008). Another study showed that Munc18c phosphorylation in activated platelets enhanced exocytosis, increased thrombin activation, and reduced its binding to syntaxin4 and syntaxin2 (Schraw et al., 2003). Together, these studies suggest that Munc18s undergo reversible phosphorylation at specific sites to modulate their affinity for their cognate partners and alter the exocytosis kinetics. In addition to these site-specific studies, proteomic discovery-mode mass spectrometry has unraveled multitudes of putative phosphorylation sites in Munc18 isoforms (Fig.1.5). Hence, Munc18 phosphorylation is a common regulatory mechanism in exocytosis that links the signaling cascade to the fusion machinery (Xu et al., 2018).

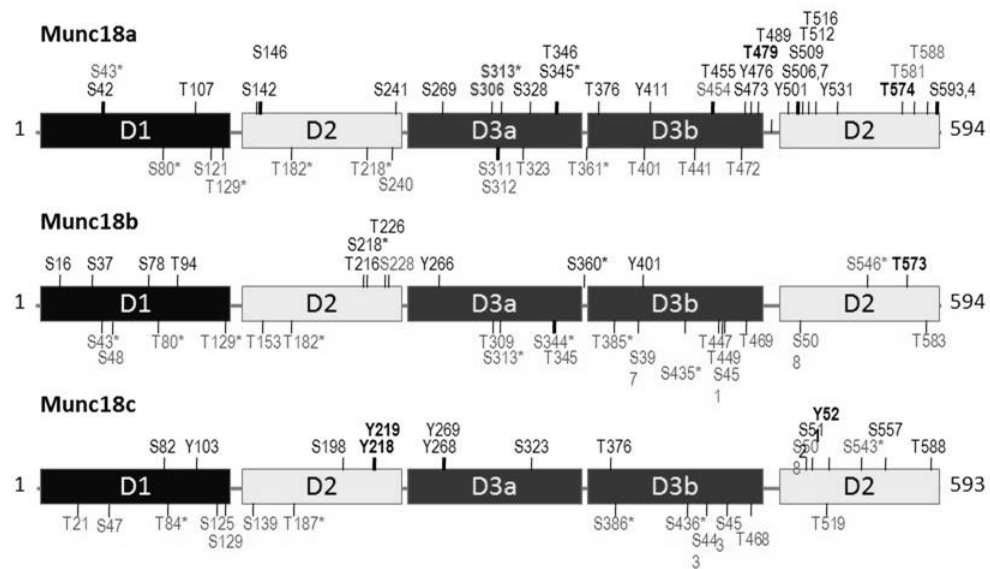


Figure 1.5 *Known or predicted phosphorylation sites in Munc18s.*

High throughput proteomics studies and site-specific studies (in bold) identified the sites above domain structure from various tissues and cells. The sites underneath the domain are predicted PKC sites. * indicates the conserved or semi-conserved PKC sites. Adapted from (Xu et al., 2018)

In addition to phosphorylation, other post-translational modifications take place on proteins involved in exocytosis. S-nitrosylation of cysteine residues was found to

occur in synaptic vesicle fusion proteins, including syntaxin1, SNAP25, and synaptobrevin (Prior & Clague, 2000). Meanwhile, Vrljic et al. (2011) showed that synaptotagmin 1, a calcium sensor in synaptic vesicle fusion, undergoes tyrosine nitrasylation in the C2 domain; phosphorylation in lumenal domain and O-glycosylation that regulated protein binding with the partners and interactions with various lipids. This suggests in response to cell-surface signaling; a fusion factor may undergo several post-translational modifications to regulate exocytosis.

1.11 Experimental models to study mast cell exocytosis

Over the years, various biochemical and well cell-based (involving cell lines and mast cells from mice) approaches have been utilized for mast cell exocytosis studies. To study the SNARE function invitro, fusion of liposomes containing mast cell SNARE proteins have been used. However, the findings from these cell-free reconstituted systems need to be validated in cell-based studies for physiological relevance. Mast cell lines or primary mast cells have been widely used, with each system having its own advantages and disadvantages. The models I utilized to study mast cell exocytosis are described briefly below.

Developed by the Rothman group to study the neuronal SNAREs (Weber et al., 1998), liposome-based membrane fusion still holds a powerful method for studying the SNAREs functions. I utilized a cell-free reconstitution system to study the interaction of SNAREs and Munc18s invitro. It is an artificial vesicle fusion system engineered from pure proteins and phospholipids to form proteoliposomes which have been extensively used to study synaptic vesicle fusion. (Brunger et al., 2015). Proteoliposomes are relatively easy to make from purified membrane proteins, and fusion of liposomes can be

readily monitored via Fluorescence resonance energy transfer (FRET) based assays. The pure exocytic SNARE proteins are reconstituted into two classes of proteoliposomes- donor liposomes (v-SNAREs) that contain fluorescent-labeled dyes (NBD-PE and Rh-PE), while acceptor liposomes (t-SNAREs) are unlabeled. Initially, Rhodamine quenches the fluorescence of NBD on donor vesicles because of the close vicinity. Upon fusion of donor and acceptor vesicles, the effect posed by Rh is relieved due to dilution resulting in NBD fluorescence. The increase in fluorescence can be measured to calculate the dequenching rate called lipid mixing (Brunger et al., 2015; Shen et al., 2013). The limitation of FRET is that it depends on correct orientation, concentration, and distance of fluorophores. It confers advantages as steps in the assembly to fusion can be dissected further by order of adding the components; incorporation of inhibitory proteins (cytoplasmic soluble VAMP domains) etc. Thus, cell-free invitro lipid mixing assay is a potent tool to directly examine the stimulatory or inhibitory effects of soluble Munc18s/ Munc18 mutant proteins in the fusion of cognate exocytic SNARE liposomes, enhancing our understanding of the regulation of SNARE-mediated fusion mechanism in mast cells.

As a complement to the in-vitro studies, cell-based studies provide direct physiological evidence of the exocytosis mechanism. Mast cells generated from bone marrow progenitors, isolated from peritoneal cavity of rats and mice along with immortalized mast cell lines such as Rat basophilic leukemia (RBL-2H3) from rats, MC-9 from mice, HMC-1 and LAD2 from human origin are commonly used in the field of mast cell biology (Jiménez et al., 2021). For my research, I used RBL-2H3 (also called RBL) cells. It is a tumor analog of mucosal mast cells and is a widely used mast cell line in immunological, allergic, and inflammation research. They are easy to grow, allow

genetic manipulations, recapitulate the responses by external stimulation, and contain plethora of mediators. The rat basophilic cells were derived from the rat that developed granulocyte leukemia after treatment with potent carcinogen. These leukemic basophilic cells exhibited basophilic and rat peritoneal mast cell characteristics, responded to IgE sensitization, and released histamine in response to FcRI stimulation. (Passante & Frankish, 2009). The proinflammatory mediators of my research interest, such as β -hexosaminidase, histamine, and serotonin, are profoundly found in RBL-2H3 cells and undergo transcriptional activation to synthesize TNF. Hence, RBL cells comprise a useful experimental model for genetic manipulations and subsequent stimulation by a specific trigger to measure exocytosis.

Comparative investigations of differential secretion in response to various modes of activation (signaling pathways) in one cell type are essential to delineate the diverse exocytic pathways in mast cells. However, not all mast cells are activated by all ligands, lacking proper cell surface receptors. For instance, RBL-2H3 cells do not express the TLR receptors or the signaling pathway elements (Passante & Frankish, 2010). They are unresponsive to bacterial products LPS and PGN, making RBL cells not ideal for studying differential secretion based on IgE and or TLR signaling. To address it, bone marrow-derived mast cells (BMMCs) and peritoneal cell-derived culture mast cells (PCMCs) are widely used owing to the significant yield (Vukman et al., 2014) and expression of multiple cell surface receptors. BMMCs are obtained as immature progenitors from the bone marrow of mice and cultured in IL-3 and SCF-containing medium. The matured BMMCs grown invitro over four weeks and toluidine blue positive stained cells are utilized as tissue equivalent mast cells. PCMCs are developed mast cells

obtained from the peritoneal cavity. Unlike BMMCs, PCMCs are a mature source of mast cells and give more robust responses to stimuli (Meurer et al., 2016). Due to the high yield and responsiveness to many stimulants, including allergic and non-allergic triggers, have made these primary model systems extensively used to study the role of mast cells (Akula et al., 2020).

1.12 Rationale and Hypothesis

Allergies, inflammation, and autoimmune diseases are leading health concerns in the United States with no immediate cure. Mast cells are linked to the progression of these diseases via regulated secretion of a variety of pharmacologically active mediators stored in distinct secretory granules. Studies have implicated the existence of multiple exocytic pathways for the regulated release of different mast cell mediators. Multiple sets of exocytic SNAREs are required to mediate mast cell exocytosis by forming fusogenic trans-SNARE complexes. However, it is not clear how mast cell SNAREs pair to fuse with each other to form a fusogenic SNARE complex. The assembly and activation of trans-SNARE complexes are coordinated by Munc18 proteins (mast cells express three Munc18 isoforms that are associated with exocytosis). However, it is not clear how Munc18s selectively regulate the assembly of cognate SNAREs. Moreover, Munc18 isoforms undergo reversible phosphorylation in response to various physiological and pathological conditions. This modification regulates the specificity and activity of Munc18s toward their cognate SNAREs. How the site-specific phosphorylation affects mast cell exocytosis is unclear. This could be one of the intricate strategies connecting signaling cascade with fusion machinery exploited to ensure the specific release of selective mediators under different activation conditions. Hence, my objective is to define

the exocytic vesicular SNAREs that mediate the differential release of histamine, serotonin and TNF in association with specific Munc18 proteins in a fashion that is regulated via reversible phosphorylation.

Moreover, the differential role of Munc13 isoforms in mast cell exocytosis has not been studied. Each Munc13 protein may be responsible for each type of mediator release, and it is not known. Our observation of partial inhibition of TNF release from Munc13-4 knockout cells suggested a compensatory function of another Munc13 isoform for the remaining TNF secretion. BAIAP3 is the most closely related Munc13-4 homolog, so I decided to test it in the TNF release.

My study hypothesizes that mast cells consist of distinct secretory granules subsets that require a specific set of SNAREs, Munc18s or phosphorylated Munc18s and Munc13 for fusion. This study aims to systematically characterize the distinct exocytic machinery for various mediators in RBL-2H3 cells to enhance our understanding of underlying molecular mechanisms of differential mediator release.

CHAPTER II – MATERIALS AND METHODS

2.1 General materials

2.1.1 Antibodies

All the primary antibodies were used at a dilution of 1:1000 unless otherwise specified. Anti-VAMP2 (104211, Clone 69.1), anti-VAMP7 (232011, Clone 158.2) mouse monoclonal and anti-VAMP8 (104303), anti-BAIAP3 (256003), anti- Munc13-1 (126103) rabbit polyclonal antibodies were obtained from Synaptic Systems (Germany). Anti-VAMP3 (pab0055) rabbit polyclonal antibody was from Covalab (France). Anti - YKT6 (NBP2-94846) rabbit polyclonal antibody was obtained from Novus Biologicals (USA). Anti- Munc13-4 (SC-271300) mouse monoclonal antibody, anti- Beta-actin (SC-1616) goat polyclonal antibody, anti- His₆ rabbit polyclonal antibody (SC-803), and p-Unc18-1 (ser313)-R specific for Ser313 phosphorylated Munc18a (SC-28459-R) rabbit polyclonal antibodies were obtained from Santacruz Biotechnology (USA) and were used at a dilution of 1:100. HRP conjugated secondary goat anti-mouse IgG (SC-2005), donkey anti-rabbit IgG (SC-2313), and donkey anti-goat IgG (SC-2033) were obtained from Santacruz Biotechnology. The secondary antibodies were used at a dilution of 1:5000.

2.1.2 Plasmids

For recombinant SNARE expression, rat genes encoding SNAP23, syntaxin3, syntaxin4, VAMP2, VAMP3, VAMP8 were cloned into NcoI and EcoRI restriction sites of the pMBP-parallel1 vector bearing N-terminal, TEV cleavable MBP tag as described (Xu et al., 2015). VAMP7^{Y45E} (with a phosphorylation mimic at tyrosine 45 of longin domain of VAMP7) was subcloned in LIC (Ligation Independent Cloning) site of pET-

MBP-His₆ vector [a gift from Scott Gradia (Addgene plasmid # 37237; <http://n2t.net/addgene:37237>; RRID: Addgene_37237)] bearing TEV cleavable C-terminal MBP tag. Rat Munc18a was amplified from cDNA (Thermofisher Scientific; Clone ID# 7315868) and inserted into EcoRI and SalI sites of the pMBP-parallel1 vector. cDNA encoding rat Munc18b was generated from a pCMV-Munc18-2 plasmid (a kind gift from Dr. Thomas Sudhof) and cloned into BamHI and SalI sites of pFast- BAC-HT-JS vector (gift from Dr. Jingshi Shen) for insect cell line expression. pFast-BAC-HT-JS-Munc18c (mouse) expression construct for insect cell line expression was obtained as a kind gift from Dr. Jingshi Shen. The construct pFL-38 His₆-TEV for expression of TEV protein was a kind gift from Dr. William Wickner (Xu et al., 2015).

The phosphomimetic Munc18a^{T574E} cDNA was amplified from pCDNA3.1-Munc18a^{T574E} and then cloned into EcoRI and SalI sites of the pMBP-parallel1 vector. Rat Munc18a^{S306E/S313E} in pROEX-HTb His₆ tagged vector was received as a gift from Dr. Axel Brunger. Rat Munc18b^{T572D} and mouse Munc18c^{Y521E} mutants were generated by site-directed mutagenesis from WT Munc18b and Munc18c respectively and cloned into BamHI and SalI sites of pFast-BAC- HT-JS vector for insect cell line expression. The vector contained a 6x His tag at N-terminal. All the constructs were verified by sequencing.

2.2 Protein expression and purification

For all MBP tagged proteins expression, the plasmids pMBP-TCS (TEV cleavable site)-SNAP23, pMBP-TCS-syntaxin3 pMBP-TCS-syntaxin4, pMBP-TCS-VAMP2, pMBP-TCS-VAMP3, pMBP-TCS-VAMP8, pET-VAMP7^{Y45E}-TCS-MBP-His₆, pMBP-TCS-Munc18a, and pMBP-TCS-Munc18a^{T574E} were transformed in *E. coli*.

Rosetta 2 (Novagen) cells, and proteins were purified according to published protocols (Xu et al., 2015). For expression of His₆-tagged proteins, the plasmids pROEX-HTb-Munc18a, pROEX-HTb-Munc18a^{S306E/313E}, pFL-38 His₆-TEV were transformed in *E. coli*. Rosetta2(DE3) and purified according to previously published procedure (Arnold et al., 2017; Xu et al., 2015).

For expression of the pFast-BAC plasmids- His₆-Munc18b, His₆-Munc18b^{T572D}, His₆-Munc18c, and His₆-Munc18c^{Y521E} were transformed into MAX Efficiency DH10Bac *E. coli*. competent cells for the bacmid transposition. The transformed cells were screened by blue-white screening. The recombinant bacmids were expressed in Sf9 insect cell line (gift from Dr. Fengwei Bai) using baculovirus infection. Sf9 insect cells were maintained as non-adherent cells in Sf-900 III SFM (Gibco) media at 28°C. For baculovirus production, cells were counted in a hemocytometer and then 8x10⁵ Sf9 cells were added to one of the wells on a 6 well plate containing 2 ml of Sf-900 medium. The cells were transfected with 2 µg of bacmid DNA in the presence of 8 µl of Cellfectin II reagent following the manufacturer's protocol (Bac-to-Bac Baculovirus Expression System; Thermofisher Scientific). Following 72 h of transfection, the media containing the virus was collected and centrifuged at 500xg for 5 min to remove cell debris. The obtained clarified supernatant, known as "P1 viral stock," was stored at 4°C. The baculoviral stock was amplified by adding all the P1 viral stock (~2 ml) to 15 ml of Sf9 cells grown at a density of 0.5x10⁶ cells/ml. The cells were incubated at 28°C with 220 rpm shaking until signs of viral infection appeared (enlarged and vesiculated cells) to generate P2 stock and stored at 4°C. The P3 viral stock was then generated by adding 5 ml of P2 stock to 250 ml of Sf9 culture grown at a density of 0.5x10⁶ cells/ml (1:50 ratio)

and then incubated at 28°C at 220 rpm for 72 h. The cell culture was centrifuged at 500xg for 5 min, and the cell pellet was washed with 250 ml of PBS, pH 7.4 (Gibco). The final cell pellet was resuspended in 20 ml of resuspension buffer (25 mM HEPES-KOH, pH 7.5, 400 mM KCl, 10% Glycerol, 2 mM β -mercaptoethanol, 1X PIC (Protease Inhibitor Cocktail containing 0.62 μ g/ml leupeptin, 4 μ g/ml pepstatin A, and 24.4 μ g/ml pefabloc-SC), 5 mM Benzidine HCl, 20 mM Imidazole, 1 mM PMSF) and snap frozen as baby beads (BBs) in liquid N₂ and stored at -70°C. The His₆ tagged fusion protein expression was verified by immunoblotting with Anti-His₆ antibody.

The proteins expressed in Sf9 insect cells were purified as reported (Yu et al., 2013). Cells were lysed by adding 2.7 ml of 10% Triton X-100 to 25 ml of cell suspension (see above), and the mixture was nutated at 4°C for 30 min. The lysates were homogenized 10 times in a Dounce homogenizer. and then centrifuged in a Type 70 Ti rotor at 18,500 rpm at 4°C for 30min. The resulting supernatant (~25ml) was added to 5 ml of Ni-NTA resin (Qiagen) pre-equilibrated with 25 ml of wash buffer (resuspension buffer containing 20 mM imidazole). The mixture was nutated at 4°C for 2 h. Then, the resin was washed with 25 ml of wash buffer as above. Proteins were eluted with 20 ml of elution buffer (resuspension buffer containing 200 mM imidazole), with 1ml eluate in each fraction. The eluted proteins were dialyzed 1,000,000-fold in RB100 buffer (20 mM HEPES-NaOH, pH 7.4, 100 mM NaCl, 10% glycerol) overnight at 4°C. The proteins were then concentrated to desired concentration using Macrosep Advance Centrifugal Device (30 K MWCO) (Pall Corporation) at 4000xg for 1.5 h at 4°C. Bradford assay was done to determine protein concentration, and then proteins were stored by flash freezing in 10 μ l aliquots in liquid N₂ and stored at -70°C.

2.3 Preparation of Proteoliposome

The proteoliposomes were prepared according to a published protocol (Xu et al., 2015). Briefly, donor proteoliposomes consisted of 60% POPC (1-palmitoyl-2-oleoyl-sn-glycero-3-phosphocholine), 17% POPE (1-palmitoyl-2-oleoyl-sn-glycero-3-phosphoethanolamine), 10% DOPS (1,2-dioleoyl-sn-glycero-3-phosphoserine), 10% cholesterol, 1.5% NBD-DHPE [N-(7-Nitrobenz-2-Oxa-1,3-Diazol-4-yl)-1,2-Dihexadecanoyl-sn-Glycero-3-Phosphoethanolamine] and 1.5% rhodamine DHPE (Lissamine™ Rhodamine B 1,2-Dihexadecanoyl-sn-Glycero-3-Phosphoethanolamine) and acceptor proteoliposomes consisted of 60% POPC, 19% POPE, 10% DOPS or POPS, 10% cholesterol and 1% Dansyl DHPE [N-(5-Dimethylaminonaphthalene-1-Sulfonyl)-1,2-Dihexadecanoyl-sn-Glycero-3-Phosphoethanolamine]. The lipids were dried under gentle stream of N₂ gas to prevent lipid oxidation. Respective SNARE proteins were added at a ratio of 1: 200 protein: lipid for donor RPLs and at 1: 500 for acceptor RPLs. Protein-free donor liposomes (PF) were prepared without any SNARE proteins. In each reconstitution, 60 µg/ml of His₆-TEV protease was added for the removal of N-terminal tags from SNAREs. The protein-lipid film was resuspended in RB500 (20 mM HEPES-NaOH, pH 7.4, 500 mM NaCl, 10% glycerol) containing 40 mM CHAPS by nutating at 4°C for 2 h. The mix was then transferred to a 20 MWCO dialysis cassette and dialyzed in RB150 (20 mM HEPES-NaOH, pH 7.4, 150 mM NaCl, 10% glycerol) buffer overnight. The proteoliposomes were then harvested on a Histodenz density gradient floatation as previously described (Shen et al., 2007). RPLs were stored by flash freezing in 10 µl aliquots in liquid N₂ and stored at -70°C.

2.4 Lipid-mixing assay

As described in (Xu et al., 2015), a 20 μ l standard fusion reaction containing 50 μ M donor RPLs and 400 μ M acceptor RPLs in RB75 (20 mM HEPES-NaOH, pH 7.4, 75 mM NaCl, 10% glycerol) buffer was prepared and incubated on ice overnight. Munc18s were added at a concentration of 5 μ M (unless otherwise specified), and His₆-TEV protease was added in a 2:1 molar ratio to remove tag in Munc18 protein. The reaction contained 1 mM DTT. Following incubation, the fusion reaction mix were transferred to 384 well black Corning microplate, and the lipid mixing was monitored by measuring the dequenching rate of NBD fluorescence at ($\lambda_{\text{ex}}= 460$ nm, $\lambda_{\text{em}}= 538$ nm, $\lambda_{\text{cutoff}}= 515$ nm) in a Spectra MAX Gemini XPS plate reader (Molecular Devices) at 37°C. The early rate of dequenching was calculated as the increased fluorescence at the given time divided by the maximal fluorescence increase in 1% Triton X-100 [(Ft-Fo)/(Fd-F0)x100].

2.5 Proteoliposome clustering assay

Clustering assay was performed as described in (Arnold et al., 2017). Briefly, a standard fusion reaction (as described above) was prepared in RB150 and incubated on ice overnight. The mixture was diluted 40 folds in ice chilled RB150. Four μ l was placed on a microscope slide covered with a 22 mm coverslip. A Zeiss confocal fluorescent microscope was used to collect random images and the particle size were measured in Image J (NIH) software. Using Kaleida Graph, the values were plotted on a logarithmic scale against their cumulative distribution.

2.6 Cell culture

The rat mast cell line RBL-2H3 cells (ATCC) were maintained in DMEM complete medium (Gibco) containing 4.5 g/l D-Glucose, 110 mg/l sodium pyruvate, 1X

Glutamax (Gibco), and 10% FBS (Gibco, heat-inactivated) at 37°C, 5% CO₂. For the routine culture, cells at around 70-90% confluency in a T-25 culture flask were treated with 1.2 ml of 0.25% Trypsin-EDTA (Gibco) and neutralized with 6.8 ml of DMEM complete medium. Then the cell suspension at a dilution of 1:3 was transferred to a 6 well plate (in 2ml of DMEM complete medium) and grown to around 80% confluency for secretion assays.

2.7 RBL-2H3 mast cell activation

For stimulation by IgE cross-linking, sub-confluent (around 80-90%) RBL-2H3 cells grown on a 6 well plate was sensitized with anti-TNP IgE (BD Biosciences, 557079) at 1:1000 dilution in 1 ml of DMEM complete medium at 37°C, 5% CO₂. After 3 h, the cells were washed once with 2 ml of phenol red-free RPMI 1640 (Corning) and then twice with 1 ml of RPMI-BSA (RPMI 1640 containing 0.1% BSA). Cells were then stimulated with 50 ng/ml or 25 ng/ml TNP (26)-BSA (Santa-Cruz) in 1 ml of RPMI-BSA for 30 min, 1 h, or 24 h, as indicated. The cell supernatant was collected from resting (no IgE or TNP-BSA) and activated (IgE/TNP-BSA stimulated) wells in a microfuge tube and kept on ice. The cells were then lysed in 1 ml of RPMI 1640 containing 0.1% BSA and 0.5% Triton X-100 for 5 min and the cell lysates were collected in a microfuge tube on ice.

2.8 Secretion assay

The extent of degranulation was determined by analyzing the amount of granule enzyme, β -hexosaminidase, serotonin, histamine, and TNF released from the activated RBL-2H3 cells.

2.8.1 β -hexosaminidase release assay

To estimate of β -hexosaminidase activity, a colorimetric assay with *p*-nitrophenyl-*N*-acetyl- β -D-glucosaminide as substrate was used. Thirty μ l of supernatant and 15 μ l the cell lysates diluted with 15 μ l of RPMI-BSA (0.1%) +Triton X-100 (0.5%) were incubated with 50 μ l substrate solution (1.3 mg/ml *p*-NAG in 0.1 M citrate buffer, pH 4.5) for 1h at 37°C in a water bath. The reaction was stopped by addition of 100 μ l stop solution (0.2 M glycine, 0.2 M NaOH). The concentration of produced *p*-nitrophenol, which correlates with β -hexosaminidase activity, was measured at 405 nm in the BIOTEK Synergy H1 microplate absorbance reader. The secretion of β -hexosaminidase was expressed as a percentage of its activity in the medium (supernatant) relative to the total activity (supernatant plus cell lysate).

2.8.2 TNF assay

Eight hundred microlitre (μ l) of supernatant, cell lysate, buffer control of supernatant (RPMI with 0.1% BSA and 25 ng/ml TNP-BSA) and buffer control for cell lysate (RPMI with 0.1% BSA and 0.5% Triton X-100) were first lyophilized (Labconco freeze/dry system) to concentrate the amount of TNF in the samples. The dried pellet was then resuspended in 120 μ l of Millipore water, centrifuged at 15,000 \times g for 10 min, and 100 μ l of the supernatant was used to measure TNF level using a Rat TNF ELISA kit (BD Biosciences, 560479) according to the manufacturer's instructions.

2.8.3 Histamine assay

The cell supernatant and cell lysates were diluted 1:50 times with standard buffer (from kit below) and 20 μ l of the diluted sample were used to measure the histamine using EIA kit (Eagle Biosciences, EA213/96) following manufacturer's instructions.

2.8.4 Serotonin assay

The cell supernatant and cell lysates were diluted 1:625 times with standard buffer (from kit below) and 20 μ l of sample was used to measure the serotonin using EIA kit (Eagle Biosciences, EA630/96) according to manufacturer's instructions.

2.9 Phosphoprotein isolation and detection

As described in (Adhikari & Xu, 2018), RBL-2H3 cells were grown to around 85% confluency on three T-25 flasks. Two flasks received 2.5 ml of fresh complete medium containing 0.5 μ g/ml of anti-TNP IgE while the 3rd one received just fresh DMEM complete medium. Following 2 h incubation, 20 μ M of Ro-03-0432 or DMSO were added to IgE-sensitized cells while the unsensitized cells received DMSO. After 30 min of further incubation, cells in all three flasks were washed twice with 2.5 ml of RPMI 1640 (phenol red-free) and incubated with 2.5 ml of RPMI 1640 containing 1% BSA and 50 ng/ml of TNP-BSA for 20 min. After removing the medium, cells in the flasks were washed three times with 7 ml of 5 mM HEPES-Na, pH 7.4, 150 mM NaCl by brief incubation at RT. Phosphoproteins were then isolated using a Qiagen PhosphoProtein Purification kit by following the manufacturer's instructions. Five ml of lysis buffer (supplied in the kit which included protease inhibitors to prevent degradation of protein) was used for each T-25 flask. Phosphoproteins were eluted from the PhosphoProtein Purification column, 0.5 ml eluates and 2 ml of Flowthrough were concentrated respectively via Nanosep ultrafiltration device (10 kDa cutoff) and subjected to SDS-PAGE and immunoblotting with affinity-purified antibodies specific for Ser313 phosphorylated Munc18a.

2.10 siRNA knockdown

SMARTpool siGENOME siRNA oligos for rat VAMP2 (M-090962-01-005), VAMP7 (M-094480-01-0005), and VAMP8 (M-099039-01-0005) were purchased from Dharmacon-Horizon Discovery Group (USA). VAMP3 siRNAs (s131634 and s131635) and Silencer select negative control siRNA (4390843) were obtained from Ambion. The siRNAs were resuspended in nuclease free water and stored as stock of 100 μ M at -20°C. siRNA knockdown of VAMPs was verified by quantitative real time PCR using TaqMan Gene Expression Cells-to-CT kit (Thermofisher Scientific, AM1728) for cell lysates harvest. To analyze gene expression via qPCR, TaqMan Gene expression assays- Beta-actin (Rn00667869_m1), VAMP2 (Rn01465442_m1), VAMP3 (Rn00588964_m1), VAMP7 (Rn00585478_m1), and VAMP8 (Rn00582868_m1) were obtained from Thermofisher Scientific (USA).

2.10.1 siRNA transfections

RBL-2H3 cells were transfected using Amaxa SF cell line Nucleofector kit (V4XC-2024) from Lonza Biosciences (Germany). RBL-2H3 cells were counted in Invitrogen Countess II FL automated cell counter following manufacturer's instructions. 1×10^6 cells were pelleted at 90xg for 5min at room temperature and resuspended in 100 μ l SF nucleofection solution provided in the nucleofector kit. From siRNA stock, 1 μ l of siRNA (VAMP3, VAMP7, and VAMP8) or 2 μ l of siRNA (VAMP2) was added to 100 μ l of cell suspension, mixed gently, transferred to nucleofection cuvette and electroporated under optimized program EQ151 in a Lonza 4D-Nucleofector (Lonza Biosciences). Five hundred μ l of DMEM complete medium prewarmed at 37°C, 5% CO₂ was added to each cuvette containing electroporated cells. The mixture was pipetted

gently up and down 3 times and about ~100 μ l of it was transferred to a well in a 24 well plate containing 500 μ l of DMEM complete medium for qPCR analysis. The remaining ~500 μ l of mix were added to a 6 well plate containing 2 ml of DMEM complete medium for secretion assays. The cells were incubated at 37°C, 5% CO₂ for 24 h for qPCR assay and 48 h for secretion assay.

2.10.2 Reverse transcription and Quantitative Real-time PCR

The siRNA transfected cells were analyzed for silencing at 24 h post-transfection. Quantitative real time PCR (qPCR) was used to determine the mRNA levels of VAMPs in siRNA transfected RBL cells. siRNA transfected cells in 24 well plate was treated with 250 μ l of 0.25% Trypsin-EDTA and neutralized with 750 μ l of DMEM complete medium. 10⁵ cells were collected for lysate preparation using TaqMan Gene Expression Cells-to-CT kit that does not require isolating or purifying RNA. In brief, the cells were pelleted at 500xg for 5min, followed by washing with 100 μ l PBS, pH 7.4. The cell pellet was resuspended in 49.5 μ l lysis buffer containing 0.5 μ l DNase. A 50 μ l reverse transcription mixture containing 22.5 μ l of prepared cell lysate (45% of reaction volume) was subjected to reverse transcription following manufacturer's protocol. Nine μ l of cDNA (45% of reaction volume) was used for qPCR using TaqMan Gene Expression assay in Bio-Rad CFX96-Real time System. The Cq values of VAMPs were normalized to the β -actin and data was analyzed using Bio-Rad CFX Maestro software.

2.11 Cell lysate harvest and Immunoblotting

RBL-2H3 cells grown to ~90% confluency on T-25 culture flask were harvested for immunoblotting. The flasks were washed twice with 8 ml of ice-cold PBS. The cells were then lysed in 500 μ l RIPA buffer [25 mM HEPES-NaOH (pH 7.4), 150 mM NaCl,

1% NP40 alternative, 1% deoxycholate, 0.1% SDS and 10 mM EDTA] containing 1 mM PMSF and 1X PIC followed by brief sonication of the lysate on ice to shear DNA.

Prepared cell lysates (from 10 to 150 μ g as indicated in figure legends) were run on 12-15% SDS PAGE gel and subjected to immunoblotting with a specific primary antibody (1:100- 1:1000 dilution), respective secondary antibodies (1:5000 dilution) and developed in 1:1 Supersignal West Femto Maximum Sensitivity Substrate.

2.12 Densitometry and band quantification

The immunoblots were imaged with Bio-Rad ChemiDoc MP imager. Using Biorad-Image Lab 6.0 software, the blots were subjected to densitometry analysis. A standard curve was plotted with the intensity values of recombinant TEV cleaved VAMP proteins. The intensity of VAMP protein in the cell lysates (unknown values) was then determined from the standard curve. The intensity of bands was standardized to their actin level in different batches of lysates. The obtained protein amount from the software was then divided by the total protein loaded (μ g) to get a concentration per μ g of cell lysate. The concentration value obtained was divided by the molar mass of each VAMP to get moles of proteins per microgram of cell lysate. It was then represented as percentage distribution of VAMPs as nanomoles per μ g of cell lysate.

2.13 Generation of CRISPR/Cas9 mediated VAMP3 KO RBL-2H3 cells

2.13.1 Digestion of vector

pSpCas9(BB)-2A-GFP (PX458) gRNA cloning vector [a gift from Feng Zhang (Addgene plasmid # 48138; <http://n2t.net/addgene:48138>; RRID: Addgene_48138)] was purchased from Addgene. The vector plasmid was isolated using QIAprep Spin Miniprep kit (Qiagen, 27106) following manufacturer's protocol. Four μ g of vector DNA was

digested in a 20 μ l reaction containing 1X NEB Buffer 2.1, and 4 μ l BbsI enzyme (NEB, R0539S, 10000 U/ml) and incubated at 37°C for 3 h in water bath followed by heat inactivation at 65°C for 20 min. The mix was then treated with 1 μ l of rSAP (NEB, M0371S, 1000 U/ml), incubated at 37°C for 1 h in water bath followed by heat inactivation at 65°C for 5 min. The digested reaction was then ran on 0.7% agarose gel and the vector DNA band was excised out from the gel with a clean scalpel. The DNA from the gel slice was purified using QIAquick Gel Extraction kit (Qiagen, 28704) following manufacturer's instructions. The DNA was eluted in 50 μ l of autoclaved millipore water and concentration was determined using Nanodrop.

2.13.2 gRNA selection

Guide RNA (gRNA) targeting the rat VAMP3 was designed using an online IDT CRISPR gRNA design tool. A 20-nucleotide sequence 5'GAGTCTTCGATTACTGCCAG 3' on exon 2 of rat VAMP3 (based on IDT's on target and off-target scores' rank) was selected and synthesized as oligonucleotide pair- sense (5' CACCGAGTCTTCGATTACTGCCAG 3') and anti-sense (5' AACCTGGCAGTAATCGAAGACTC 3') that were compatible with BbsI restriction site. Oligonucleotide pair each at 100 μ M concentration were annealed in a 10 μ l reaction buffer containing 1ul T4 Polynucleotide Kinase (NEB, M0201S, 10,000 U/ml) and 1X T4 ligation buffer with ATP (NEB, B0202A). The reaction occurred at 37°C for 1 h followed by 5 min incubation at 95°C and gradual cooling down at RT for 1 h. The annealed mix was diluted 10 times, and then 1 μ l was added for the ligation.

2.13.3 Ligation of gRNA into the CRISPR vector

A 10 µl ligation reaction consisting of 100 ngs of digested and gel purified PX458 vector, 1µl of annealed gRNA, 0.5 µl T4 DNA ligase (NEB, M0202S, 400,000 U/ml), and 1X T4 DNA ligase was incubated at RT for 1 h. The reaction was heat inactivated 65°C for 10 min. Then, 5 µl of the ligated mix was transformed into 50 µl of DH5 alpha competent *E. coli* cells (home made using Xu lab Protocol 007) following directions on Xu lab Protocol 008 (2b). The transformed colonies on LB+ Ampicillin (100 µg/ml) agar plate were further streaked into a new LB+ Amp agar plate to isolate the colonies from single cell. The plasmid was isolated and then sent sequencing to verify the integration of gRNA in the pCas9 vector.

2.13.4 Homologous Recombination (HR) vector design

For Homology Directed Repair-based CRISPR knockout, the HR target vector (HR110PA-1) was purchased from System Biosciences to clone the 5' and 3' homologous sequences (homology arms). A 600 bp homology arm on the left and right side of the double-strand break site was amplified from the RBL-2H3 genome via PCR using primers (HXO_E24: 5'AAAACGACGGCCAGTGAATTCCTGGCTTGAG CAATCC 3' and HXO_E25: 5' AAAACGACGGCCAGTGAATTCCTGGCTT GAGCAATCC 3') for left arm, and (HXO_E26: 5' GAAATAACCTAGATCGGAT CCGCACTGGACCCTGAAG 3', and HXO_E27: 5' GATTACGCCAAGCTT GCATGTGCTTCAGACTTTGGTC 3') for right arm (Table 2.1). These primers contained a 15 bp of homology to the linearized vector ends. Left Homologous Arm was cloned into the EcoRI and BglII site of MCS1 of HR vector and Right Homologous Arm was cloned into BamHI and SphI sites of MCS2 of HR vector using cold fusion cloning

kit (System Biosciences, MC010B-1). The cold fusion cloning was based on homologous recombination and allowed the homologous ends (on homologous arm and linearized vector) to fuse efficiently. The integration of homologous arms in HR vector was verified by sequencing.

2.13.5 Transfection of CRISPR plasmids and screening of clones

Five μg of PX458 plasmid containing VAMP3 gRNA was co-transfected with an equal amount of HR target plasmid containing homology arms into RBL-2H3 cells using electroporation as described in section 2.10.1. Cells were transferred to a 6 well plate containing 2 ml of DMEM complete medium. After 48 h of electroporation, cells were replaced with 3 $\mu\text{g}/\text{ml}$ puromycin containing medium to enrich cells. Cells were grown in puromycin-containing media until discrete cell colonies were visible. Using the cloning discs (Scienceware, F37847-001), single clone cells were transferred to each well of 24 well plate containing 0.5 ml media and grown until cells reached confluency of $\sim 60\%$. Then cells on the 24 well plate were trypsinized with 250 μl of 0.25% Trypsin-EDTA and neutralized with 750 μl of DMEM complete medium. The cells were centrifuged at 300xg for 5 min followed by wash with 100 μl PBS. Cells were resuspended in 25 μl buffer containing 10 mM Tris-HCl (pH 8.5), 25 mM KCl, 1% Triton X-100, and 2% Proteinase K. The cell lysates were incubated at 37°C for 1 h followed by 5 min incubation at 95°C to inactivate proteinase K. To screen the potential knockout clones, 1 μl of cell lysate was used as a template in a 20 μl PCR reaction containing 1X OneTaqMM (NEB, M0482) and 200 nM of forward and reverse primers (Table 2.1). Three sets of primers were designed for the amplification of edited clones. Primer sets 5F (HXO_E37: 5' GCTTCTACAAAGACCTGCC 3') and 3R (HXO_E38: 5'

GCCACAGCAAAAAGGTAC 3') amplified the region left to right of the edited site. Primer sets 5F and 5R (HXO_E41: 5' GGCCGCTGTCTAGATTTTTG 3') amplified the left side integration into the edited cells. The primer sets 3F and 3R (HXO_E42: 5' TTAGGGCCCATTGGTATGGC 3') amplified the right integration into the edited cells. The candidate clones screened via PCR were then expanded in a T-25 flask, and cells lysates were harvested as described in 2.11. To validate the knockout of VAMP3, the expression of VAMP3 protein was examined by western blotting (Fig. 4.7).

2.14 Generation of stable VAMP3 rescue cells

For the generation of stable VAMP3 rescued RBL knockout cells, the rat VAMP3 expressing plasmid (pMBP-TCS-VAMP3) was amplified via PCR using primers HXO_F30: 5' GGAATTCGCCACCATGTCTACAGGGGTG 3' and HXO_F31: 5' CGGGATCCAGAGACACACCACACA 3' (Table 2.1). The amplicon was then cloned into EcoRI and BamHI sites of modified pLVX-EmGFP-IRES-blast vector (a kind gift from Dr. Shuzo Sugita). The cloned construct was verified by sequencing. The recombinant lentivirus was generated in Human embryonic Kidney (HEK)-293FT cells (a gift from Dr. Shuzo Sugita). HEK-293FT cells were cultured on a 6 well plate in 2 ml of DMEM complete medium at 37°C, 5% CO₂ to reach 70% confluency. To generate lentivirus, 3 plasmids were co-transfected- a) 1.8 µg of VAMP3 expression plasmid, b) 2.4 µg of lentiviral packaging plasmid (psPAX2), and c) 0.8 µg of lentiviral envelope plasmid (pCMV-VSVG) into Human embryonic Kidney (HEK)-293FT cells using Lipofectamine 3000 reagent (Thermofisher, L3000001) following manufacturer's protocol. Cell supernatant was collected from transfected cells at 24 h and 52 h time point and centrifuged in Beckman Coulter at 2000 rpm for 5 min at 4°C to pellet down cells.

The supernatant was then filtered through a 0.45 µm pore size filter (VWR, 28145-481). The lentiviral particles thus harvested were stored at -70°C, while 1.2 ml of it was applied to a T-25 flask of VAMP3 KO cells in the presence of 8 µg/ml Polybrene. After 48 h, the transduced cells were selected with 20 µg/ml blasticidin. The fluorescence was monitored under Leica Microsystems (DFC3000 G) fluorescence microscope. The cells were further grown in presence of blasticidin to harvest cell lysate. The rescue of KO with GFP tagged VAMP3 expression was verified by western blotting (Fig.4.11).

2.15 Generation of CRISPR based Base-edited BAIAP3 KO RBL-2H3 cells

gRNA cloning vector pGL3-U6-sgRNA-PGK-puromycin [a gift from Xingxu Huang (Addgene plasmid # 51133; <http://n2t.net/addgene:51133>; RRID: Addgene_51133)], and pCMV-BE4max plasmid vector [a gift from David Liu (Addgene plasmid # 136918; <http://n2t.net/addgene:136918>; RRID: Addgene_136918)] were obtained from Addgene. pGL3-U6-sgRNA-PGK-puromycin was modified by incorporating the RFP tag upstream of puromycin to create pGL3-U6-sgRNA-PGK-RFP-puromycin (Ayo and Xu, unpublished). The gRNA targeting the rat BAIAP3 was designed using an online benchling tool (<https://www.benchling.com/crispr/>). A 20-nucleotide sequence 5' CGACCAGGTAGACGACGAGG 3' on exon 5 of rat BAIAP3 (based on base editing scores) was selected and synthesized as oligonucleotide pair- sense (5' CCGGGCGACCAGGTAGACGACGAGG 3'), and antisense (5' AAACCCTC GTCGTCTACCTGGTCCG 3') that was compatible with BsaI (NEB) restriction site. Oligonucleotide pairs were annealed and then ligated into the vector (as described in section 2.13.2). The pGL3-U6-sgRNA-PGK-RFP-puromycin plasmid (4 µg) was digested with 4 µl BsaI enzyme (NEB, R3733S, 20000 U/ml) in a 20 µl reaction

containing 1X rCutSmart Buffer. The reaction was incubated at 37°C for 1 h in water bath followed by heat inactivation at 80°C for 20 min. The purification of digested vector and then ligation with gRNA was performed as described in section 2.13.3.

Seven μg of pCMV-BE4-max plasmid and 3 μg of pGL3-U6-BAIAP3-sgRNA-PGK-RFP-puromycin were transfected into RBL-2H3 cells. After 48 h of transfection, the cells were selected using 1.5 $\mu\text{g}/\text{ml}$ puromycin (concentration that killed all wild-type RBL cells). The cells were grown to confluency (~70%) and then electroporated again with same amount of plasmids as the first electroporation. The transfected cells were screened with 1.5 μg of puromycin. The second round of transfection was performed to increase the chance of base editing in both alleles to get a biallelic mutant. After the second round of puromycin enrichment, the single cells were transferred to a 24 well plate using the cloning discs. Single-cell dilution in a 96 well plate was also performed to screen many clones. From the clones, cell lysate was harvested (described in section 2.13.5). Two μl of cell lysate was used as a template in a 50 μl PCR reaction containing 1X OneTaqMM, 200 nM of forward (HXO_E89: 5' GGCTGAGGACTGGATG 3') and reverse primer (HXO_E90: 5' GACACACATACCACACC 3') to generate the RFLP amplicon. The PCR products were purified using wizard PCR Preps DNA Purification System (Promega, A2180) following manufacturer's instructions and further subjected to restriction enzyme digestion. A 20 μl reaction consisting of 100 ngs of RFLP amplicon, 1X NEB Buffer 3.1, 0.5 μl BstNI (NEB, R0268S, 10000 U/ml) was incubated at 60°C for 1 h. The digested product (20 μl) was run on 2% agarose gel, and the digestion in edited clones was compared with WT. The PCR product was sent for Sanger sequencing to verify the base modification. The potential clones were then expanded in a T-25 flask to

harvest lysates. The cells were lysed in 500 μ l RIPA buffer (as described in section 2.11) containing Pierce Protease Inhibitor Mini tablet (ThermoFisher, 88669) for immunoblotting with BAIAP3 antibody.

2.16 Isolation of primary mast cells

The isolation of primary mast cells was performed as described (Meurer et al., 2016; Vukman et al., 2014). The surgical procedures were performed in clean environment (USM animal facility). Peritoneal cell-derived mast cells (PCMC) or bone marrow-derived mast cells (BMMCs) were obtained from C57BL/6 mice of about 10-14 weeks old. PCMCs were obtained by injecting a 10 ml syringe into the abdominal cavity of mice containing 3 ml sterile PBS and 2 ml of air. The peritoneal cells were collected with a syringe, placed on ice, and then centrifuged at 1200 rpm at 4°C. The pellet was dissolved in 3 ml of Primary mast cell medium [RPMI 1640, 10% FBS, 1X Penicillin /Streptomycin (ATCC, 30-2300), 10 mM HEPES, 4 mM Glutamax, 50 μ M β -mercaptoethanol, 5 ng/ml Interleukin-3 (PeproTech, 213-13) and 10 ng/ml Stem cell factor (PeproTech, 250-03)]. Cells were cultured in one well in a 6 well plate at 37°C, 5% CO₂ for about a week.

BMMCs were obtained from the femurs of mice. The heads of the femur were cut with sterile scissor in sterile environment (culture hood) to leave the shaft intact, transferred to the flow tube, and then centrifuged at 1500 rpm for 10 min. The collected cells were cultured in a T-25 flask containing 8 ml of Primary mast cell medium as described above. For both types of cells, the medium was changed every 3-4 days by moving non-adherent cells into a new flask. During medium change, the cells were centrifuged at 150xg for 8 min at RT, and the cell pellet (BMMCs) was resuspended in 8

ml of medium and grown on a T-25 flask. PCMCs were resuspended in 3ml of medium and grown in a well in a 6 well plate. BMDC were cultured for 4-6 weeks until the culture was 90% mast cells as showed by Toluidine blue staining (1% Toluidine blue stock in 70% ethanol and 1% NaCl, pH 2.2 at 1:10 ratio).

2.16.1 Secretion of primary mast cells

Cells were counted in Invitrogen Countess II FL automated cell counter following manufacturer's instructions. About 5×10^5 cells were cultured in 24 well plates containing 500 μ l primary MC medium (as described above). For stimulation with IgE (described in section 2.7), anti-TNP mouse IgE was added to the cells for 24 h. Following incubation, cells were washed once with 1 ml of phenol red-free RPMI 1640 and then once with 1 ml of RPMI-BSA by centrifuging the cells at 150xg for 8 min at RT. Then cells were stimulated with 25 ng/ml TNP-BSA in 250 μ l of RPMI-BSA for 1 h. One μ M of Ionomycin or 1 μ M Ionomycin along with 20 nM PMA were added to the respective wells for 1 h. The control well received equal amount of DMSO. For LPS (Lipopolysaccharide) stimulation, cells were stimulated with varying concentrations (as indicated) of LPS from Escherichia coli (055: B5; Sigma-Aldrich; L6529), for 1 h at 37°C, 5% CO₂. Following incubation, supernatant and cell lysates were collected, and the β -hexosaminidase assay was performed by colorimetric assay (described in section 2.8.1). The mouse TNF was then quantified using Mouse TNF ELISA kit (BD Biosciences, 560478) following the manufacturer's instructions.

2.17 Data analysis

All data analysis is expressed as mean values of three or more biological replicates. Error bars represent standard deviations. Statistical significance between two

samples was determined by Students t-test. $p < 0.05$ was considered statistically significant. Data were analyzed with GraphPad prism 6.05 (Graph Pad Prism, La Jolla, USA) unless otherwise specified.

Table 2.1 *List of primers used*

Primer #	Name	Sequence (5'-3')	Vector
HXO_C80	M18b ^{T572D} -BamHI-F	CCCACATCCTCGATCCAAC CCGCTTCC	pFastBac HT-JS
HXO_C81	M18b ^{T572D} -SalI-R	GGA AGC GGG TTG GAT CGA GGA TGT GGG	pFastBac HT-JS
HXO_D13	Munc18c ^{Y521E} -BamHI-F	ATGGGATCCATGGCGCCG CCGGTATC	pFastBac HT-JS
HXO_D14	Munc18c ^{Y521E} -SalI-R	ACGC GTCGACTTA CTCATCCTTAAAGGAAAC	pFastBac HT-JS
HXO_E22	rVAMP3-gRNA-F	CACCGAGTCTTCGATTACT GCCAG	PX458
HXO_E23	rVAMP3-gRNA-R	AAACCTGGCAGTAATCGA AGACTC	PX458
HXO_E24	V3-gRNA-LHA-F	AAAACGACGGCCAGTGAA TTCCTGGCTTGAGCAATCC	HR target vector
HXO_E25	V3-gRNA-LHA-R	ATGTTTTGAGTGGAAAGAT CTCGAAGACTCCAGCAGA C	HR target vector
HXO_E26	V3-gRNA-RHA-F	GAAATAACCTAGATCGGA TCCGCACTGGACCCTGAA G	HR target vector
HXO_E27	V3-gRNA-RHA-R	GATTACGCCAAGCTTGCAT GTGCTTCAGACTTTGGTC	HR target vector
HXO_F30	rVAMP3-EcoRI-F	GGAATTCGCCACCATGTCT ACAGGGGTG	pLVX-IB-EmGFP
HXO_F31	rVAMP3-BamHI-R	CGGGATCCAGAGACACAC CACACA	pLVX-IB-EmGFP
HXO_E37	VAMP3-5F	GCTTCTACAAAGACCTGCC	
HXO_E38	VAMP3-3R	GCCACAGCAAAAAGGTCA C	
HXO_E41	5R HR-RFP-Puro	GGCCGCTGTCTAGATTTTT G	
HXO_E42	3F HR-RFP-Puro	TTAGGGCCCATTTGGTATGG C	
HXO_E89	RFLP-BAIAP3-BE-F	GGCTGAGGACTGGATG	

Table 2.1 (continued).

HXO_E90	RFLP-BAIAP3-BE-F	GACACACATACCACACC	
HXO_E91	rBAIAP3-gRNA-F	CCGGGCGACCAGGTAGAC GACGAGG	pGL3-U6-sgRNA- PGK-RFP-puro
HXO_E92	rBAIAP3-gRNA-R	AAACCCTCGTCGTCTACCT GGTCGC	pGL3-U6-sgRNA- PGK-RFP-puro

CHAPTER III – MUNC18 DEPENDENT MAST CELL EXOCYTOSIS

3.1 Characterizing wild-type and phosphomimetic mutant Munc18s in reconstituted degranulation assays

Mast cells exploit multiple sets of exocytic SNAREs to release mediators important in immunity, allergy, and inflammation. These SNAREs operate with specific Munc18 isoforms that undergo reversible phosphorylation in response to various physiological and pathological conditions. In this study, I investigated the activities of three Munc18 isoforms- Munc18a, Munc18b, and Munc18c in reconstituted fusion reactions. To characterize the site specific phosphorylation important in mast cells, the phosphorylation sites essential in other secretory cells such as- Munc18a^{S306/S313}, Munc18a^{T574}, Munc18b^{T572}, and Munc18c^{Y521} were tested in fusion reactions (Fletcher et al., 1999; Genç et al., 2014; Kioumourtzoglou et al., 2014; Liu et al., 2007). I investigated the activities of WT and phosphomimetic Munc18s proteins side by side to address two questions: i) do phosphomimetic mutations alter the specificity of Munc18s (selectivity of trans-SNARE complex formation), and ii) do phosphomimetic Munc18s change the activity of Munc18s (enhance/reduce the effects in fusion reactions).

As shown in (Fig.3.1 A, lane 11), Munc18b selectively stimulated VAMP8/syntaxin3/SNAP23-based lipid mixing reaction in a modest yet in a statistically significant fashion. Munc18b did not interact functionally with any other SNARE complexes tested (Fig.3.1 A, all lanes other than 11). In contrast, when Thr572 was substituted to Asp (D), the phosphomimetic Munc18b^{T572D} mutant did not stimulate any of the SNARE combinations tested (Fig.3.1 B). The phosphomimetic mutation abolished Munc18b's capability to promote V8/stx3/SNAP23-based reaction (Fig.3.1 B lane 11)

suggesting that this mutation may impair Munc18 b's interaction with individual SNARE or SNARE complex. The phosphorylation of Thr572 could potentially inactivate the cells' Munc18b dependent degranulation reactions.

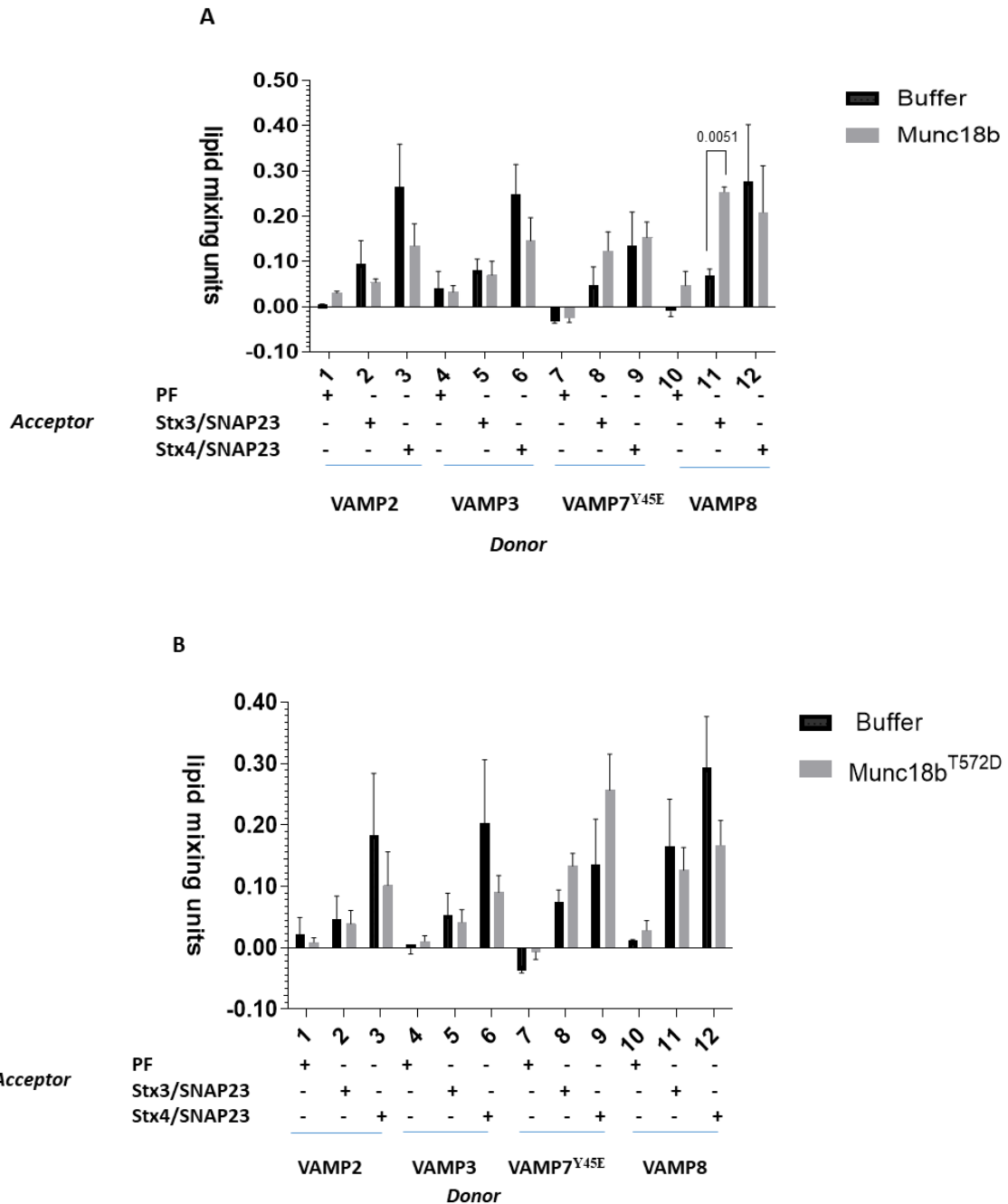
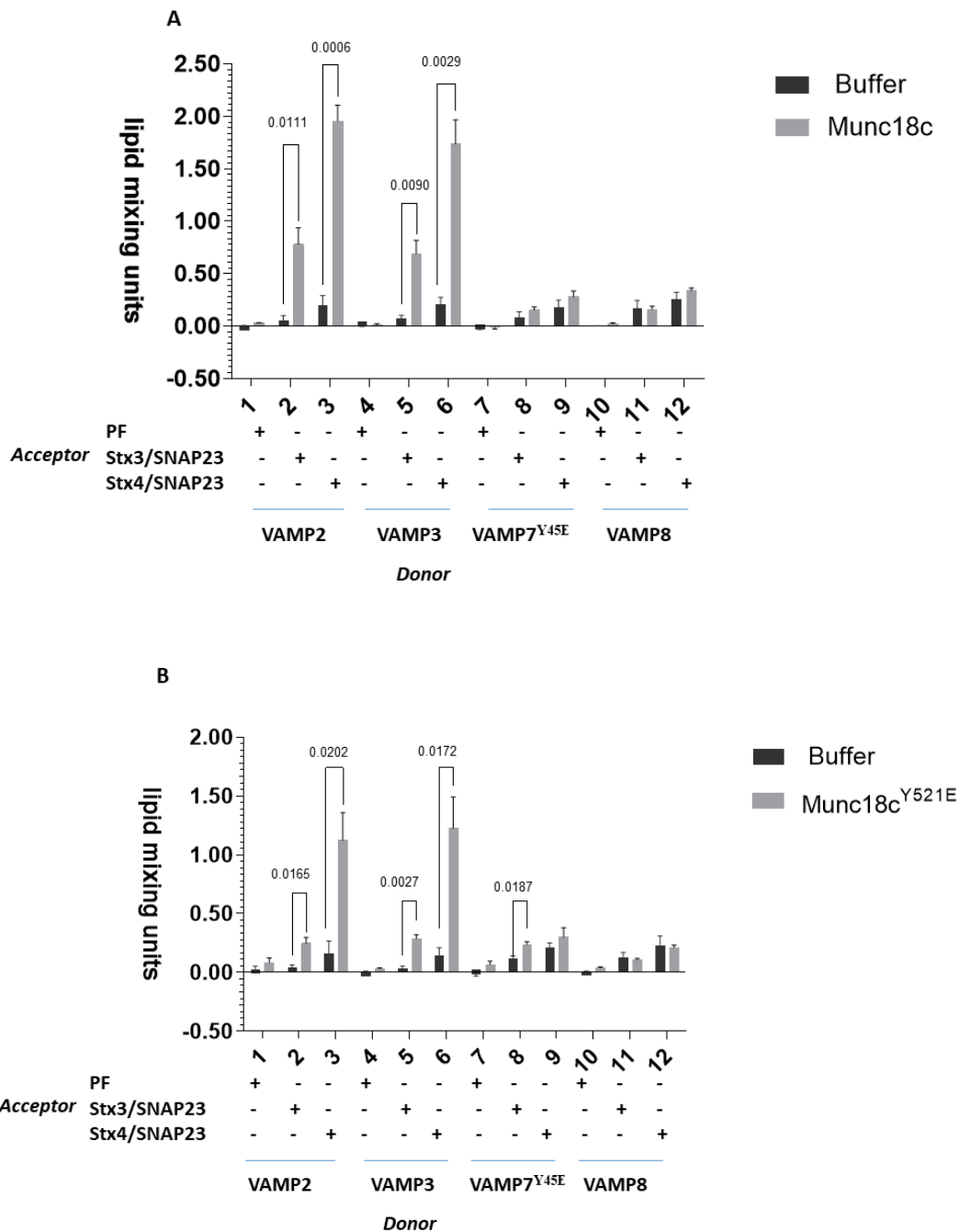


Figure 3.1 *Munc18b* based lipid mixing.

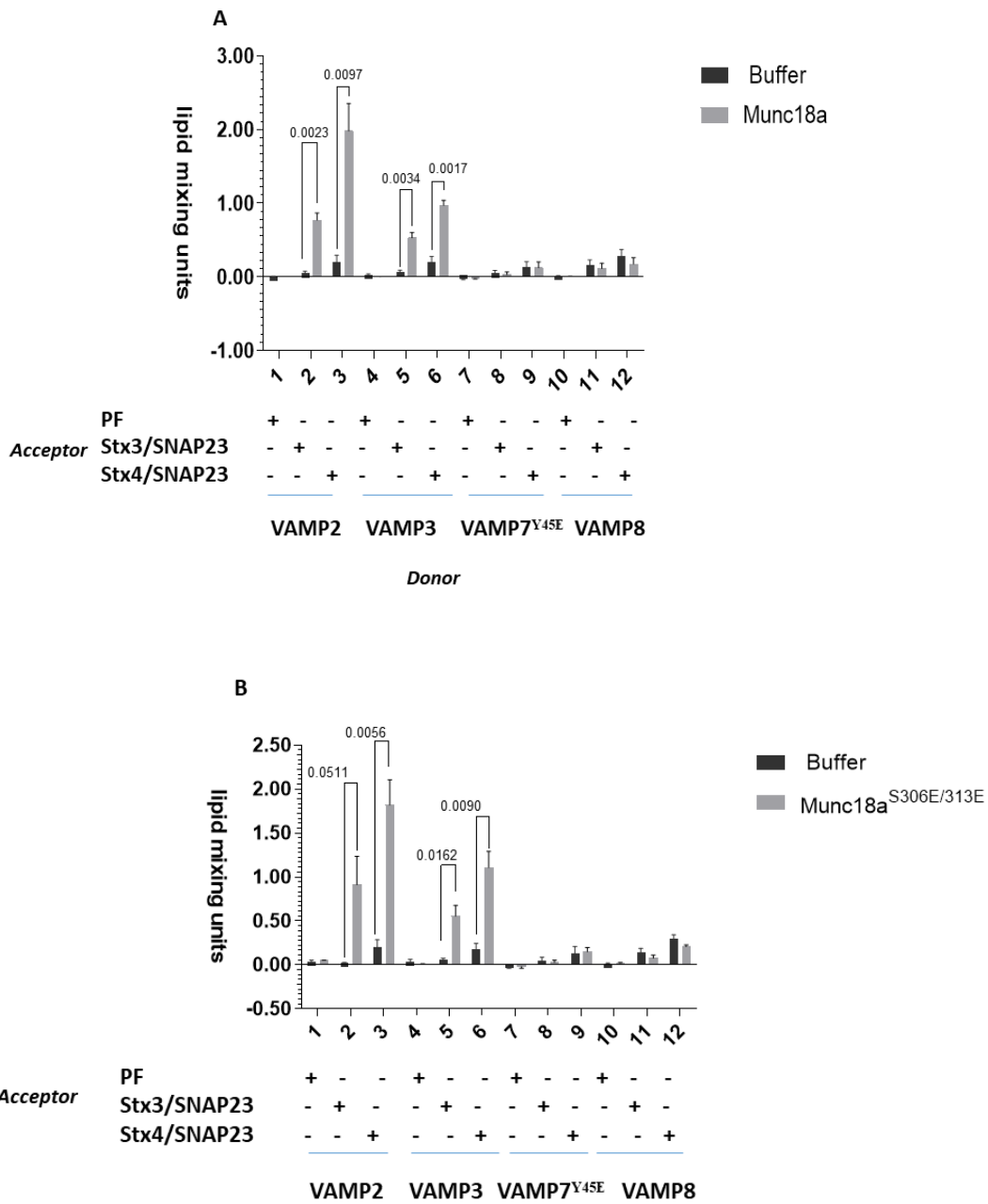
Various combinations of donor (50 μ M) and acceptor (400 μ M) reconstituted proteoliposomes as specified were incubated overnight at 4 $^{\circ}$ C in reconstitution buffer containing 75mM NaCl, 5 μ M of recombinant Munc18b or Munc18b T572D proteins or their respective buffer controls and lipid mixing read at 37 $^{\circ}$ C. Error bars represent standard deviations from 3 independent experiments. Students t-test was used to calculate p values. p<0.05 statistically significant.

Munc18c accelerated VAMP2 and VAMP3-based lipid mixing (Fig.3.2 A, lanes 1-6) in a similar fashion as previously observed by Xu et al., (2015) for Munc18a. This suggests there might be some functional redundancy in Munc18a and Munc18c. The activity of Munc18c was observed when the salt concentration in the reconstitution buffer was kept low, i.e., at RB75 (75mM). Similar Munc18c activity was reported by Yu et al., (2013) in VAMP2/syntaxin4/SNAP23-mediated GLUT4 translocation. This suggests that the activity of purified Munc18c protein may be affected by the concentration of salt (crowding effect) in the fusion buffer. Phosphomimetic Munc18c^{Y521E}, on the other hand, was also able to stimulate VAMP7^{Y45E}/syntaxin3/SNAP23 reaction at low but detectable levels (Fig.3.2 B, lane 8), suggesting the phosphorylation of Munc18c might facilitate phosphorylated VAMP7 trans-SNARE complex formation.



The reason of using phosphomimetic VAMP7 (i.e. VAMP7^{Y45E}) in all my reconstitution assays is because Xu et al. (2015) did not observe lipid mixing activity with reconstituted VAMP7 donor liposomes. VAMP7 is known to have an N-terminal longin domain that binds with the SNARE domain to form a self-inhibitory structure, preventing it from binding to other SNAREs (Vivona et al., 2010). Studies have shown that phosphorylation at Tyr45 of longin domain relieves this self-inhibition, and mimicking phosphorylation at Tyr45 enhanced exocytosis in insulin-treated cells (Burgoyne et al., 2013). Hence, donor liposomes with a phosphorylation mimic at Tyr45 of longin domain of VAMP7 were prepared and tested in fusion reactions.

Furthermore, to assess the functional impact of Munc18a phosphorylation in reconstitution degranulation reactions, I analyzed Munc18a phosphomimetic mutants if they alter the Munc18a's specificity (i.e., switching VAMP2- and VAMP3- based reactions to VAMP8-based reactions) and or its activity. The phosphorylation sites critical in neurotransmission, Munc18a^{S306/S313} (Genç et al., 2014), and Munc18a^{T574} (Fletcher et al., 1999) were studied. The phosphomimetic mutants- Munc18a^{S306E/S313E} and Munc18a^{T574E} had the same specificity as their wildtype (WT) counterparts and stimulated VAMP2 and VAMP3-based reactions (Fig.3.3, lanes 1-6). Like the WT Munc18a, neither of the Munc18a mutants promoted VAMP8-based lipid mixing (Fig.3.3, lane 11-12).



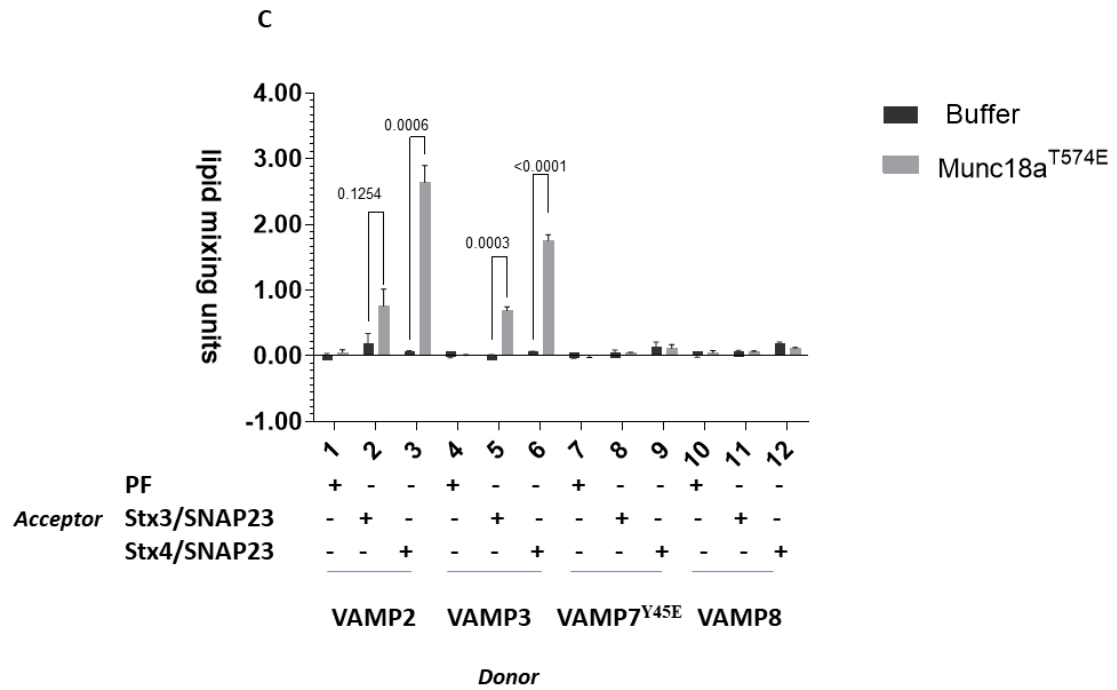


Figure 3.3 *Munc18a* based lipid mixing.

Donor (50 μ M) and acceptor (400 μ M) proteoliposomes as specified were added in a standard fusion reaction containing 75mM NaCl, 5 μ M of Munc18a WT (A) or Munc18a^{S306E/313E} (B) or Munc18a^{T574E} (C) or the respective buffer controls. Error bars represent standard deviation (n=3). p<0.05 is statistically significant.

These reconstitution data support the notion that there is some selective activity of Munc18s, and site-specific phosphorylation might regulate this function. The cell-based studies would reveal directly the phosphorylation sites important in stimulated mast cells.

3.2 PKC-dependent phosphorylation of Munc18a at Ser313 in activated RBL-2H3 cells

Based on the reported studies highlighting the importance of phosphorylation in Munc18 activity and Protein Kinase C (PKC) phosphorylation of Munc18a to be critical in neurotransmission (Genç et al., 2014), first I tested PKC inhibition in mast cells. A selective, cell-permeable PKC inhibitor Ro-32-0432 was used in RBL-2H3 cells-based secretion assay. At 5 μ M, Ro-32-0432 inhibited over 65% of β -hexosaminidase secretion from RBL-2H3 cells, and at 20 μ M, about 95% (Fig.3.4 A). Meanwhile, Ro-32-0432 does not interfere with either β -hexosaminidase activity or the enzymatic assay at the concentrations used (hatched column) (Fig.3.4 A).

I then investigated if PKC-dependent modification of Munc18a occurs in RBL-2H3 cells just as it does in neuronal cells and chromaffin cells (Barclay et al., 2003; Genç et al., 2014). To do so, I extracted proteins from resting and activated RBL-2H3 cells, with or without Ro-32-0432. Phosphorylated and non-phosphorylated proteins were separated into two fractions (Eluate and FT), and subject to SDS-PAGE and immunoblotting. While actins exist in unphosphorylated states regardless of the treatment, phosphorylated Munc18a at Ser313 was detected exclusively in activated RBL-2H3 cells (Fig.3.4 B), using anti-phospho-Munc18a (pSer313) raised against a phosphopeptide derived from Munc18a. The phospho-Munc18a band disappeared (middle panel) as expected, when the antibody had been pre-incubated with the phosphopeptide. Importantly, this phosphorylated Munc18a was not observed in RBL cells activated in the presence of Ro-32-0432, demonstrating that Munc18a phosphorylation at Ser313 in RBL cells is PKC dependent. These findings suggest that

PKC-dependent phosphorylation is a prevalent mechanism in activated RBL-2H3 cells and Munc18a at S313 is a conserved PKC phosphorylation site among secretory cells. The lipid mixing by Munc18a^{S306E/S313E} phosphomimetic mutant had similar activities like WT Munc18a (Fig.3.3 B) suggesting that additional PKC sites might be critical in mast cell function.

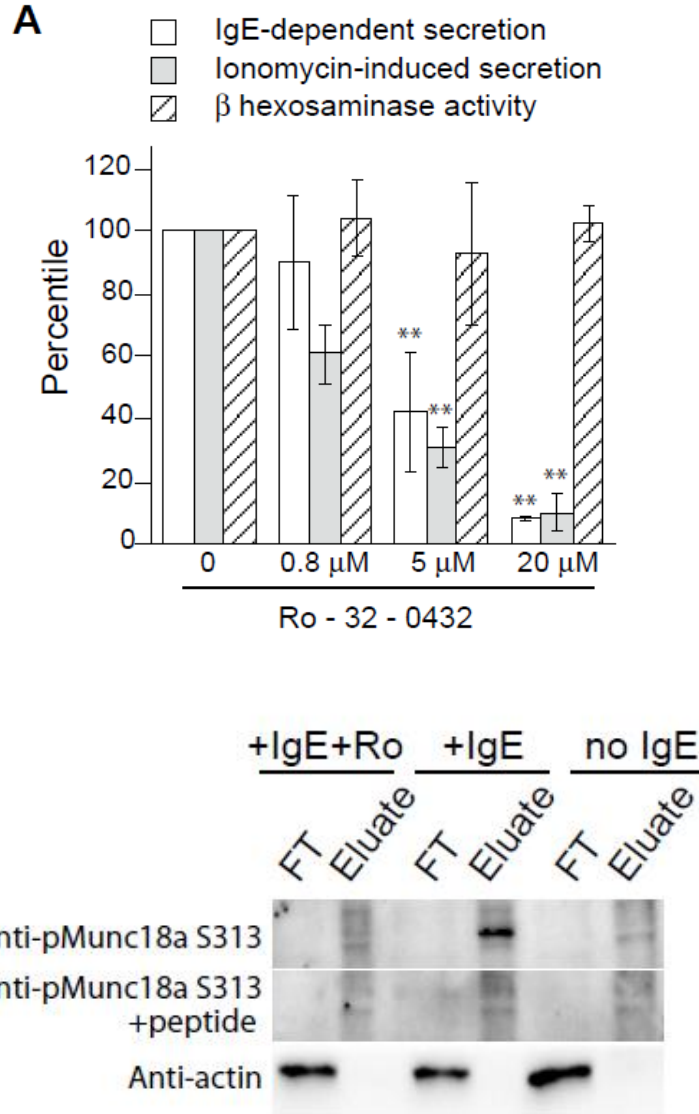


Figure 3.4 *PKC inhibitor prevents mast cell degranulation and Munc18a phosphorylation at Ser313.*

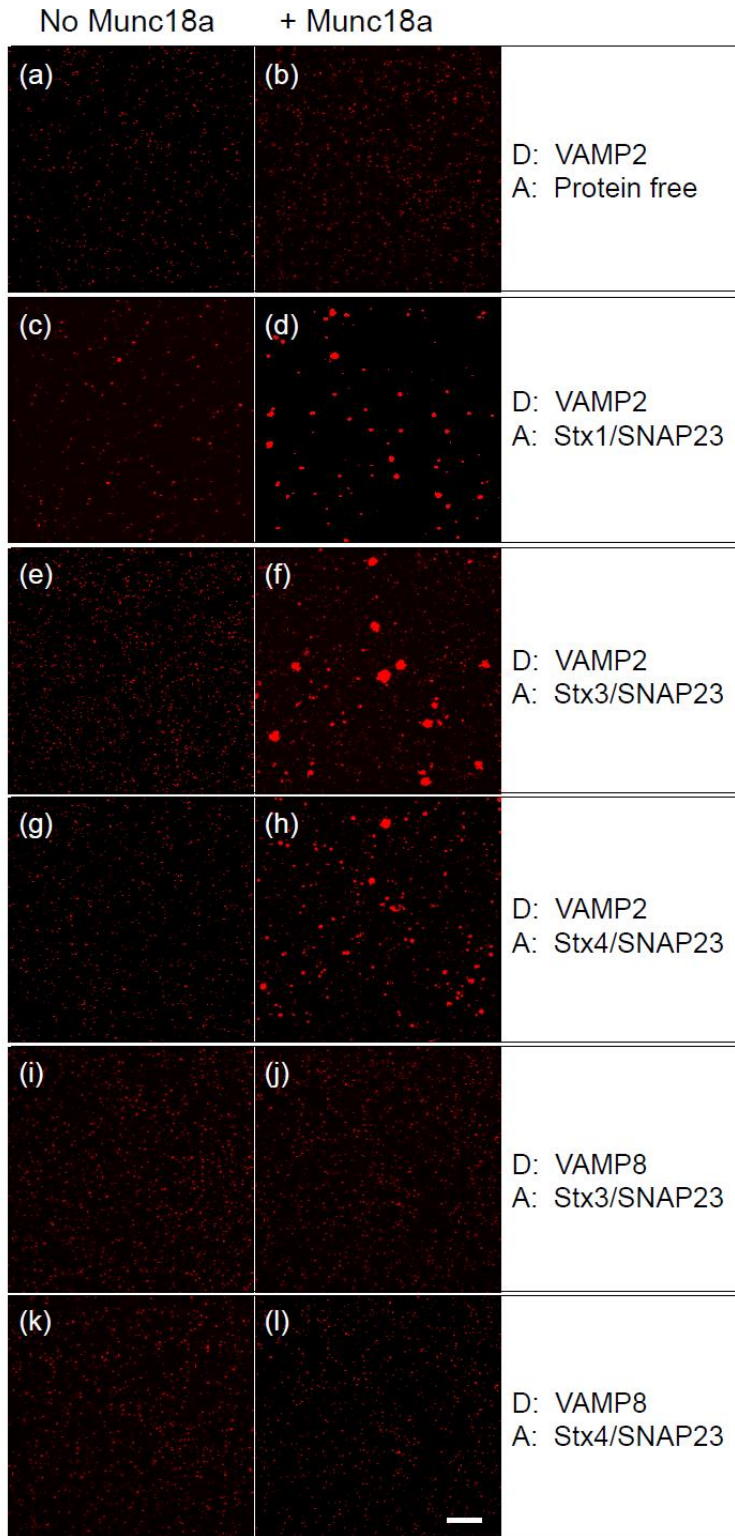
A) RBL-2H3 cells treated with Ro-32-0432 or DMSO were activated with either anti-TNP IgE/TNP-BSA (white columns) or ionomycin (gray columns) and then assayed for β -hexosaminidase release. The value of the DMSO-treated sample was set as 100% and used to determine the relative values of other conditions. Likewise, the effect of Ro-32-0432 on β -hexosaminidase activity was also measured and the values relative to the DMSO-treated sample were presented (hatched columns). Error bars indicate SD (n=3). Student t-test was used for statistical analysis. * means p<0.05; ** means p<0.01. B) RBL-2H3 cells incubated under specified conditions were lysed by CHAPS, with phosphorylated proteins and non-phosphorylated proteins separated into the FT (Flow-through) and the Eluate fractions. Two μ g of total protein from each fraction were used subsequently in SDS-PAGE and western blotting. The data is representative of 3 independent experiments.

3.3 Munc18a clusters SNARE-bearing liposomes prior to trans-SNARE zippering

Munc18 proteins are integral component of SNARE fusion machinery and required for the optimal fusion of their cognate SNARE pairs (Shen et al., 2007). Munc18 exhibit various binding modes and regulate the SNARE assembly and fusion (McNew, 2008). Accumulating evidence suggests the additional role of Munc18 protein in early steps of fusion cascade where Munc18 can bind simultaneously with Q- and R-SNAREs and facilitates SNARE complex assembly (priming) (Baker et al., 2016; Yu et al., 2013). With our observation that Munc18a can promote fusion of trans-SNARE complex formed by VAMP2/VAMP3 and Stx3/Stx4 and SNAP23, I decided to investigate the Munc18a function in membrane clustering underlying the vesicle docking during exocytosis. I examined if Munc18 could bring SNARE bearing membranes together in a condition when there was no fusion (on ice/4°C). When the donor proteoliposomes were incubated with SNARE-free acceptor liposomes, Munc18a had no impact on the cluster size distribution (Fig.3.5 B-box A, B). In contrast, when VAMP2-bearing liposomes were incubated with acceptor liposomes bearing any of the three Q-SNARE complexes (syntaxin1/SNAP25, syntaxin3/SNAP23, or syntaxin4/SNAP23), larger clusters were detected as long as Munc18a had been added (Fig.3.5 B-box C, E, G). The Munc18a effect on cluster size is specific to VAMP2 because replacing VAMP2 with VAMP8 in the donor liposome abolished the Munc18-dependent cluster size increase (Fig.3.5 B-box D, F, H) This VAMP2-specific clustering by Munc18a mirrors the reported lipid-mixing results (Shen et al., 2007; Xu et al., 2015), and suggests that unique motif(s) on VAMP2 might be responsible for direct interactions with Munc18a. All three Q-SNARE complexes (with different combinations of Qa- and Qbc- SNAREs) in my assay

supported Munc18a-dependent clustering. Inhibition of fusion and trans SNARE complex formation by soluble VAMP proteins did not interfere with Munc18a mediated tethering, indicating that Munc18a mediated tethering occurs prior to trans-SNARE complex formation as described in (Arnold, Adhikari, et al., 2017). These findings suggest the positive role of Munc18 in bringing the exocytic SNAREs closer together to for trans-SNARE complex formation that underlie physiological processes such as GLUT4s secretion and mast cell degranulation.

A



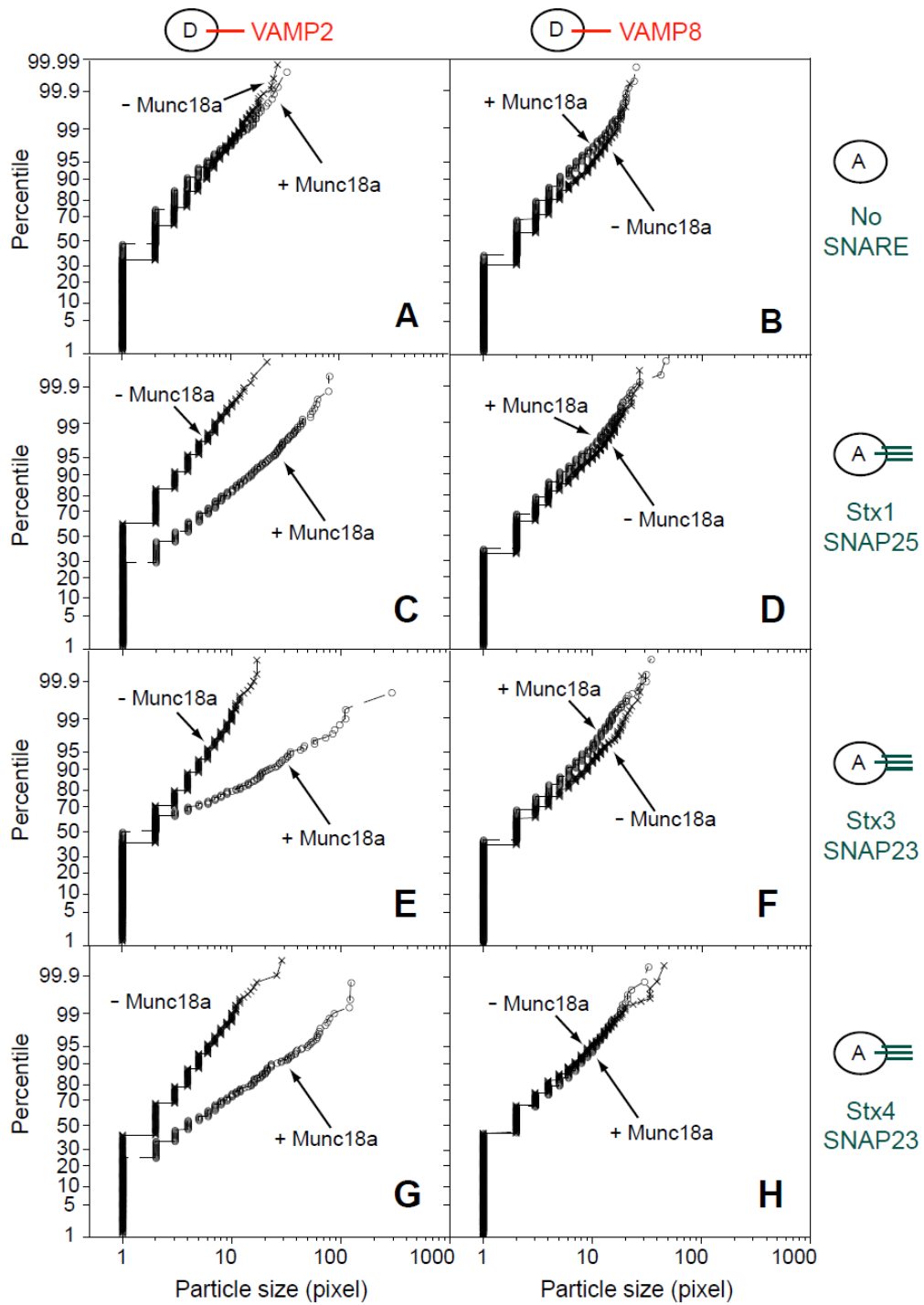
B

Figure 3.5 *Munc18a selectively promotes the clustering of SNARE-bearing proteoliposomes.*

As specified, donor and acceptor proteoliposomes were mixed in a 1:8 molar ratio, with either Munc18a or Munc18a buffer.

Following overnight incubation on ice, diluted samples were subject to confocal fluorescence microscopy. A) Original microscopic images used for cluster size measurement. The white bars equal 20 μ m. Particle sizes in four randomly collected images were measured and B) their cumulative distribution is presented. The Wilcoxon test indicates that the particle size distributions for the – Munc18a condition and the + Munc18 condition; are significantly different ($p < 0.001$). This experiment is a representative of 3 repeats.

CHAPTER IV – DELINEATING THE EXOCYTIC PATHWAYS OF MAST CELL
MEDIATORS

4.1 Differential release of RBL-2H3 mast cell mediators via VAMP homologs

The presence of multiple sets of SNAREs in mast cells suggests the presence of different exocytic events in mast cells. It is not clear if there is a differential requirement of the SNAREs in distinct mediator release. Here, I investigated the requirement of four vesicular SNAREs in secretion of mediators from RBL-2H3 cells. The reported VAMPs in mast cell degranulation from various studies include VAMP2, VAMP3, VAMP7, and VAMP8 (Lorentz et al., 2012). First the homology of the members of VAMP protein family in rat was determined (Fig.4.1 A). Based on the sequence similarity with conserved and similar residues colored, a phylogenetic tree was drawn (Fig.4.1 B). Based on homology and branches they occupy in the phylogenetic tree, VAMP2 and VAMP3 (which are primary neuronal VAMPs) were closely related, while VAMP7 and VAMP8 (major endolysosomal SNAREs) were close relatives.



Figure 4.1 *Sequence alignment of rat VAMPs.*

(A) Using the online Phylogeny.fr platform, the rat VAMP sequences were aligned. The conserved residues are colored. (B) Based on the alignment of the sequence, a phylogenetic tree was constructed.

To determine the expression level of the VAMPs as mentioned above in RBL-2H3 cells, I exploited antibodies specific for each VAMP homolog. As shown in (Fig. 4.2 A), MBP-tagged recombinant VAMP proteins were purified from bacterial lysates and used to confirm the specificity of the antibodies via immunoblotting. On immunoblots, the antibodies tested were specific to their target VAMP and sensitive enough to recognize as little as 10ngs of recombinant proteins (Fig.4.2 B). Using these antibodies, I then checked the expression of VAMP 2, 3, 7, and 8 in RBL-2H3 cell lysate (Fig.4.2 C). These are representative blots from 3 independent experiments. Each VAMP protein in RBL-2H3 cell lysate was quantified using densitometry from the respective VAMP immunoblots. The four exocytic v-SNAREs are expressed at a molar ratio of 17% (VAMP2): 25% (VAMP3): 18% (VAMP7): 40% (VAMP8) in RBL cell lysates (Fig.4.2 D).

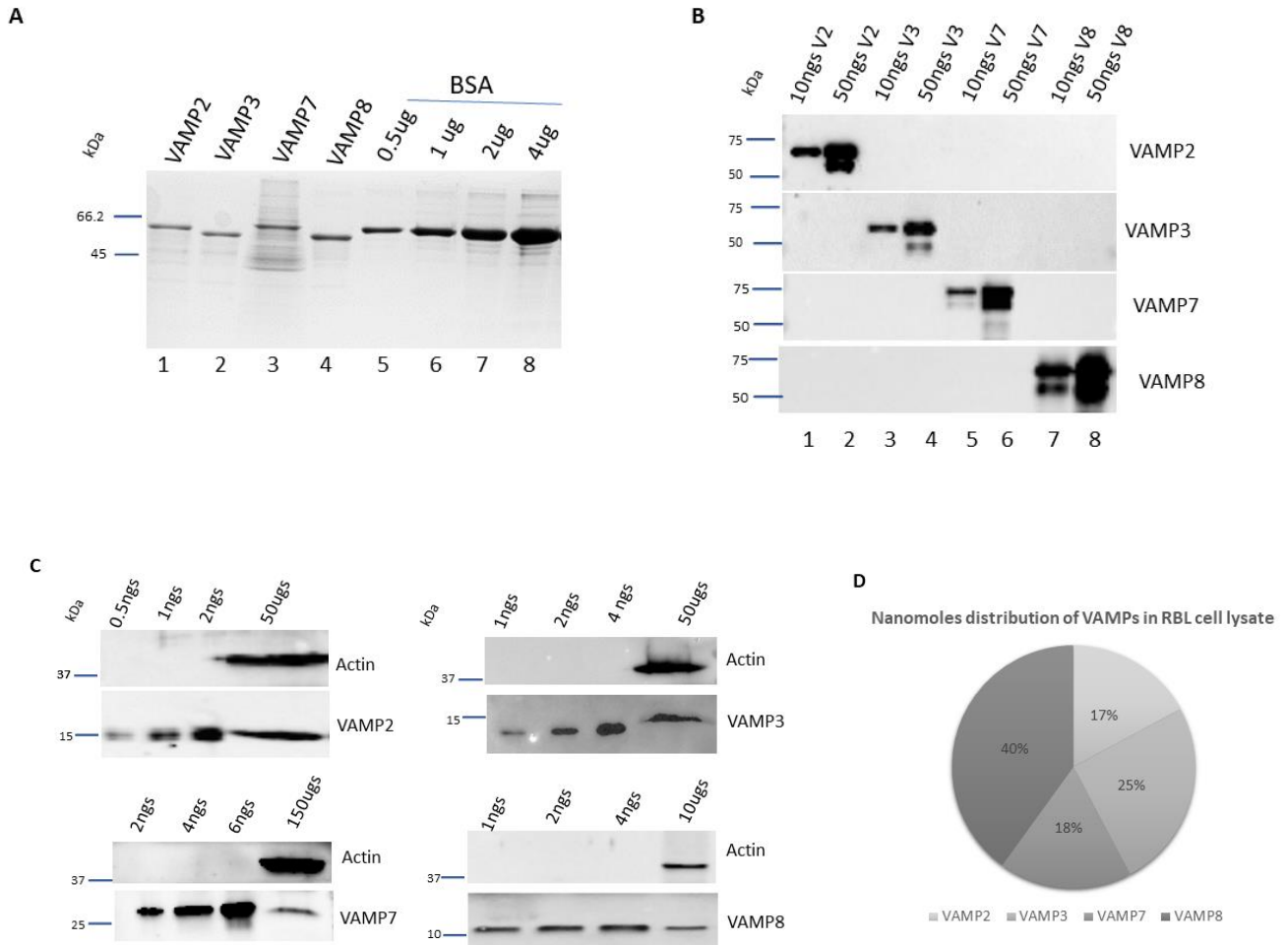


Figure 4.2 *Characterization of VAMPs in RBL-2H3 cell lysates using VAMP-specific antibodies.*

(A) Recombinant MBP-tagged VAMP proteins (0.5ug) were run along with a BSA standard on 15% SDS PAGE and the gel was subjected to Comassie Brilliant Blue R-250 staining. (B) Recombinant MBP-tagged VAMP proteins (10ngs and 50ngs) were run on 15% SDS PAGE gel and subjected to immunoblotting with respective VAMP2 (V2), VAMP3 (V3), VAMP7 (V7) and VAMP8 (V8) specific antibody. (C) Recombinant TEV cleaved VAMP proteins for specific blots at varying concentrations (as labelled) along with RBL-2H3 cell lysate (last lane for each blot) were run on 15% SDS PAGE gel. The blots were cut and subjected to immunoblotting with anti-actin and respective anti-VAMP specific antibodies. (D) Percentage distribution of nanomoles of each VAMP protein per microgram of RBL-2H3 cell lysate. Data presented are mean of 3 biological replicates.

To examine the roles of these four exocytic VAMPs in IgE/allergen-induced mast cell exocytosis, I used RNAi to deplete the expression of VAMP2, VAMP3, VAMP7, and VAMP8 respectively from RBL-2H3 cells. I then monitored the regulated release of

β -hexosaminidase, histamine, serotonin, and TNF from knockdown cells. Quantitative real-time PCR (qPCR) indicated that VAMP2 mRNA was reduced on average by 80%, VAMP3 by 85%, VAMP7 by 90%, and VAMP8 by 95% (Fig.4.3 A). Partial silencing of the expression of VAMP2, VAMP3, or VAMP7 does not seem to reduce IgE/allergen triggered mediator release (Fig.4.3 B-E, lanes 2-4). Inhibition of VAMP8 expression, on the other hand, significantly reduced the exocytosis of β -hexosaminidase, histamine, and serotonin without affecting TNF release (Fig.4.3, lane 5 in labels B-E). The selective effect of VAMP8 observed in RBL-2H3 cells corroborates findings in BMDCs isolated from VAMP8 KO mice (Tiwari et al., 2008), suggesting that TNF must exploit a different exocytic R-SNARE for release. It also implies that TNF is probably pre-stored in an intracellular compartment other than the classic secretory granules enriched with β -hexosaminidase, histamine, or serotonin.

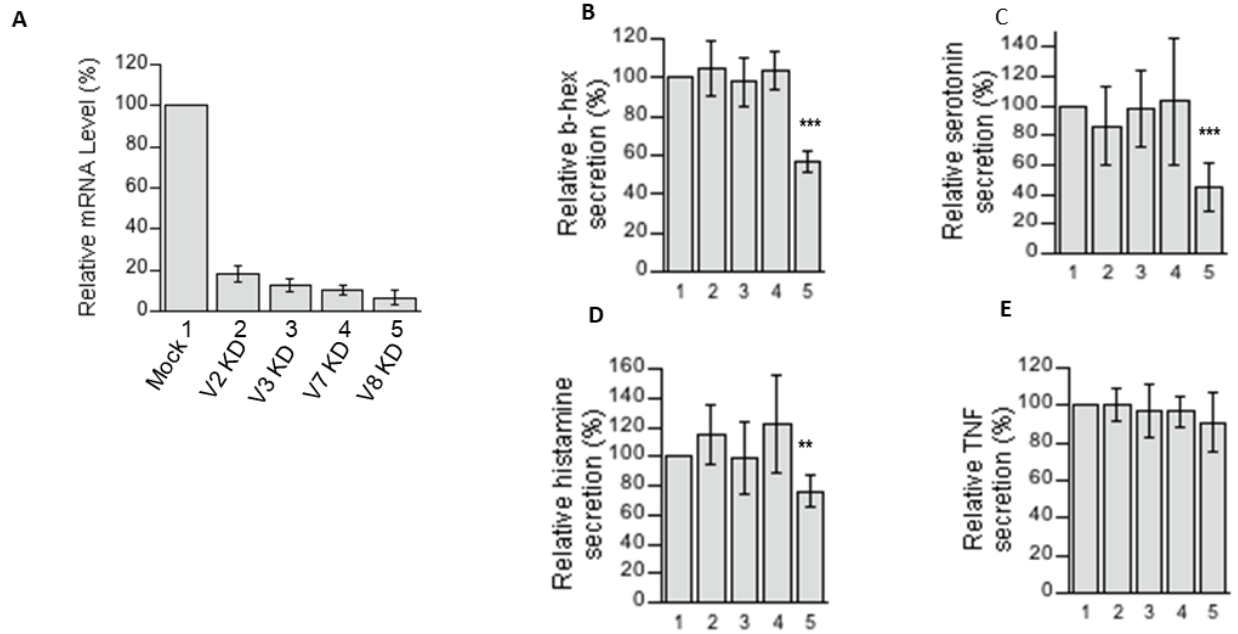


Figure 4.3 *Assessing the involvement of VAMPs in the differential release of mediators.*

(A) Verification of siRNA knockdown of VAMPs via qPCR. (B-E) Secretion of preformed mediators in siRNA treated RBL-2H3 cells. After 48 h post siRNA transfection, cells were sensitized with anti-TNP IgE and then stimulated with TNP-BSA for 1 h. (A) β -hexosaminidase activity was first measured in supernatants and lysates using a colorimetric enzyme assay. The β -hexosaminidase release was expressed as a percentage of the activity released into the medium relative to the total activity (released plus cell-associated). (C-D) The release of endogenous serotonin, histamine, and preformed TNF- α was determined as a percentage of the total amount in the supernatant and remaining in the cells using ELISA kits. Data from 6 independent experiments. $p < 0.05$ *; $p < 0.01$ **; $p < 0.001$ ***

4.2 Deciphering the role of VAMP3 in RBL-2H3 mast cell exocytosis

Because RNAi does not eliminate gene expression, my findings above do not rule out the possible involvement of any of the four VAMPs in TNF secretion. Colocalization studies suggest that TNF colocalized with VAMP3 positive compartment at plasma membrane in BMMCs however, its involvement in regulated release was not examined (Tiwari et al., 2008). Considering that VAMP3 has been shown to mediate TNF secretion in human synovial sarcoma cells (Boddul et al., 2014) and in phagocytosing macrophages (Murray et al., 2005), I went on to knock out VAMP3 from RBL-2H3 cells using Homology Directed Repair mediated CRISPR/Cas9 system.

HDR based CRISPR/Cas9 technology requires an exogenous homologous repair template that effectively induces desired and precise genome modifications (Ran et al., 2013). The guide RNA (gRNA) on exon 2 of the rat VAMP3 genome was targeted (the yellow highlighted region in Fig.4.4 A). The orange arrow indicates the double-strand break site (Fig.4.4 A). A plasmid-based donor repair template consisting of homology arms on each side (left homology arm and right homology arm) flanking the double strand break site was generated via PCR (Fig.4.4 B) and then cloned into the HDR vector (Fig.4.4 C). The resulting construct had a Red Fluorescent Protein (RFP) tag and a puromycin resistance marker between the two homology arms to insert these reporter genes in the edited cells.

(Fig.4.5 B).

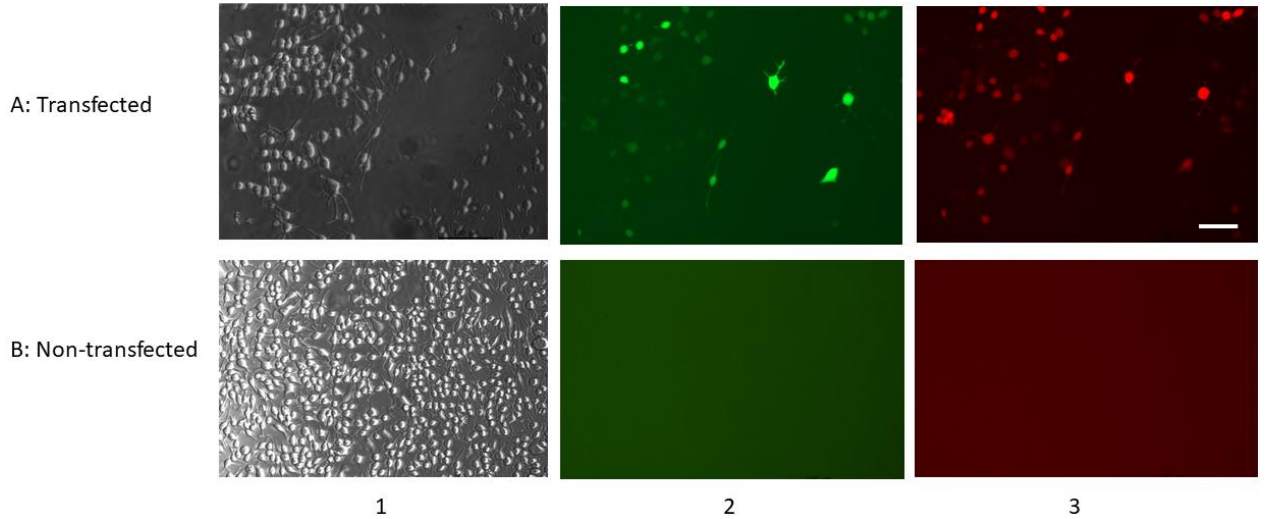


Figure 4.5 *Fluorescence microscopy of transfected cells.*

(A) 48 h post-electroporation, RBL cells were observed in fluorescence microscope under bright field (1), green (2) and red (3) fluorescent light at 20X objective. (B). As a control, the non-transfected cells were observed parallelly. White bar scale=100 μ m

The cells were further enriched with 3 μ g/ml of puromycin. In the edited cells, the RFP and puromycin marker would be inserted into the repaired site thus causing it to be stably expressing the fluorescence and resistance to the puromycin. The puromycin-resistant cells were isolated with the cloning discs so that a clonal population arising from single edited cell would be expanded in 24 well plate. Twenty-four such clones were then subjected for PCR to identify VAMP3 KO mutants.

PCR amplification was done using three sets of primers (5F, 5R; 3F, 3R and 5F, 3R) (Fig.4.6 A) to identify 5' integration, 3' integration, and modification of targeted sites respectively. PCR amplified targets on agarose gel showed that all clones via 5F and 3R primers amplification yielded a WT-like DNA band (Fig.4.6 B). Clone #17 and Clone #18 gave a shorter band than WT, hinting that it might be a deletion mutant that had undergone a NHEJ repair pathway. Then, with the 5F and 5R primers (Fig.4.6 C), Clones

#7, #16, #22, #24 gave a band for 5' integration band suggesting the integration of HDR vector in the genome, while the 3F and 3R did not show successful amplification (data not shown). Despite the latter, I moved on to further examine the positive hits obtained from gel analysis (Fig.4.6).

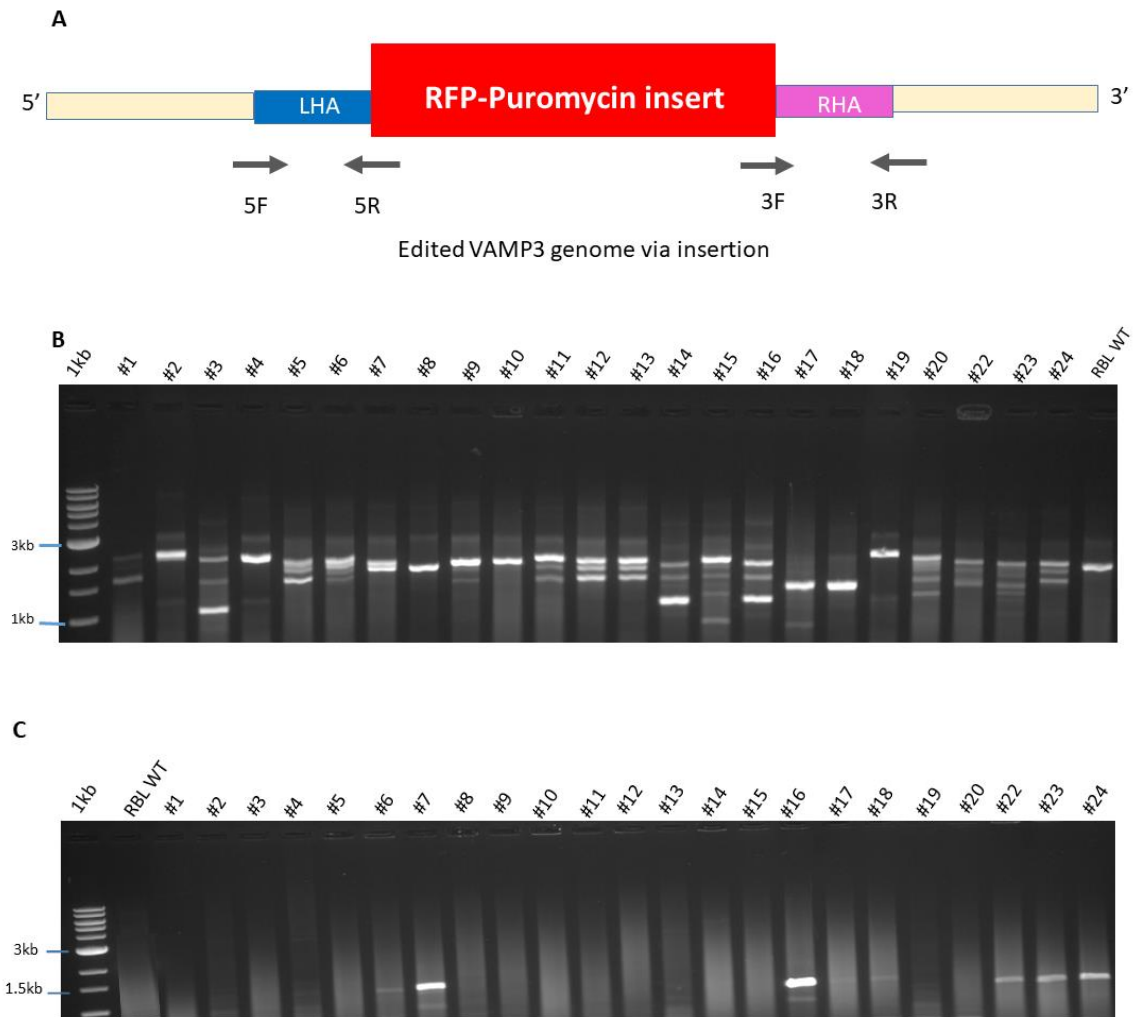


Figure 4.6 *PCR-based screening of CRISPR/Cas9 edited clones.*

(A) Strategy of PCR based screening of CRISPR-Cas9 clones where 3 sets of primers were designed for the amplification of edited clones. (B) PCR of clones with primer sets 5F and 3R that spans left to right of the edited site. (C) PCR of clones with primer sets 5F and 5R that amplifies the left side integration into the edited cells.

The potential edited (knockout) clones were expanded in a T-25 flask to harvest cell lysate for immunoblotting. As shown by immunoblotting (Fig.4.7), eight clones showed complete elimination of VAMP3 expression, suggesting they are biallelic KOs. Meanwhile, Clone #7 showed reduced VAMP3 protein expression compared to RBL controls suggesting it could be a monoallelic KO. The success of obtaining the biallelic knockout as determined by western blotting (Fig.4.7) was found to be 88%.

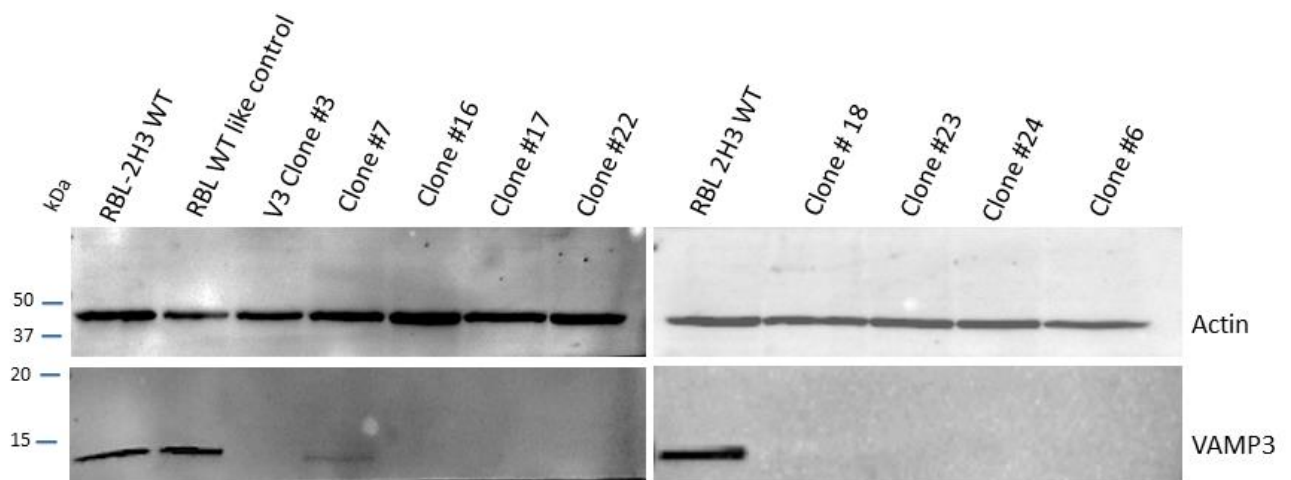


Figure 4.7 *Immunoblotting of WT and VAMP3 KO RBL-2H3 clones.*

50 micrograms of total cell lysate on each lane were run on 15% SDS PAGE gel. The blots were cut and subjected to immunoblotting with anti-actin (Santacruz; 1:100 dilution) and anti-VAMP3 antibody (Covalab, 1:500 dilution). The blots were developed in 1:1 Supersignal West Femto Maximum Sensitivity Substrate. First lane is precision plus protein standard. RBL WT like control is the clone screened on PCR that behaved like WT. Two blots are shown side by side to compare all the VAMP3 KO clones.

The biallelic knockouts verified on immunoblotting were further subjected to sequencing to confirm the genome editing. Clone #3, Clone #16, Clone #17, and Clone #18's PCR amplicons (as shown in Fig. 4.6) were sent for Sanger sequencing. The representative Sanger sequence view (Fig.4.8) is showing edited (upper chromatogram; Clone #16) and wildtype (lower chromatogram; WT control) sequences in the region around the guide sequence. In WT chromatogram guide RNA sequence (5'

GAGTCTTCGATTACTGCCAG 3') is underlined and vertical black dotted line is the cut site. Compared to the intact guide RNA sequence in control sample, the KO Clone #16 is different from the wildtype in having an insertion (extra C in 18th position) and 7 base modifications (represented by black arrows). This suggests that Clone #16 had undergone random insertions and base modifications around the cut site rather than precise insertion of homologous template via homologous recombination. NHEJ occurs in a higher frequency than HDR during DNA repair (Kuscu et al., 2017; Ran et al., 2013). These base modifications and insertion in VAMP3 genome would have induced the amino acid changes and potentially affected the protein function. Thus, a nonfunctional VAMP3 protein was not recognized in immunoblotting (Fig.4.7). The other clones sent for sequencing did not yield a clean sequence (a lot of N's in sequence); thus, I could not further analyze them.

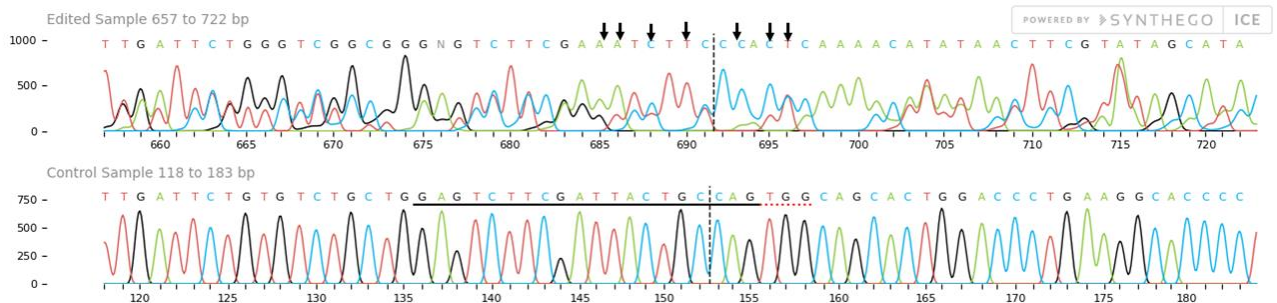


Figure 4.8 *Sequence analysis of edited clone.*

The target region of control and edited sample (clone #16) was amplified by PCR and analyzed by Sanger sequencing using Synthego's Inference of CRISPR Editing (ICE) web tool. Upper chromatogram is for edited clone while lower chromatogram represents RBL WT.

Clone #16 (a biallelic VAMP3 knockout clone) was further analyzed in secretion assay to assess the role of VAMP3 in RBL-2H3 mast cell exocytosis. Sensitizing the VAMP3 KO cells with IgE followed by subsequent stimulation with antigen for 30 min, I

observed an enhanced release of β -hexosaminidase (Fig.4.9 A); however, the release of acute TNF was unaffected compared to the wildtype control (Fig.4.9 B). To test if the newly synthesized TNF relies on VAMP3 for delayed, constitutive exocytosis, the cells were sensitized with IgE and stimulated with antigen for 24 h (instead of 30 min previously). No defect was observed in the secretion of newly synthesized TNF from VAMP3 KO cells (Fig.4.9 C, D). Monitoring the release of β -hexosaminidase at 24 h showed a slight increase; however, the difference was not statistically significant as observed for earlier time point (Fig 4.9, compare A and C).

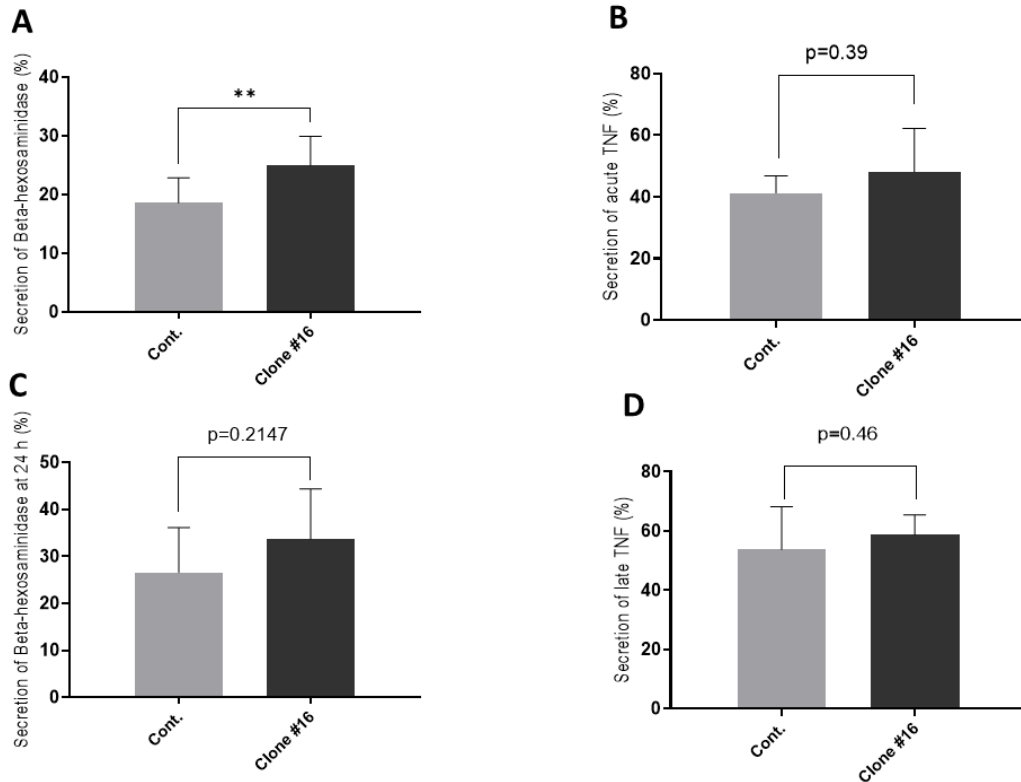


Figure 4.9 Analyzing VAMP3 KO clone in secretion assays.

Secretion analysis β -hexosaminidase (A and C), acute TNF (B) and late phase TNF (D). The WT RBL-2H3 (Cont.) and VAMP3 KO Clone#16 cells were sensitized with anti-TNP IgE and then stimulated with TNP-BSA for 30 min (acute TNF) or 24 h (for late TNF). Data from at least 4 independent experiments and p value calculated Student's t-test. Acceptable $p < 0.05$; ** means $p < 0.01$.

Since, knocking out VAMP3 did not affect the release TNF, I reasoned if other VAMP isoforms compensate for the loss of VAMP3. Hence, I performed immunoblotting to analyze any compensatory changes in the expression of other VAMPs in the absence of VAMP3. In mammalian and *Drosophila* cells, another R-SNARE, YKT6 was involved in vesicular secretion of newly synthesized proteins in association with VAMP3 in the siRNA studies (Gordon et al., 2017). Hence, the expression of YKT6 was also analyzed in VAMP3 KO cells. Knocking out VAMP3 did not increase expression of the other exocytic R-SNAREs, suggesting that the loss of VAMP3 is not compensated by the overexpression of any other R-SNAREs (Fig.4.10).

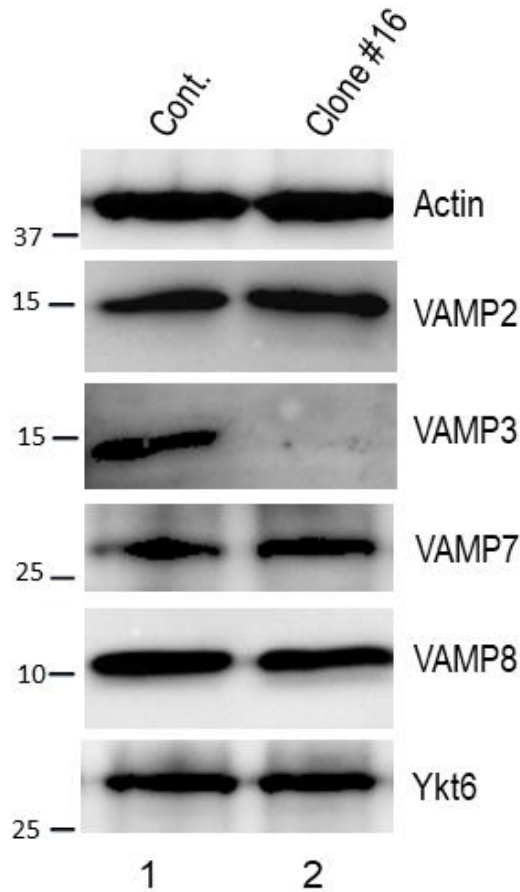


Figure 4.10 *Expression of R-SNAREs in VAMP3 KO RBL-2H3 cells.*

To observe compensatory modifications in the expression of other VAMPs in VAMP3 KO cells, immunoblot analyses for VAMP2, 7, 8 and YKT6 were performed in WT (lane 1) VAMP3 KO (lane 2) cell lysates. 100 micrograms of total cell lysate on each lane were run on 15% SDS PAGE gel. The blots were cut and subjected to immunoblotting with anti-actin or respective antibodies as labeled.

Next, I generated a VAMP3 expression construct cloned into a modified lentiviral pLVX-IRES-Blasticidin vector. The resulting construct would express a fused VAMP3-GFP protein and would serve two purposes i) it would be used to monitor colocalization of VAMP3 and TNF, and ii) it would rescue the VAMP3 knockout phenotypes. As evidenced by fluorescence microscopy, I generated a VAMP3-GFP expression construct that expressed a functional GFP fluorescence into transfected cells (Fig.4.11 A). In immunoblotting, lentivirus expressing VAMP3-GFP construct successfully reintroduced

VAMP3 into the KO clone (Fig.4.11 B, lane 3). The naked lentiviral vector itself did not induce any changes in protein expression (Fig.4.11 B, lane 1 and 2)

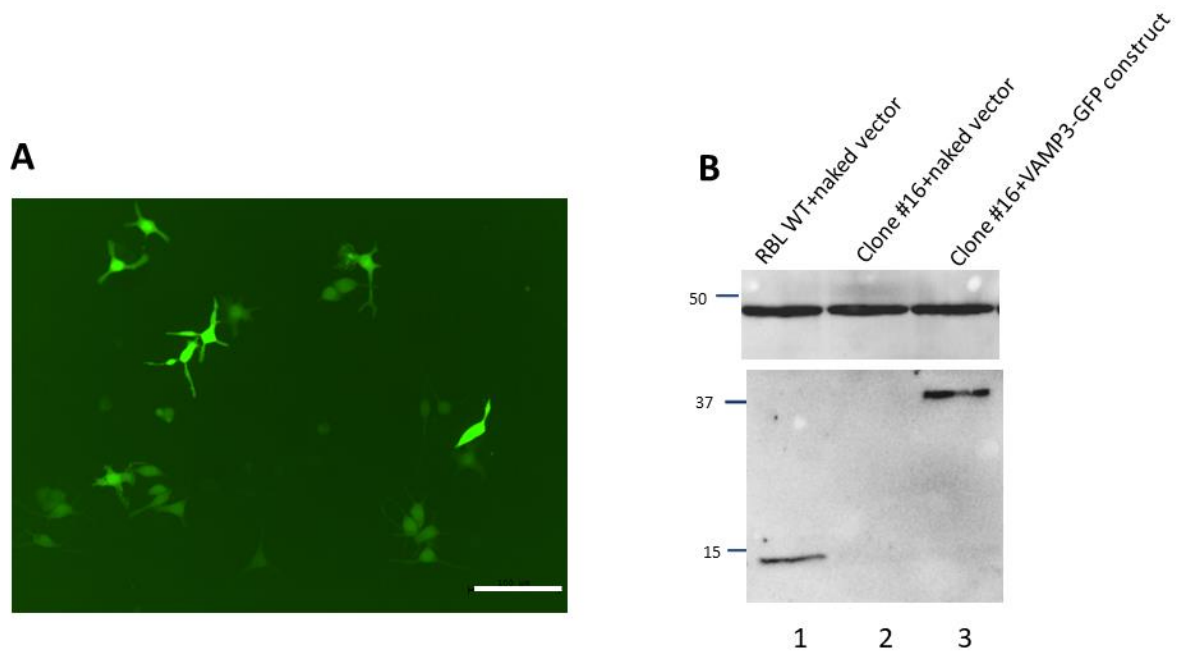


Figure 4.11 *Lentiviral mediated rescue of VAMP3 KO.*

(A) Fluorescence microscopy of transduced cells with VAMP3-GFP expression construct. (B) RBL WT and VAMP3 KO cells transduced with lentivirus containing naked GFP vector (lane 1 and 2) or VAMP3 KO cells transduced with lentivirus containing GFP fused VAMP3 (lane 3). Lane 3 showed the VAMP3 fused with GFP protein expression in lentivirus rescue cells. White bar scale=100 μ m

CHAPTER V – CHARACTERIZING BAIAP3 IN MAST CELL EXOCYTOSIS

We have recently shown that when Munc13-4 was knocked out in RBL-2H3 cells, it caused partial reduction of TNF secretion after IgE/antigen stimulation (Ayo et al., 2020), suggesting Munc13 group of protein play a critical role in the secretion of mediators from activated mast cells. Mast cells are known to express Munc13-1, Munc13-2, and Munc13-4 (Ayo et al., 2020; Higashio et al., 2017; Rodarte et al., 2018; Woo et al., 2017). BAIAP3 is a newly identified member of Munc13 group of proteins and the closest homolog of Munc13-4 (Fig.5.1 A). We also observed that in Munc13-4 KO cells, there is an increased (12 folds more) expression of BAIAP3 at mRNA level, suggesting the compensatory role of BAIAP3 in Munc13-4 KO cells (Fig.5.1 B). To elucidate the role of BAIAP3 in mast cell exocytosis, I decided to knock out the BAIAP3 in RBL 2H3 cells via CRISPR base editing.

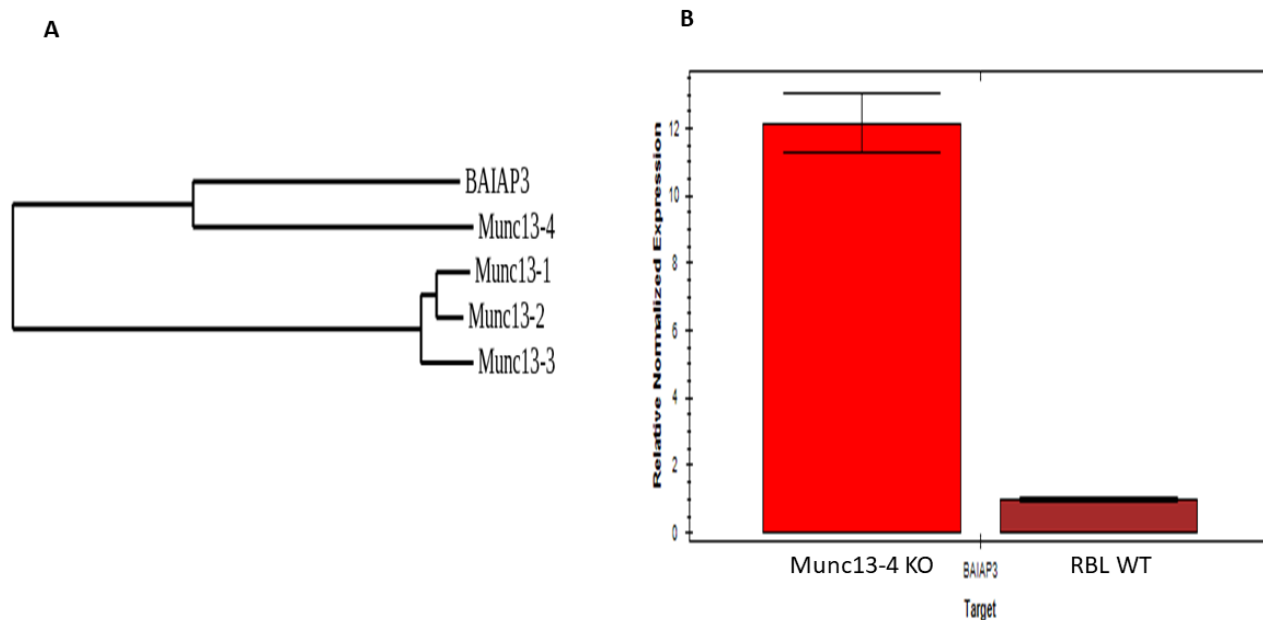


Figure 5.1 *Phylogeny of Munc13 proteins and expression of BAIAP3 in RBL-2H3 cells.*

(A) A phylogenetic tree based on the rat Munc13 group of proteins sequence alignment was constructed. (B) qPCR analysis of BAIAP3 in RBL WT and Munc13-4 KO RBL cells. Data is representative of 3 independent experiments. Error bars represent standard deviation.

CRISPR/Cas9 dependent base editing strategy precisely modifies C to T or G to A, so the codons like CAA, CAG, CGA, and TGG can be modified to stop codons. CRISPR based base editors comprise of a nicked/ deadCas9 which is not able to induce double strand breaks, a cytidine deaminase (called APOBEC) and a uracil glycosylase inhibitor (UGI) (Billon et al., 2017). I used an optimized BE4max cytidine base editor that converts C to T (Koblan et al., 2018). The base editor requires target C within the editing window of Protospacer adjacent motif (NGG) site. Hence, I first looked for BAIAP3 gRNA that have potential edit sites. Using benchling web tool, the gRNA (5' **CGACC**AGGTAGACGACGAGG 3') on exon 5 of rat BAIAP3 sequence was chosen (Fig.5.2). The gRNA has three Cs (highlighted in yellow) within the editing window. The

conversion of third C would change the nucleotide sequence CAG to TAG, which would prematurely stop the protein synthesis, forming a truncated BAIAP3.

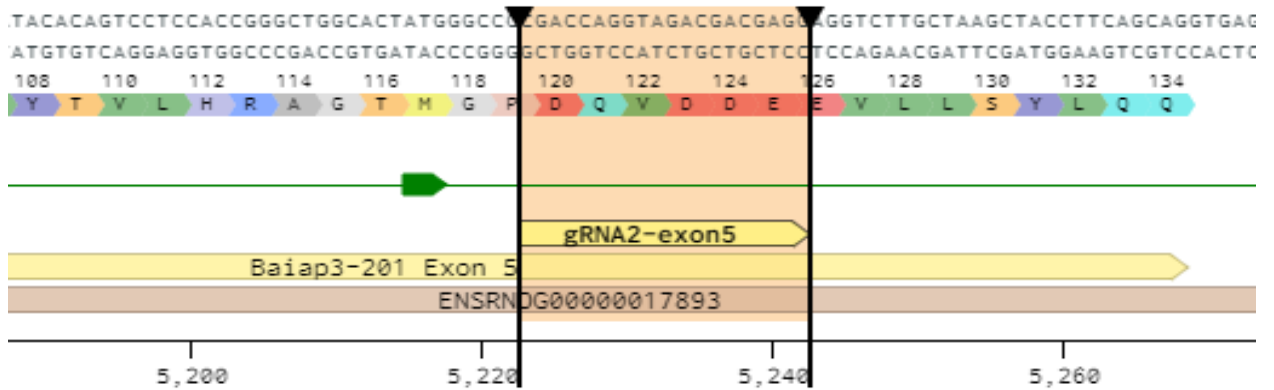


Figure 5.2 Gene structure and target sequence location of BAIAP3.

Using benchling web tool, the gRNA (20bp nucleotide) on exon 5 of rat BAIAP3 gene was selected for the base editing.

For the screening of base edited clones, the RFLP (restriction fragment length polymorphism) sites were identified to be BstNI and BfaI. Upon conversion of CAG to TAG, there would be either loss or gain of RFLP sites. Hence, each type of mutant would yield a characteristic DNA fragment (Fig.5.3). Because the loss of the BstNI site (Fig.5.3 A) prevents the restriction site from digesting the DNA, biallelic mutants will show one uncut DNA band, monoallelic will show three and WT will show two bands. The gain of sites (as for BfaI) would digest the biallelic mutant to produce two bands, the monoallelic mutant to produce three bands, and the WT to produce a single DNA band. to give two bands, monoallelic mutant three bands and WT will show as a single DNA band (Fig.5.3 B).

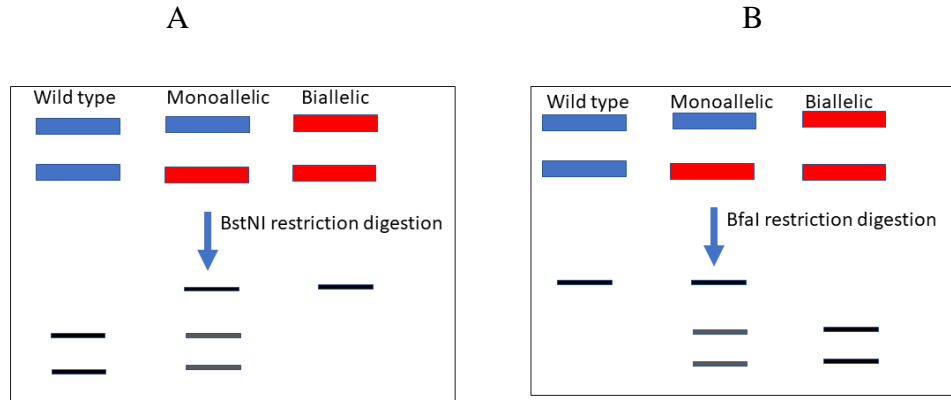
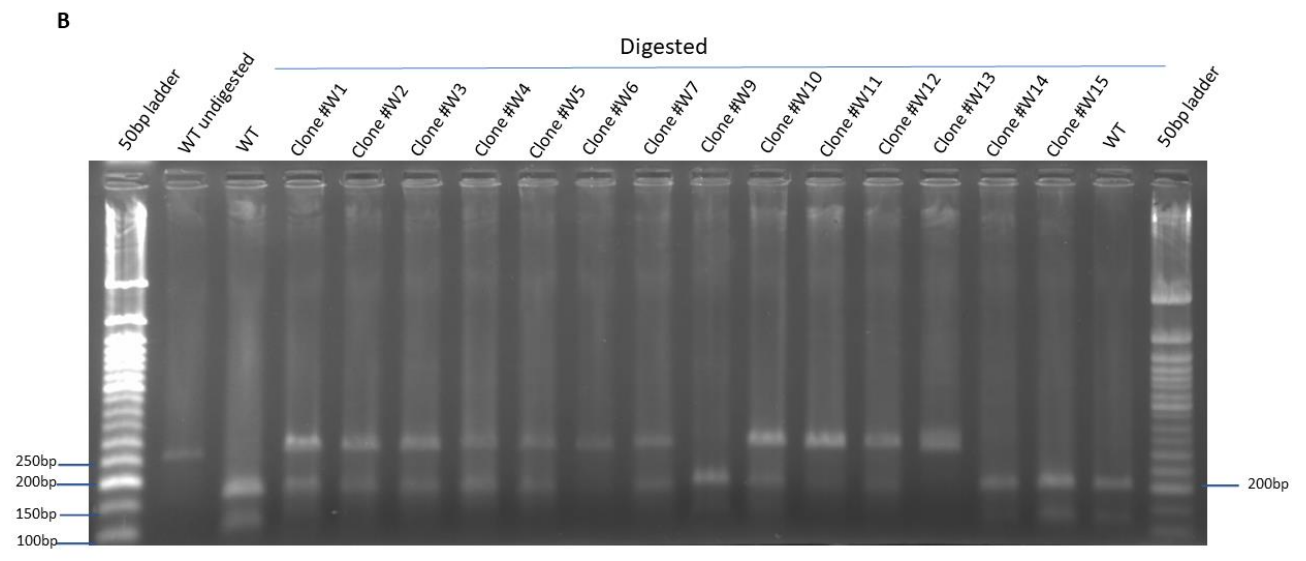
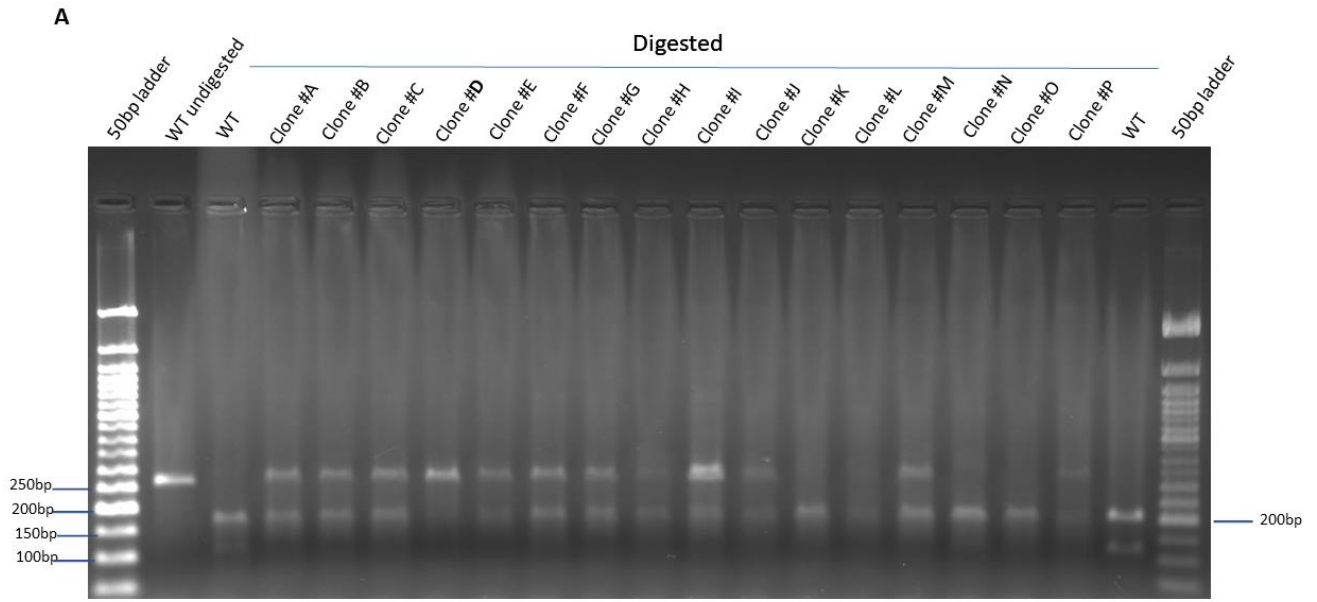


Figure 5.3 *Schematic representation of genotype determination of base edited clones by RFLP.*

(A) Loss of site in edited clones- BstNI enzyme cleavage. (B) Gain of site- BfaI enzyme cleavage. Lower black bands display DNA fragments after cleavage resolved on agarose gel.

Two successive rounds of base editing plasmid transfection were performed in the RBL-2H3 cells to enhance the efficiency of base modifications. The clones were further isolated by cloning discs on 24 well-plate or by single-cell dilution on a 96 well plate. The single isolated clones were then genotyped by amplifying the gene target by PCR. The amplicon was then digested by BstNI restriction enzyme. The product, when ran on 2% agarose gel, Clone #D showed one upper band comparable to the undigested WT band suggesting it to be a biallelic mutant (Fig.5.4 A). On the other hand, the other clones (A, B, C, E, F, G, H, I, J, M, P) showed an upper undigested WT-like band and lower digested WT-like band suggesting them to be monoallelic. The remaining clones (K, N, O) showed WT-like digested bands, suggesting unedited clones (Fig.5.4 A). The DNA fragments displayed by clones isolated from single cell dilution are shown in Fig.5.4 B. Clone W13 showed an upper undigested WT-like band, suggesting that it could be a biallelic mutant. However, upon reanalysis the Clone W13 showed the band pattern for monoallelic mutant (data not shown). This could have been result of mixture of clones in

W13 (WT, monoallelic or biallelic). Hence, I performed single cell dilution to isolate discrete clones. Of such, six clones were subjected to BstNI digestion and found that all six discrete clones showed the upper undigested and lower two digested bands, though at a varying intensity (Fig.5.4 C). The frequency of monoallelic mutants was highest among all analyzed clones suggesting the BE4 max base editor enzyme has high efficiency in generating the monoallelic mutants (~70%).



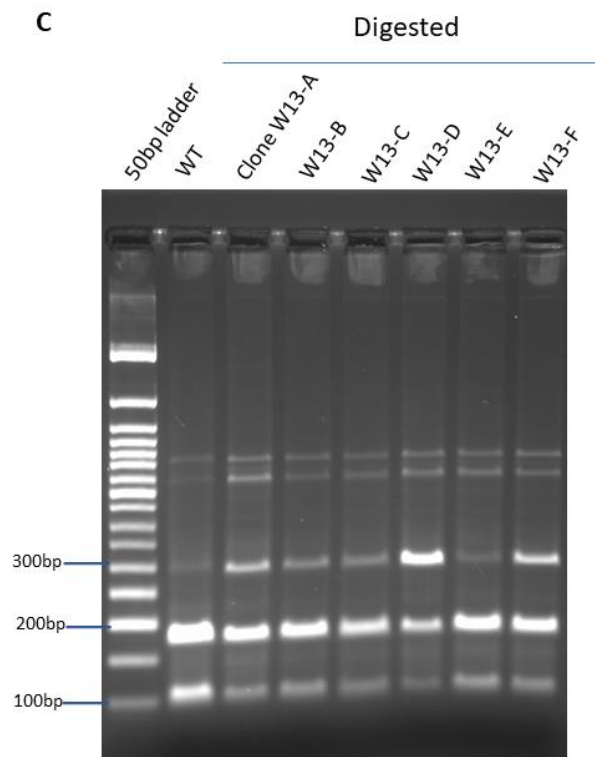


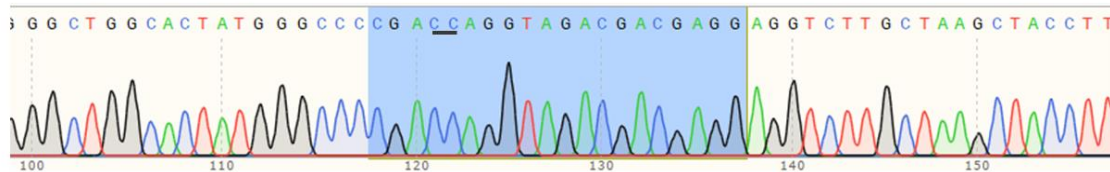
Figure 5.4 Target amplification and RFLP analysis of base edited clones.

(A) The clones isolated using cloning disc on 24 well plate. (B) Clones isolated from single cell dilution. (C) Clones isolated from single cell dilution of Clone W13. The cell lysate containing genomic DNA (from RBL WT or edited clones) was amplified via PCR and subjected to BstNI restriction digestion. The products were run on the 2% agarose gel along with 50 bp DNA ladder. Undigested wild type PCR product was ran as a control in A and B.

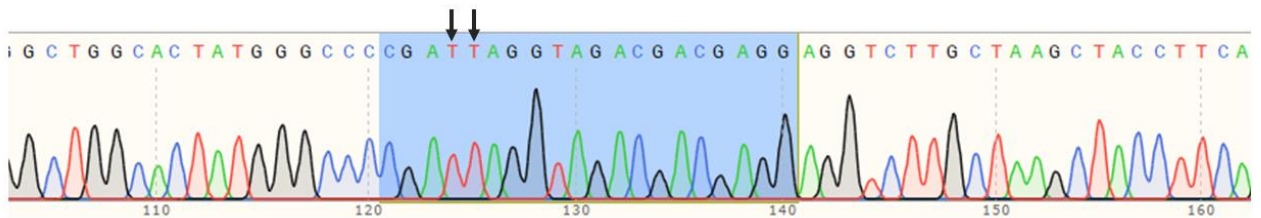
To validate the base change that occurred in Clone D and Clone W13; PCR was performed to amplify the target RFLP amplicon. The target amplicon was sent for Sanger sequencing. Upon sequence analysis, as compared to the wild type (Fig.5.5 A), there was indeed the base change in the Clone D (Fig.5.5 B), with two 'C's changed to 'T' within the editing window (represented by arrows). The chromatogram showed one peak of base at the edit site, confirming that it is a biallelic mutant. While Clone W13 showed two base peaks at the edit site, one allele had edits while the other allele was intact (Fig.5.5 C), suggesting it to be a heterozygous and a monoallelic mutant. Conversion of desired C

to T introduced a TAG stop codon into the BAIAP3 genome for Clone D which would prematurely truncate the BAIAP3 protein synthesis.

A. RBL WT



B. Clone D



C. Clone W13

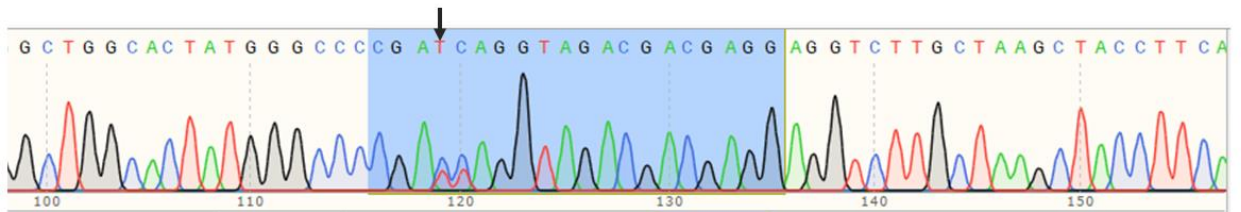


Figure 5.5 *Sequence analysis of base edited clones.*

The target region of control and edited sample was amplified by PCR and analyzed by Sanger sequencing. (A) Chromatogram of RBL wild type, (B) Clone D and (C) Clone W13 with gRNA region highlighted.

The base edited BAIAP3 (Clone D) was further analyzed in secretion assay. β -hexosaminidase was monitored as a degranulation marker and showed slight increase in β -hexosaminidase release than WT (Fig.5.6 A). TNF secretion seems to be affected by BAIAP3 deletion but is not statistically significant (Fig.5.6 B). More experimental

repeats of secretion and rescue with a BAIAP3 expression construct in future will further decipher the involvement of BAIAP3 in TNF secretion.

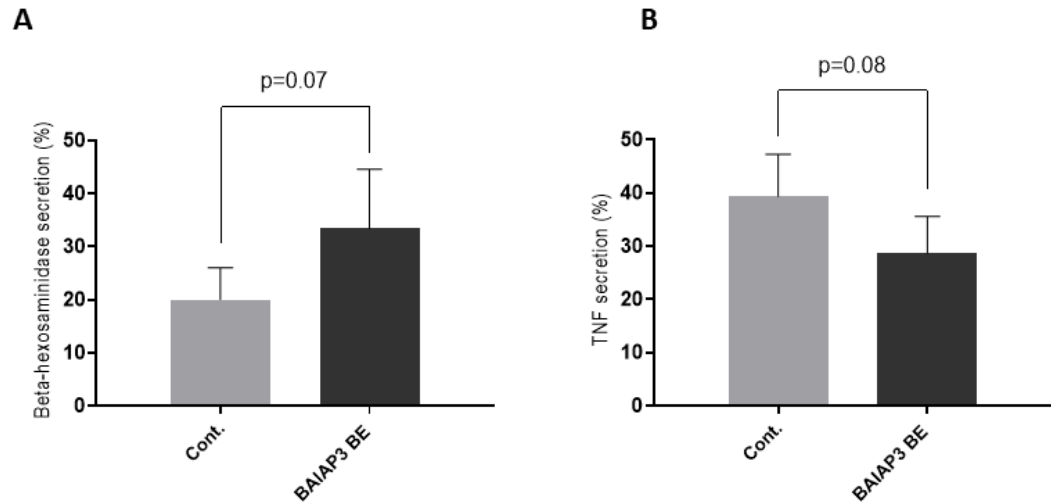


Figure 5.6 Analyzing BAIAP3 base edited clone in secretion assays.

Secretion of preformed β -hexosaminidase and TNF from IgE sensitized/ TNP-BSA stimulation. The WT RBL-2H3 (Cont.) and BAIAP3 biallelic base edited (BE) cells were sensitized with anti-TNP IgE and then stimulated with TNP-BSA for 30 min. Data from 4 independent experiments. p value <0.05 statistically significant.

To analyze the base edited knockout clone in immunoblotting, cell lysates were harvested from a T-25 flask. Due to the non-specificity of the available anti-BAIAP3 antibody, the loss of BAIAP3 protein was not detected (data not shown). To monitor if the loss of BAIAP3 protein would compensate the expression of other Munc13 proteins, immunoblotting for Munc13-1 expression was performed. There was no change in the expression of Munc13-1 in BAIAP3 base edited cells compared to WT control (Fig.5.7). The expression of Munc13-4 was also tested in immunoblotting; however, the Munc13-4 antibody did not detect the band at predicted molecular weight (data not shown) indicating that our Munc13-4 antibody has a low affinity due to sensitivity loss over time.

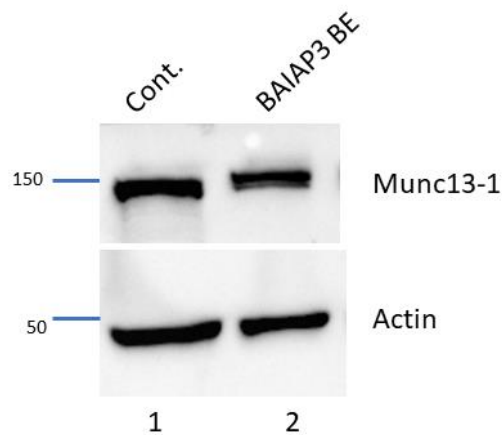


Figure 5.7 *Expression of Munc13-1 in BAIAP3 base edited clone.*

To observe if there is a change in the expression of other Munc13 in BAIAP3 base edited (BE) cells, immunoblot analyses for Munc13-1 was performed in WT (lane 1) and BAIAP3 base edited (BE) (lane 2) cell lysates. 15µg of total cell lysate on each lane were run on 12% SDS PAGE gel. The blot was cut and subjected to immunoblotting with anti-actin or Munc13-1 antibody.

These initial findings on the BAIAP3 base edited cells serve as a basis for future investigations underlying the essential role of Munc13 proteins in differential regulation of mast cell exocytosis.

CHAPTER VI – DISCUSSION

6.1 Munc18s in mast cell exocytosis

The specificity of the secretory pathway involves the specific interaction of SNAREs with their cognate Munc18 proteins (Shen et al., 2007). The presence of multiple sets of exocytic SNAREs and three Munc18 proteins in mast cells suggests there are diverse exocytosis in these cells. My reconstitution data shows that Munc18c (Fig.3.2 A) has the same specificity as Munc18a (Fig.3.3 A) and promoted VAMP2 and VAMP3 based lipid mixing. Meanwhile, Munc18b modestly activated the VAMP8/syntaxin3/SNAP23-dependent fusion reaction (Fig.3.1 A). This indicates differential effects of Munc18 proteins in achieving the specificity of fusion underlying the differential mediator release. There may be functional redundancy in Munc18a and Munc18c, while the function of Munc18b may be distinct.

VAMP8 is required for the release of β -hexosaminidase. The effect of loss of VAMP8 was not absolute and only partially inhibited β -hexosaminidase (Puri & Roche, 2008; Tiwari et al., 2008), suggesting additional VAMP may be functional. Tiwari et al., (2009) observed that in the absence of VAMP8, there was an enhanced SNARE complex formation by VAMP2 and VAMP3, indicating some compensatory effect. Based on the positive role of Munc18a in RBL-2H3 exocytosis (Bin et al., 2013), my reconstitution data (Fig.3.3 A), and previous observation by Xu et al., (2015) for Munc18a, I speculate that in the events where VAMP8-dependent degranulation is compromised, VAMP2 and VAMP3 based trans-SNARE complexes might form an association with Munc18a and Munc18c in mast cells. This distinct set of trans-SNARE complex may be required for a small unique secretion such as piecemeal exocytosis rather than the evident immediate

degranulation. This correlates with Gutierrez et al., (2018) observation, where Munc18b was reported to be the only Munc18 isoform mediating anaphylactic response, while Munc18a and Munc18c deficient mature mast cells did not show any defect.

VAMP8/syntaxin4/SNAP23 is the best characterized trans-SNARE complex for the release of β -hexosaminidase release from the mast cells (Lorentz et al., 2012; Puri & Roche, 2008; Tiwari et al., 2008). Intriguingly, in reconstitution, none of the Munc18 isoforms promoted VAMP8/syntaxin4/SNAP23 based membrane fusion, which led me to the notion that Munc18s might receive post-translation modifications to activate the fusion machinery. Numerous studies have suggested that Munc18s are phosphorylated, which modifies their activity in various secretory cells. (Genç et al., 2014; Kioumourtzoglou et al., 2014; Liu et al., 2007). PKC-dependent phosphorylation of Munc18a at serine residues 306 and 313 enhanced neurotransmitter release (Genç et al., 2014). In neuroendocrine cells, phosphorylation of Munc18a at threonine 574 residue by CDK5 enhanced secretion (Fletcher et al., 1999). CDK5 mediated Munc18b phosphorylation at threonine 572 promoted gastric acid secretion in epithelial cells (Liu et al., 2007). Insulin-dependent phosphorylation of Munc18c at tyrosine 521 residue facilitated the delivery of GLUT4 to the cell surface in fat muscle cells (Kioumourtzoglou et al., 2014). As a starting point for further investigation into the phosphorylation-dependent regulation of mast cell exocytosis, I tested all these known phosphorylation sites (phosphomimetic mutants of Munc18a, b, and c) in reconstitution.

The tested phosphomimetic mutants- Munc18a^{S306E/313E} (Fig.3.3 B) and Munc18a^{T574E} (Fig.3.3 C) had activity just like WT Munc18a (Fig.3.3 A), suggesting that these phosphorylation events are either irrelevant in mast cells or affect Munc18a

interaction with SNARE-independent partners in the fusion reactions. The PKC targets S306 and S313 in Munc18a are located in domain 3a in the region that undergoes conformational change to promote trans-SNARE zippering and activation (Baker et al., 2015; Hu et al., 2011). There are additional phosphorylation sites predicted in Munc18a at this domain (Fig.1.5), and these may be important for mast cell functioning. However, this needs future investigations. The C-terminal Thr572 on domain D2 serves as a syntaxin3 binding site, and CDK5 phosphorylation of T572 weakens the Munc18b-syntaxin3 interaction and promotes complex formation with SNAP25 (Liu et al., 2007). In contrast, Munc18b^{T572D} did not stimulate any fusion reactions and abolished the lipid mixing signal of Munc18b/VAMP8/Stx3/SNAP23 (Fig.3.1 B). As unmodified VAMP8, Munc18b, and syntaxin3 are essential components for mast cell exocytosis (Gutierrez et al., 2018; Puri & Roche, 2008; Sanchez et al., 2019; Tiwari et al., 2008), this Munc18b phosphorylation site may not be necessary for mast cells. It may have inactivated the degranulation machinery by inducing conformational changes that alter the interaction with syntaxin3, and its subsequent interaction with other SNAREs. However, these await future investigations. In future, WT Munc18b, phosphomimetic (Munc18b^{T572E}), and phosphoresistant mutants (Munc18b^{T572A}) expression constructs can be expressed into the Munc18b KD RBL-2H3 cells via lentivirus transduction. The secretion of mediators can be monitored from the activated lentivirus transduced cells. If these sites have functional relevance (i.e., inhibition of degranulation machinery), phosphomimetic mutations would inhibit the secretion while phosphoresistant mutants would restore the defect as it cannot be phosphorylated.

Munc18c^{Y521E} promoted VAMP7^{Y45E}/Stx3/SNAP23 lipid mixing to some extent (Fig.3.2 B); however, the difference is minimal to pinpoint any physiological relevance. The WT and phosphomimetic mutant Munc18c activate the VAMP2 and VAMP3 dependent lipid mixing reactions similarly (Fig.3.2). More experimental repeats in the future would reveal if WT Munc18c would stimulate the VAMP7^{Y45E} based response to a statistically significant extent. VAMP7 is essential for histamine release in human mast cells (Sander et al., 2008). Using the VAMP7^{Y45P} antibody, we observed that VAMP7 is always phosphorylated in resting and activated RBL-2H3 cells, suggesting that the longin domain's inhibition is minimal and can easily form trans-SNARE complexes. This SNARE complex may be required explicitly for distinct mediator release in RBL-2H3 cells. Moreover, the low lipid mixing for VAMP7^{Y45E} based reaction (Fig.3.2, lanes 8 and 9) suggests that this SNARE may require conditions in reconstitution that enhance artificial tethering. In reconstitution studies, agents such as Polyethylene glycol (PEG) have been used to promote tethering and bring the liposomes together to increase the rate of lipid mixing (Dennison et al., 2006). Xu et al., (2015) observed an enhanced SNARE-mediated lipid mixing when 4% PEG was added to the SNARE-dependent fusion reaction. This may be a starting PEG concentration to be tested in the future. The incorporation of molecular crowding agents may precisely recapitulate the physiological membrane fusion invitro and drive efficient membrane fusion (Yu et al., 2015).

Intriguingly, Munc18s or phosphomimetic Munc18 mutants did not activate VAMP8/syntaxin4/SNAP23-based fusion reaction, which are the three SNAREs underscoring the release of β -hexosaminidase in cultured cells (Lorentz et al., 2012; Puri & Roche, 2008; Tiwari et al., 2008). This has raised the possibility that VAMP8 might

require SM proteins other than Munc18s to be activated. VAMP8 has been implicated in endolysosomal fusion, and it is possible that mast cells, which is a secretory lysosome, might require additional SM proteins. VPS33A, an SM protein, is involved in endolysosomal fusion and has been shown to stabilize the SNARE assembly formed by VAMP7 (Saleeb et al., 2019). In the future, VPS33A can be purified and tested in reconstituted degranulation tests to see if it activates VAMP8 based reactions.

These findings suggest that Munc18s have some specificity towards their cognate SNARE complexes, and phosphorylation might regulate their specificity; however, future investigations, including cell-based assays, will be required to recapitulate the reconstitution results in physiological settings.

6.2 PKC dependent Munc18a phosphorylation

To exploit the regulatory mechanism of phosphorylation on exocytosis, I investigated the site-specific phosphorylation of Munc18a in activated RBL-2H3 mast cells. Protein kinase C is an integral component of IgE/antigen activation pathways and modulates the exocytosis via phosphorylation of fusion factors. I found that targeted phosphorylation of Munc18a occurs at Ser313 by PKC in activated RBL-2H3 mast cells. PKC inhibitor RO-03-0432 prevented the phosphorylation of Munc18a at Ser313 as well as inhibited the RBL-2H3 exocytosis. This PKC-dependent phosphorylation of Munc18a at S313 could serve as a missing link between signaling and exocytosis. The physiological consequence of this modification has not been determined. My reconstitution study shows that the lipid mixing by Munc18a^{S306E/S313E} phosphomimetic mutant did not show any biochemical difference from wild type Munc18a (Fig.3.3 A, and B). I speculate that PKC-dependent Munc18a phosphorylation is a side reaction of the

PKC activation pathway with no importance. In addition to S313, there are additional PKC sites on Munc18a (there are four others identified and 12 predicted PKC sites) that can be phosphorylated. Furthermore, in Munc18b, there are at least nine identified and 12 predicted PKC sites. Munc18c has five identified and 10 predicted PKC sites (Xu et al., 2018). Munc18s might go modifications at the predicted PKC sites, modulating the biochemical and physiological outcomes. This may be part of intricate strategies mast cells exploit to ensure the specific release of selective mediators under different activation conditions. Identification of novel phosphorylation sites in Munc18 proteins would enhance our understanding of site-specific Munc18 phosphorylation in the regulation of mast cell exocytosis.

The potential phosphorylation sites in Munc18s can be identified by immunoprecipitation using phosphospecific Munc18 antibodies. It will aid in isolating phosphorylated proteins from activated mast cell lysate. Such protein can then be peptide fractionated, digested, enriched with phosphopeptides and subjected to Mass Spectrometry to determine the phosphorylated residues. Mass spectrometry will generate a list of identified sites of Munc18s that are phosphorylated in RBL-2H3 cells. The task would be to determine the critical sites for RBL-2H3 function. Strategically important phosphorylation sites of Munc18, such as the syntaxin-binding site or the sites undergoing conformational changes, can be subjected to further validation. A phosphomimetic mutant for each identified residue, created using site-directed mutagenesis can be tested (in reconstituted degranulation assays) to determine its functional relevance. Phosphomimetic mutant Munc18 proteins activating or diminishing the lipid mixing compared to their wild-type counterpart can be further tested for their

physiological significance in mediator's release. For this, Munc18 knocked down cells would be rescued using phosphoresistant mutant constructs via lentivirus transfection. In the absence of putative phosphorylation sites in phosphoresistant mutant constructs, the secretion will be altered compared to wild-type. This will determine if site-specific phosphorylation is vital for secretion in mast cells. These cell-based phosphorylation studies would reveal temporal regulation of Munc18s in mediator release by differential regulation of distinct trans-SNARE complexes.

6.3 Munc18a in clustering

In eukaryotic cells, activation of cognate trans-SNARE complexes by SM protein facilitates membrane fusion. This study underpinned the novel role of Munc18a in non-neuronal fusion and played a favorable function in the early stages of the fusion cascade. These findings suggest that Munc18 proteins promote proteoliposome clustering underlying vesicle docking during exocytosis in eukaryotic cells. This facilitates bringing the vesicles and target membranes closer together before activating the zippered trans-SNARE complex for fusion suggesting a positive role in physiological processes such as GLUT4 secretion and mast cell degranulation.

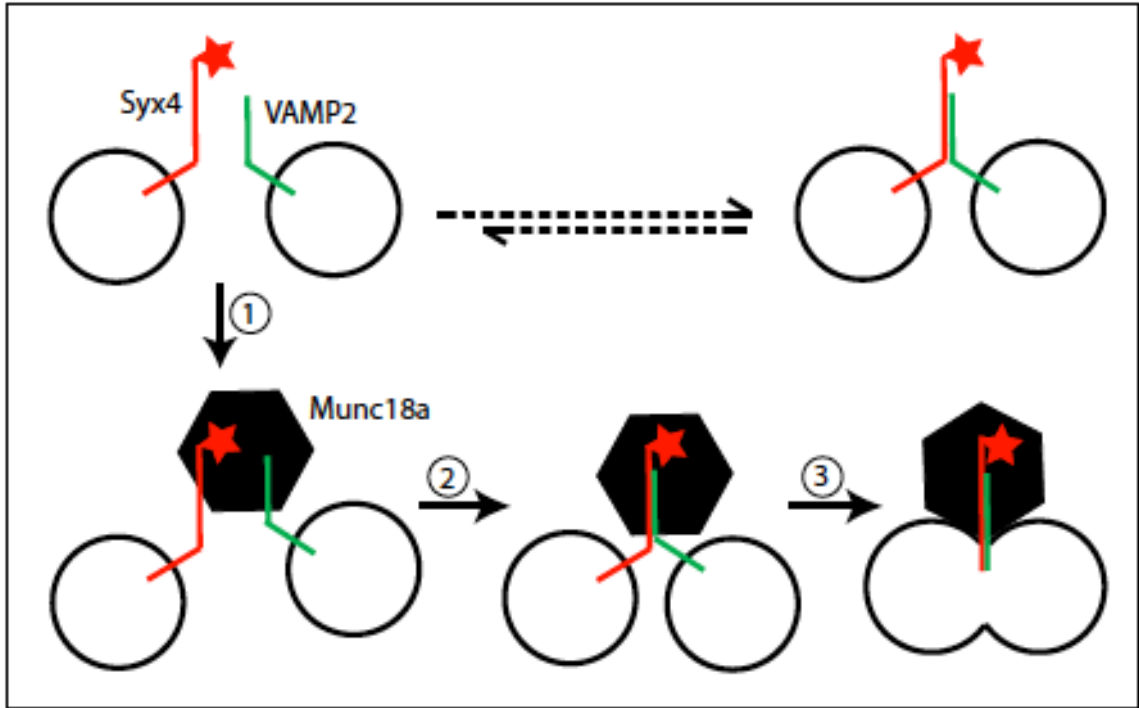


Figure 6.1 *Model for Munc18a action in membrane fusion.*

Munc18a binds to the N-terminal peptide of syntaxin (represented by *) and VAMP2, mediating the membrane tethering before the membrane fusion.

Munc18a mediates multiple roles in the fusion cascade (Fig.6.1). Without Munc18a, SNAREs undergo reversible pairing to form a partially zipped trans-SNARE complex (on ice/4°C) (Fig.6.1, dotted arrow). It's unclear whether Munc18 links two membranes directly during the docking process. The tethering activity of Munc18a depends on direct interaction with the N-peptide of syntaxin and unique motifs in VAMP2 (Fig.6.1, step 1). N- peptide bridges VAMP2 and Munc18a and facilitates membrane tethering and trans-SNARE assembly (Fig.6.1, step 2). The conformational change in Munc18a and/or SNAREs facilitates the fusion of the opposing membranes (Fig.6.1, step 3). The clustering activity of Munc18a is R-SNARE specific as Munc18a dependent clustering was only observed with VAMP2 but not with VAMP8. This

suggests that unique motifs in R-SNARE VAMP2 are responsible for interaction with Munc18a. Munc18a interacts with the short proline-rich N-terminal region of VAMP2 and the C-terminal SNARE domain (Shen et al., 2007). Munc18a's structural elements (regions) that interact with specific domains of VAMP2 are not understood, nor is the consequence of such interaction in vesicle tethering clear. Utilizing the Munc18 mutations at conserved and semi-conserved regions relevant to the Munc18a functioning and testing them in recapitulated fusion reactions will help determine the structural components responsible for the defined role of Munc18a in fusion cascade in the future. Munc18c, which acts similarly in reconstitution, can be tested in the future to see if clustering is unique to Munc18a or a general mechanism of SM function.

6.4 Differential release of mast cell mediators via VAMPs

The presence of multiple exocytic SNAREs in mast cells suggests the presence of multiple secretory pathways. It's yet unclear what role these exocytic SNAREs play in the differential release of specific mediators. In this study, I investigated the functional requirements of four VAMPs (VAMP2, VAMP3, VAMP7, and VAMP8) in RBL-2H3 mast cell exocytosis. When VAMP8 was silenced by siRNA, IgE/antigen-induced release of β -hexosaminidase, histamine, and serotonin were all inhibited (Fig.4.3 B-E, panel 5). TNF release on the other hand, was unaffected (Fig.4.3 E, panel 5), in line with previous studies from VAMP8 knockout mice (Puri & Roche, 2008; Tiwari et al., 2008). On the other hand, silencing of VAMP2, VAMP3, and VAMP7 did not inhibit the release of any of the mediators (Fig.4.3 B-E, panel 2-4).

VAMP8 knockdown resulted in a 50% reduction in β -hexosaminidase release, which corroborates previous studies in RBL cells (Woska & Gillespie, 2011) and

BMMCs from VAMP8 knockout mice (Puri & Roche, 2008; Tiwari et al., 2008). Partial inhibition of preformed mediators in VAMP8 siRNA transfected cells suggests that another VAMP homolog might compensate for its function. Compensation by other genes in the same protein family is a potential issue in RNAi-mediated gene depletion studies (Gordon et al., 2017). In VAMP8-deficient murine mast cells, VAMP2 had an increased association with SNAP23 that increased upon stimulation, but not in WT BMMCs, suggesting that VAMP2 may play a role or compensate for VAMP8 loss in secretory fusion events (Tiwari et al., 2008). Woska & Gillespie, (2011) proposed that t-SNAREs (syntaxin 4/ SNAP23) on mast cell plasma membrane can form a functional SNARE complex with v-SNAREs VAMP7 or VAMP8 and mediates the release of β -hexosaminidase and histamine. Sander et al., (2008) reported the involvement of VAMP7 and VAMP8 in histamine release from human mast cells. These suggest there might be a redundancy to the VAMP8 function. A double knockdown of redundant VAMPs would reveal if they act synergistically.

The potential redundancy of VAMPs could be detected by expression of VAMP proteins in immunoblotting for the level of VAMP expression. Puri and Roche (2008) reported no increased expression of other VAMP proteins in mast cells derived from VAMP8 knockout mice. I did not test this compensation mechanism in my VAMP8 knocked down RBL-2H3 cells because immunoblotting with VAMP antibodies required a large amount of cell lysates post-transfection. qPCR to measure the mRNA levels of other VAMPs can be used to assess the changes in gene expression directly. I did not measure the transcript level in silenced cells in this study and can be tested in the future.

It is critical to confirm that the phenotypes observed in any siRNA screen are specific and not simply the result of off-target effects. This is accomplished by conducting rescue experiments in which cells are rescued by transfecting with siRNA-resistant gene construct. Malmersjö et al., (2016) had generated a siRNA resistant VAMP8 sequence by introducing silent mutations in VAMP8 cDNA and cloned into a lentiviral vector so that the siRNA transfected cells can be rescued via lentivirus transduction. Using the construct described above, the rescue experiments can be pursued. If the effect of VAMP8 knockdown is specific, the rescue construct should restore the secretion of β -hexosaminidase, histamine, and serotonin.

The partial inhibition of secretion by VAMP8 also suggests that the pre-formed mediators might be present in another pool of VAMP8 free granular compartments. This pool may represent the distinct granule population as evidenced by Puri & Roche, (2008). They observed that serotonin and histamine localize to distinct granule populations and utilized distinct VAMP proteins for their release. Colocalization of serotonin with VAMPs and histamine with VAMPs would precisely reveal the potential granule subsets and suggest which VAMP might be responsible for a specific mediator release. Nevertheless, the reported studies, including mine suggest that VAMP8 is located on granules packed with preformed mediators β -hexosaminidase, serotonin, and histamine waiting for a trigger to undergo regulated exocytosis.

Despite an 80-90% reduction of target VAMP mRNAs upon introducing the siRNAs, no defective secretory phenotype was evident in VAMP2, VAMP3, and VAMP7 knockdowns, failing to impair the exocytosis. Gordon et al., (2010) reported that knockdown of multiple post-Golgi-specific R-SNAREs did not inhibit the constitutive

protein secretion in human cell lines suggesting functional redundancy. Similarly, the VAMPs I have tested may be functionally redundant, and disrupting just one is unlikely to show a defect. Hence, future studies involving combinatorial knockdown of VAMP2, VAMP3 and VAMP7 would reveal if they act synergistically in RBL-2H3 mast cell exocytosis. Similarly, colocalization studies would reveal the potential redundancy as the functional redundant would colocalize with each other. However, for these, each VAMP should carry a different fluorescent tag to differentiate them.

There remains a possibility that these VAMPs are instead required for the release of other mediators from activated mast cells. The differential release of chemokines required VAMP7 and VAMP8 (Frank et al., 2011). There are plentiful other cytokines readily synthesized upon transcriptional activation and then released from stimulated mast cells. Further quantification of release of other endogenous cytokine via ELISA based assay and cytokine arrays can be performed. Because siRNA does not eliminate gene expression, the possibility that the remaining VAMPs after transient knockdown would compensate for the secretory deficiency cannot be ruled out. SNAREs have been found in reserved pools, such as multimolecular clusters, generally in greater abundance, sequestered, and only released as per cellular needs, and even at a minimal level, SNAREs can perform normal functions (Bethani et al., 2009). Hence an 80-90% reduction in VAMP mRNA expression as determined by qPCR would not cause perturbation of exocytosis. Genetically altered knockout cells would be suitable for further studies.

Since knockdown of either VAMP isoform had no effect on TNF release, based on the studies in other immune cells such as macrophages undergoing phagocytosis and

human synovial cells (Boddul et al., 2014; Murray et al., 2005), I proposed VAMP3 to be involved in TNF release from activated RBL-2H3 cells. To study the role of VAMP3 in TNF release, I created CRISPR/Cas9 based VAMP3 knockout RBL-2H3 cells. In contrast to findings in human synovial cells, my results showed that VAMP3 is not required for TNF from IgE/antigen-activated RBL-2H3 mast cells (Fig.4.9 B,D) suggesting the TNF secretion to be cell type-specific. TNF release from different cells may determine their distinct physiological roles, ranging from innate immunity to autoimmune disease pathogenesis. TNF's distinct functions and release in response to specific activation may necessitate unique secretory machinery (Efimov et al., 2016). Moreover, mast cells are the only cells capable of storing TNF in their cytoplasmic granules and synthesize TNF to release via small vesicles. Macrophages, in contrast, do not have granules. It is not clear if the trafficking of TNF as seen in macrophages via Golgi through recycling endosomes to the cell surface also occurs in mast cells. Colocalization studies of VAMP3 and Rab11 (a recycling endosome marker) would reveal more insights into the trafficking pathways in mast cells. TNF intracellular distribution in mast cells would be revealed by immunofluorescence studies with various subcellular compartments.

TNF synthesis soars up upon mast cell activation, and TNF is released constitutively via small vesicular carriers. As observed in macrophages undergoing phagocytosis, the newly synthesized cytokines reach the cell surface via VAMP3 bearing recycling endosomes (Murray et al., 2005; Murray & Stow, 2014) suggesting VAMP3 to be a likely R-SNARE involved in the constitutive secretion of newly synthesized TNF in mast cells. I further quantified VAMP3's involvement in releasing late-phase TNF

(quantified 24 h after TNP-BSA stimulation), which is thought to be mediated via constitutive exocytosis. The release of late-phase TNF was unaffected by loss of VAMP3 (Fig.4.9 D). In my study, the knockout of VAMP3 failed to produce a phenotype, which could be due to redundancy. Depletion of two R-SNAREs-VAMP3 and YKT6 (an ER to Golgi R-SNARE) arrested the fusion of constitutive secretory vesicles in mammalian cell lines (Gordon et al., 2017). In line with this, I performed a siRNA knockdown of YKT6 in VAMP3 KO cells to see any functional redundancy for constitutive TNF release; however, no effect on late-phase TNF release was observed (data not shown). It remains to be seen in the future whether the synergy of two longin domain-containing R-SNAREs, VAMP7, and YKT6, is involved in the constitutive secretion of newly synthesized TNF from RBL cells via simultaneous knockdown of VAMP7 and YKT6 in RBL-2H3 cells. All these studies would reveal the potential R-SNARE involved in TNF secretion.

Unexpectedly, my data shows an enhanced β -hexosaminidase secretion in VAMP3 KO cells (Fig.4.9 A). Is it the hypersecretory nature of the CRISPR modified cells due to some off target effects (based on my observation of increase in β -hexosaminidase secretion from the BAIAP3 base edited cells) or is it due to VAMP3's specific effect, requires further investigations? Rescue experiments of VAMP3 into KO cells would reveal whether the secretion defect is VAMP3 specific or not. Moreover, there remains a possibility that the β -hexosaminidase present on different pools upon VAMP3 loss might come together due to the cell's feedback mechanism and cause it to secrete more when activated. Future immunofluorescence studies monitoring the

granules' localization, size, and exocytosis would reveal the dynamics of the granular content in KO cells.

If VAMP3 is not involved in TNF release, then which R-SNARE is responsible for TNF exocytosis. Based on preliminary colocalization studies from our lab, TNF colocalized with multivesicular bodies (MVB) markers- CD63, CD81, and CD9 (Ayo and Xu, unpublished), suggesting that TNF may be present in MVBs/late endosomes. We speculate that fusion of MVBs with plasma membrane releases exosomes decorated with TNF utilizing distinct R-SNARE. Accumulating evidence shows that VAMP7 present on MVB is required for MVB fusion with the plasma membrane to release exosomes from cultured human cells (Hessvik & Llorente, 2018). VAMP7 has an N-terminal longin domain that can inhibit the SNARE complex formation, and overexpression of the N-terminal VAMP7 domain is shown to inhibit exosomes release impairing the fusion of MVBs with the plasma membrane (Fader et al., 2009). The other R-SNARE protein, YKT6, is required for exosomes release in human embryonic kidney HEK293 and human lung cancer A549 cells (Ruiz-Martinez et al., 2016). The colocalization of TNF with VAMP7 and YKT6 would serve to provide grounds to test their role in TNF release. The availability of VAMP7 and YKT6 knockout mice and ease of isolation of primary mast cells would assist in the direct assessment of these R-SNAREs in TNF release. For this, the primary mast cells-BMMCs (bone marrow-derived progenitors) and PCMCs (mature mast cells) will be isolated from the KO and WT mice and stimulated with various stimuli- IgE/antigen, LPS, and PGN. LPS and PGN selectively release TNF without degranulation(release of granular contents) (Supajatura et al., 2002). Monitoring TNF

release from variously activated cells will enhance our understanding of the stimulus dependent exocytic pathways.

Other than KO and KD studies, functional studies utilized in mast cell exocytosis include overexpression, permeabilizing antibodies, introduction of N-peptides. Paumet et al., (2000) showed that overexpression of syntaxin4 but not syntaxin2 and 3 affected IgE stimulated RBL-2H3 degranulation. Overexpression will lead to overproduction of protein and disturb the steady state of interacting proteins and subsequent inhibition of exocytosis. The N-terminal mimicking peptides introduced to permeabilized RBL-2H3 cells were found to inhibit SNARE complex formation and specifically inhibit secretion from granular subset (Yang et al., 2018). Antibodies that neutralize the endogenous SNAREs has been utilized to identify the SNARE exocytic machinery (Sander et al., 2008). Moreover, SNARE cleaving toxins such as tetanus or botulinum has been found to be effective in inhibiting SNAREs and subsequent SNARE mediated fusion. Thus, all these functional tools will aid in investigations on regulation of specific membrane fusion event.

6.5 BAIAP3 in mast cell exocytosis

Partial inhibition of TNF in Munc13-4 knockout RBL-2H3 cells led us to investigate the function of Munc13-4 homolog BAIAP3. Knocking out BAIAP3 in RBL-2H3 cells seems to reduce TNF secretion to some extent, but the difference was not statistically significant (Fig.5.6). Future repeats will reveal if the secretion defect is statistically significant. Moreover, rescuing BAIAP3 KO with a rescue construct stably expressing BAIAP3 protein will demonstrate if the effect of BAIAP3 in TNF release is specific or not. Due to the lack of a monoclonal antibody, the knockout of BAIAP3

protein was not validated in immunoblotting. There was cross-reactivity, and multiple bands appeared in blot (data not shown). Immunoblotting with RBL-2H3 cells stably expressing the BAIAP3 construct will help to characterize the antibody's sensitivity.

Since there are three Munc13 isoforms expressed in RBL cells (Ayo et al., 2020; Higashio et al., 2017), each isoform might govern a unique secretory pathway, or the function might be redundant. In immunoblotting, no change in expression in Munc13-1 was observed in BAIAP3 KO cells (Fig.5.7), while due to lack of working antibody, Munc13-4 was undetected (not shown). Localization studies using fluorescently tagged stable expression constructs would likely reveal functional redundancy in the future. Then, to investigate the role of Munc13 in mast cell secretion, a double knockout of redundant Munc13 homologs can be performed. The role of BAIAP3 in late-phase TNF secretion is yet to be determined.

6.6 CRISPR based modifications of RBL-2H3 cells

In this study, I used CRISPR-Cas9 technology to successfully target the VAMP3 and BAIAP3 gene in RBL-2H3 cells. I used the traditional CRISPR/Cas9 HDR method and the recently developed CRISPR mediated base editing. Traditional CRISPR/Cas9 precisely modifies the target genome and disrupts gene function by causing a double-strand break that is then repaired using NHEJ or HDR. Homologous directed recombination (HDR) based knockout is an efficient technique to target various mammalian cells and is dependent on the presence of exogenous homologous donor sequence. HDR is accurate yet less efficient as it is limited to occur during S and G2 phases of the cell cycle when the sister chromatids undergo homologous recombination (Ran et al., 2013).

In my study, using the traditional CRISPR/Cas9 approach in the presence of an HDR repair template resulted in the knockout of VAMP3 (Fig.4.7); however, I was unable to create a BAIAP3 KO. The inefficiency in creating a BAIAP3 (and even VAMP7) knockout could be the outcome of the design of guide RNA (gRNA) or the generation of homology arms. A 20-nucleotide gRNA on an early exon (exon 2) of the BAIAP3 genome was selected using the IDT CRISPR design tool based on their high on target and low off-target score. IDT software recommends the top hit gRNA with the best scores (on exon 3 of BAIAP3); however, I opted for a gRNA on an early exon, i.e., exon 2. Overall, the chosen gRNA had a subtle difference in scores than recommended gRNA (this was a similar case when I tried knocking out VAMP7). The reason why the guide RNA selected did not work is unknown; however, as IDT suggests, selecting the top hit gRNA as a starting point for CRISPR knockouts may be a good place to start. I chose the top-recommended IDT's gRNA for VAMP3 and successfully targeted the VAMP3 gene.

On the other hand, the homology arms of 600bp on each side of the cleavage site were synthesized in vitro using the RBL genomic DNA, while the primers for PCR were designed based on rat database sequence. As a result, there may be differences in the published rat sequence and the cell line generated DNA sequence, which may contain unknown mutations. Because of the reliance of HDR on absolute homologous donor sequences, subtle variations in arms might have affected the recombination process. The sequencing data (Fig.4.8) for the VAMP3 KO clone shows random insertions and base substitutions around the target site while the rest of the sequence aligned with the WT, suggesting the KO obtained was not HDR based. The NHEJ repair might have outcome the HDR at the double-strand break site. Random integration of the HDR template in the

genome might have occurred as the cells were red fluorescing and puromycin resistant even after subsequent generations. In the future, for an efficient knockout and choosing the best-recommended gRNA suggested by the CRISPR design tool, two guide RNAs for the targeted genome can be designed (Ran et al., 2013) for efficient targeting. Moreover, the availability of RBL-2H3 genome sequence in the database or in-house sequencing of the targeted area genome would help design more exact homologous arms and a more efficient recombination process. To minimize the random integration of exogenous HDR template, the amount of plasmid transfected could be carefully controlled. Moreover, an HDR repair plasmid without its own promoter, which gets expressed only after successful recombination events utilizing cells' endogenous promoter at the targeted site, will validate the recombination at the desired position. This would mitigate the expression of exogenous DNA due to random integration, as seen in my studies.

Due to limited success, and unexpected outcomes of the HDR approach, as an alternative to knockout BAIAP3, CRISPR-based base editing was employed. It is a highly efficient technique as it does not rely on double-strand cleavage or the presence of cell recombination machinery and homologous arms as a template (Komor et al., 2016). It efficiently disrupts the gene via direct conversion of C to T and effectively induces early stop codons, causing truncated (nonfunctional) protein synthesis. These base modifications could be readily monitored via restriction length polymorphism (RFLP) assay using specific restriction enzymes that determine the loss or gain of sites in edited cells (Billon et al., 2017). I created a biallelic BAIAP3 mutant via CRISPR base editing, analyzed by RFLP, and verified by sequencing.

Overall, CRISPR/Cas9 induces double-strand break, which is toxic to the cells, causes random insertions/ deletions with higher chances of nontargeted modifications and double-strand break formation at off-target sites and higher off-target effect (Roy et al., 2018). It is an intensive and time-consuming process requiring homologous repair template generation. Random insertions and deletions are more abundant than homology-based recombination during DNA break repair. This makes it extremely difficult to control random indels with unusual target protein modification. In contrast, base editing is advantageous in many ways as it does not produce harmful endogenous DNA breaks, does not rely on homologous donor molecules, and is less toxic than the traditional CRISPR technique (Kuscu et al., 2017). Thus, base editing mediated generation of the stop codon (CRISPR-STOP) serves to be an efficient, reliable, and more straightforward method of CRISPR gene knockout for future knockout studies. Base editing may be further improvised by the use of high fidelity cytidine deaminase, nicked Cas9 enzyme for improvised target recognition; effective off target prediction tools, use of alternative PAM sequences, thorough computational analysis tools to improve the limitations posed by the existing CRISPR-STOP approach (Billon et al., 2017; Koblan et al., 2018; Kuscu et al., 2017).

The off-target effect occurs at a higher rate in the conventional DSB mediated CRISPR knockout approach. The Cas9 can recognize up to 5 mismatched bases, thus having eminent off-target consequences. A similar off-target outcome in CRISPR-based syntaxin3 KO RBL cells was observed in our lab (data not shown). A defect in the release of β -hexosaminidase and TNF was observed in syntaxin3 KO cells; however, upon reintroduction of syntaxin3 into the KO cells did not rescue the secretion defect.

This suggests that in the KO, there was an off-target secondary effect in an essential exocytic pathway that affected the mediator release. Any off-target effect in VAMP3 KO remains to be determined.

6.7 Primary mast cells secretion

Elucidation of differential release pathways of mast cell mediators calls for the activation of several signaling pathways in one experimental system to observe the different release patterns. Primary mast cells (BMMCs and PCMCs) are more advantageous than RBL-2H3 as they express multiple cell surface receptors. Moreover, BMMCs respond to PGN and LPS via TLR receptors to release TNF without degranulation (Ikeda & Funaba, 2003), suggesting a crucial role of mast cells in host defense. The function of individual VAMPs in TNF release can be precisely monitored in BMMCs and PCMCs via TLR response when challenged with bacterial products.

As a pioneering study, I isolated and cultivated the primary mast cells. The purity of mast cells was assessed as purple stained cells with Toluidine blue dye (Fig.6.2 A, B, and C). Toluidine blue is a basic dye that binds to heparin in mast cell granules to give characteristic purple staining (Ribatti, 2018). As shown in Fig.6.2, BMMCs (B) and PCMCs (C) stained purple just like RBL-2H3 cells (A), suggesting the isolated cells are a homogenous mast cell population. The BMMCs were more abundant, while the yield of PCMCs was about 70% lower than BMMCs.

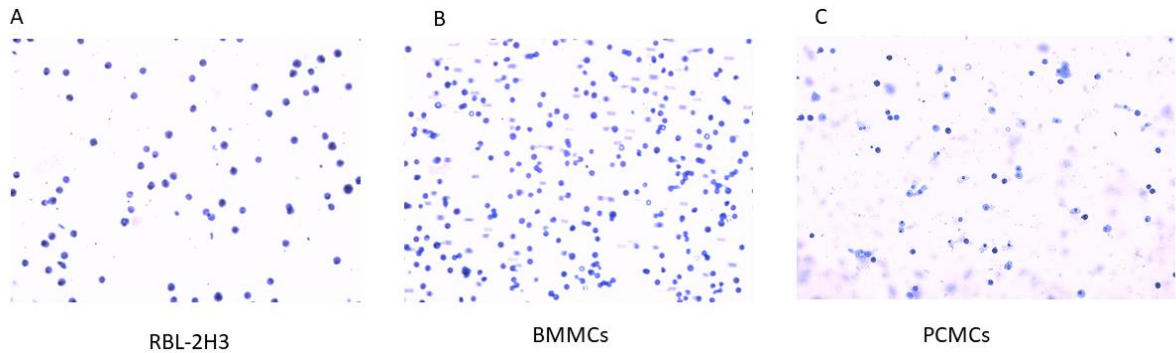


Figure 6.2 *Successful isolation and cultivation of primary mast cells.*

BMMCs and PCMCs were respectively obtained from bone marrow and peritoneal cavity of mice, cultured in medium containing SCF and IL3 (A) RBL-2H3 cells as a control; (B) BMMCs and (C) PCMCs stained purple with Toluidine blue dye and consisted of a homogenous mast cell population.

The cultured cells were further stimulated with various stimuli to undergo degranulation. The release of β -hexosaminidase release was monitored as a marker of degranulation, and IgE/antigen stimulation resulted in 50% release of prestored β -hexosaminidase from BMMCs (Fig.6.3 A). The BMMCs when triggered by calcium ionophore (Ionomycin) to release 45% of β -hexosaminidase (Fig.6.3 A). PCMCs, on the other hand, had an overall lower yield and, upon Ionomycin/PMA stimulation, released the β -hexosaminidase to around 50% (Fig.6.3 B). The secretion was comparable to the β -hexosaminidase secreted by BMMCs suggesting the isolated cells to be pure mast cells. The release of TNF from BMMCs (Fig.6.3 C) was quantified from the samples harvested for β -hexosaminidase assay and showed that TNF was secreted from stimulated cells. These results suggest that the cells isolated from bone marrow progenitors were pure mast cells, and they undergo stimulation by various triggers to release their granular contents such as β -hexosaminidase and TNF, readily. The secretion of TNF from PCMCs was not detectable (data not shown) due to the lower yield of cells. In the future,

combining the cells obtained from the peritoneal cavities of two mice may produce a higher yield.

Furthermore, BMDCs were triggered with TLR ligands known to release granular contents differentially (Supajatura et al., 2002). For this, the cells were treated with various concentrations of lipopolysaccharide (LPS) (Fig.6.3 D). The highest LPS concentration (2 μ g/ml) did not stimulate the cells to release β -hexosaminidase, while IgE/antigen stimulation caused the cells to degranulate readily. These results corroborated with published studies (Supajatura et al., 2002). The release of TNF in these cells awaits future testing. These preliminary results suggest mast cells undergo selective release of mediators via different signaling pathways, which will help in comparative investigations of various exocytic machinery in the future.

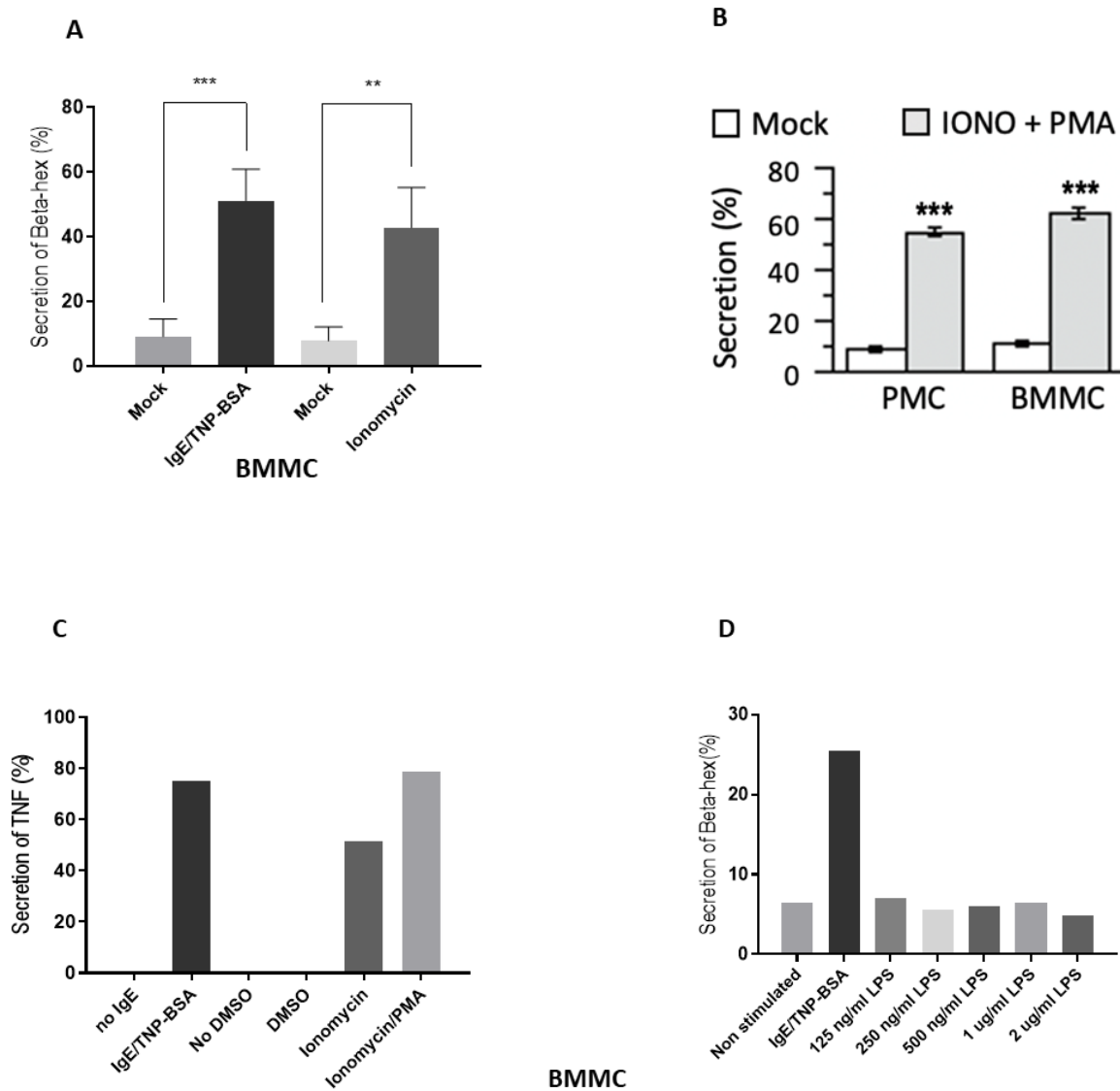


Figure 6.3 *Secretion from primary mast cells.*

After 3 weeks of culturing, secretion assays from BMMCs- (A) β -hexosaminidase from various conditions in BMMCs. Data from 4 independent experiments. (B) β -hexosaminidase secretion of PCMCs and BMMCs in response to calcium ionophore (Ionomycin 1 μ M) and PKC activator PMA (phorbol myristate acetate; 20 nM) Data from 3 independent experiments. (C) TNF release from the BMMC stimulated in A and B. (D) Secretion of β -hexosaminidase from LPS treated BMMCs at various concentrations. IgE/TNP-BSA stimulation as control of degranulation. (G) ****p<0.0001, ***p<0.03, **p<0.01

CHAPTER VII – CONCLUSION

The findings in this study suggest the differential regulation of mast cell mediators utilizing distinct exocytic pathways and set the stage to dissect further the molecular mechanisms involved in the exocytosis of distinct mast cell mediators. Munc18s selectively activated the cognate SNAREs which in turn may be regulated by Munc18 phosphorylation. VAMP8 decorated granules are enriched with the preformed mediators consisting of β -hexosaminidase, histamine, and serotonin. TNF is not present in this granular subset as my knockdown studies and studies in knockout mice show that VAMP8 is partially involved in the release of β -hexosaminidase, histamine, and serotonin but not TNF. VAMP3, on the other hand, did not show any effect in the release of TNF. However, some inhibitory effect of VAMP3 was observed in β -hexosaminidase release, which needs to be validated further with rescue studies. BAIAP3 knockout seems to affect the TNF release; however, more experimental repeats and rescue with BAIAP3 constructs need to be done. The data from our lab shows that Munc18b (Xu, unpublished) and Munc13-4 (Ayo et al., 2020) are so far involved in the secretion of TNF.

Successful isolation and stimulation of primary mast cells have set the stage for further testing of various stimuli such as LPS, PGN, and Poly: IC. This will enhance our understanding of the differential signaling-based regulation of fusion machinery. Thus, investigating the differential release of mediators at the signaling interface (activation via IgE-Fc ϵ RI or TLR; PKC dependent phosphorylation of targets) and exocytic fusion machinery will enhance our understanding of the release pre-formed mediators via immediate degranulation or through delayed response (such as TNF). This will help

identify molecules that regulate the specific effector function and, in the future, will serve to be rational therapies for mast cell-associated diseases.

REFERENCES

- Adhikari, P., & Xu, H. (2018). PKC-dependent phosphorylation of Munc18a at Ser313 in activated RBL-2H3 cells. *Inflammation Research : Official Journal of the European Histamine Research Society ... [et Al.]*, 67(1), 1–3. <https://doi.org/10.1007/s00011-017-1097-4>
- Akula, S., Paivandy, A., Fu, Z., Thorpe, M., Pejler, G., & Hellman, L. (2020). How Relevant Are Bone Marrow-Derived Mast Cells (BMMCs) as Models for Tissue Mast Cells? A Comparative Transcriptome Analysis of BMMCs and Peritoneal Mast Cells. *Cells*, 9(9), 1–19. <https://doi.org/10.3390/cells9092118>
- Arnold, M. G., Adhikari, P., Kang, B., & Xu 徐昊, H. (2017). Munc18a clusters SNARE-bearing liposomes prior to trans-SNARE zippering. *The Biochemical Journal*, 474(19), 3339–3354. <https://doi.org/10.1042/BCJ20170494>
- Ayo, T. E., Adhikari, P., Sugita, S., & Xu, H. (2020). TNF Production in Activated RBL-2H3 Cells Requires Munc13-4. *Inflammation*, 43(2), 744–751. <https://doi.org/10.1007/s10753-019-01161-4>
- Baker, R. W., & Hughson, F. M. (2016). Chaperoning SNARE assembly and disassembly. *Nature Reviews Molecular Cell Biology*, 17(8), 465–479. <https://doi.org/10.1038/nrm.2016.65>
- Baker, R. W., Jeffrey, P. D., Zick, M., Phillips, B. P., Wickner, W. T., & Hughson, F. M. (2015). A direct role for the Sec1/Munc18-family protein Vps33 as a template for SNARE assembly. *Science (New York, N.Y.)*, 349(6252), 1111–1114. <https://doi.org/10.1126/science.aac7906>
- Baker, R. W., Jeffrey, P. D., Zick, M., Phillips, B. P., Wickner, W. T., & Hughson, F. M.

- (2016). *HHS Public Access*. 349(6252), 1111–1114.
<https://doi.org/10.1126/science.aac7906.A>
- Baram, D., Adachi, R., Medalia, O., Tuvim, M., Dickey, B. F., Mekori, Y. A., & Sage-Eisenberg, R. (1999). Synaptotagmin II negatively regulates Ca²⁺-triggered exocytosis of lysosomes in mast cells. *Journal of Experimental Medicine*, 189(10), 1649–1657. <https://doi.org/10.1084/jem.189.10.1649>
- Barclay, J. W., Craig, T. J., Fisher, R. J., Ciuffo, L. F., Evans, G. J. O., Morgan, A., & Burgoyne, R. D. (2003). Phosphorylation of Munc18 by protein kinase C regulates the kinetics of exocytosis. *Journal of Biological Chemistry*, 278(12), 10538–10545. <https://doi.org/10.1074/jbc.M211114200>
- Bethani, I., Werner, A., Kadian, C., Geumann, U., Jahn, R., & Rizzoli, S. O. (2009). Endosomal fusion upon SNARE knockdown is maintained by residual snare activity and enhanced docking. *Traffic*, 10(10), 1543–1559. <https://doi.org/10.1111/j.1600-0854.2009.00959.x>
- Billon, P., Bryant, E. E., Joseph, S. A., Nambiar, T. S., Hayward, S. B., Rothstein, R., & Ciccia, A. (2017). CRISPR-Mediated Base Editing Enables Efficient Disruption of Eukaryotic Genes through Induction of STOP Codons. *Molecular Cell*, 67(6), 1068–1079.e4. <https://doi.org/10.1016/j.molcel.2017.08.008>
- Bin, N. R., Jung, C. H., Piggott, C., & Sugita, S. (2013). Crucial role of the hydrophobic pocket region of Munc18 protein in mast cell degranulation. *Proceedings of the National Academy of Sciences of the United States of America*, 110(12), 4610–4615. <https://doi.org/10.1073/pnas.1214887110>
- Black, R. A., Rauch, C. T., Kozlosky, C. J., Peschon, J. J., Slack, J. L., Wolfson, M. F.,

- Castner, B. J., Stocking, K. L., Reddy, P., Srinivasan, S., Nelson, N., Boiani, N., Schooley, K. A., Gerhart, M., Davis, R., Fitzner, J. N., Johnson, R. S., Paxton, R. J., March, C. J., & Cerretti, D. P. (1997). A metalloproteinase disintegrin that releases tumour-necrosis factor- α from cells. In *Nature* (Vol. 385, Issue 6618, pp. 729–733). <https://doi.org/10.1038/385729a0>
- Blank, U. (2011). The mechanisms of exocytosis in mast cells. *Advances in Experimental Medicine and Biology*, 716, 107–122. https://doi.org/10.1007/978-1-4419-9533-9_7
- Blank, U., Huang, H., & Kawakami, T. (2021). The high affinity IgE receptor: a signaling update. *Current Opinion in Immunology*, 72, 51–58. <https://doi.org/10.1016/j.coi.2021.03.015>
- Blank, U., Madera-Salcedo, I. K., Danelli, L., Claver, J., Tiwari, N., Sánchez-Miranda, E., Vázquez-Victorio, G., Ramírez-Valadez, K. A., Macias-Silva, M., & González-Espinosa, C. (2014). Vesicular trafficking and signaling for cytokine and chemokine secretion in mast cells. In *Frontiers in Immunology* (Vol. 5, Issue SEP). Frontiers Media S.A. <https://doi.org/10.3389/fimmu.2014.00453>
- Blank, U., & Rivera, J. (2004). The ins and outs of IgE-dependent mast-cell exocytosis. *Trends in Immunology*, 25(5), 266–273. <https://doi.org/10.1016/j.it.2004.03.005>
- Boddul, S. V., Meng, J., Dolly, J. O., & Wang, J. (2014). SNAP-23 and VAMP-3 contribute to the release of IL-6 and TNF α from a human synovial sarcoma cell line. *FEBS Journal*, 281(3), 750–765. <https://doi.org/10.1111/febs.12620>
- Bradding, P., & Arthur, G. (2016). Mast cells in asthma - state of the art. *Clinical and Experimental Allergy*, 46(2), 194–263. <https://doi.org/10.1111/cea.12675>
- Brandie, F. M., Aran, V., Verma, A., McNew, J. A., Bryant, N. J., & Gould, G. W.

- (2008). Negative regulation of syntaxin4/SNAP-23/VAMP2-mediated membrane fusion by Munc18c In Vitro. *PLoS ONE*, 3(12), 1–7.
<https://doi.org/10.1371/journal.pone.0004074>
- Brunger, A. T., Cipriano, D. J., & Diao, J. (2015). Towards reconstitution of membrane fusion mediated by SNAREs and other synaptic proteins. *Critical Reviews in Biochemistry and Molecular Biology*, 50(3), 231–241.
<https://doi.org/10.3109/10409238.2015.1023252>
- Bulfone-Paus, S., & Bahri, R. (2015). Mast cells as regulators of T cell responses. *Frontiers in Immunology*, 6(AUG), 6–11. <https://doi.org/10.3389/fimmu.2015.00394>
- Burgo, A., Casano, A. M., Kuster, A., Arold, S. T., Wang, G., Nola, S., Verraes, A., Dingli, F., Loew, D., & Galli, T. (2013). Increased activity of the vesicular soluble N-ethylmaleimide-sensitive factor attachment protein receptor TI-VAMP/VAMP7 by tyrosine phosphorylation in the Longin domain. *Journal of Biological Chemistry*, 288(17), 11960–11972. <https://doi.org/10.1074/jbc.M112.415075>
- Cao, J., Papadopoulou, N., Kempuraj, D., Boucher, W. S., Sugimoto, K., Cetrulo, C. L., & Theoharides, T. C. (2005). Human Mast Cells Express Corticotropin-Releasing Hormone (CRH) Receptors and CRH Leads to Selective Secretion of Vascular Endothelial Growth Factor. *The Journal of Immunology*, 174(12), 7665–7675.
<https://doi.org/10.4049/jimmunol.174.12.7665>
- Carr, C. M., & Rizo, J. (2010). At the junction of SNARE and SM protein function. *Current Opinion in Cell Biology*, 22(4), 488–495.
<https://doi.org/10.1016/j.ceb.2010.04.006>
- Carroll-Portillo, A., Cannon, J. L., te Riet, J., Holmes, A., Kawakami, Y., Kawakami, T.,

- Cambi, A., & Lidke, D. S. (2015). Mast cells and dendritic cells form synapses that facilitate antigen transfer for T cell activation. *Journal of Cell Biology*, *210*(5), 851–864. <https://doi.org/10.1083/jcb.201412074>
- Cavalcante, M. C. M., de Andrade, L. R., Du Bocage Santos-Pinto, C., Straus, A. H., Takahashi, H. K., Allodi, S., & Pavão, M. S. G. (2002). Colocalization of heparin and histamine in the intracellular granules of test cells from the invertebrate *Styela plicata* (Chordata-Tunicata). *Journal of Structural Biology*, *137*(3), 313–321. [https://doi.org/https://doi.org/10.1016/S1047-8477\(02\)00007-2](https://doi.org/https://doi.org/10.1016/S1047-8477(02)00007-2)
- Chen, Y. A., & Scheller, R. H. (2001). SNARE-mediated membrane fusion. *Nature Reviews. Molecular Cell Biology*, *2*(2), 98–106. <https://doi.org/10.1038/35052017>
- Chen, Y. A., Scales, S. J., Patel, S. M., Doung, Y., & Scheller, R. H. (1999). *Cell 166 Figure 1. Proposed Mechanism by which S25-C Rescues Exocytosis.* 97, 165–174. https://ac.els-cdn.com/S0092867400807278/1-s2.0-S0092867400807278-main.pdf?_tid=6918a0d8-b34a-11e7-9086-00000aacb35f&acdnat=1508251963_656ec21dc16f66ae8c93c1b7fd8ebf48
- Coward, W. R., Okayama, Y., Sagara, H., Wilson, S. J., Holgate, S. T., & Church, M. K. (2002). NF- κ B and TNF- α : A Positive Autocrine Loop in Human Lung Mast Cells? *The Journal of Immunology*, *169*(9), 5287–5293. <https://doi.org/10.4049/jimmunol.169.9.5287>
- Crivellato, E., Beltrami, C. alberto, Mallardi, F., & Ribatti, D. (2003). Paul Ehrlich's doctoral thesis: a milestone in the study of mast cells. *British Journal of Haematology*, *123*(1), 19–21. <https://doi.org/10.1046/j.1365-2141.2003.04573.x>
- da Silva, E. Z. M., Jamur, M. C., & Oliver, C. (2014). Mast Cell Function: A New Vision

- of an Old Cell. In *Journal of Histochemistry and Cytochemistry* (Vol. 62, Issue 10).
<https://doi.org/10.1369/0022155414545334>
- Dennison, S. M., Bowen, M. E., Brunger, A. T., & Lentz, B. R. (2006). Neuronal SNAREs do not trigger fusion between synthetic membranes but do promote PEG-mediated membrane fusion. *Biophysical Journal*, *90*(5), 1661–1675.
<https://doi.org/10.1529/biophysj.105.069617>
- Dulubova, I., Sugita, S., Hill, S., Hosaka, M., Fernandez, I., Südhof, T. C., & Rizo, J. (1999). A conformational switch in syntaxin during exocytosis: Role of munc18. *EMBO Journal*, *18*(16), 4372–4382. <https://doi.org/10.1093/emboj/18.16.4372>
- Efimov, G. A., Kruglov, A. A., Khlopchatnikova, Z. V., Rozov, F. N., Mokhonov, V. V., Rose-John, S., Scheller, J., Gordon, S., Stacey, M., Drutskaya, M. S., Tillib, S. V., & Nedospasov, S. A. (2016). Cell-type-restricted anti-cytokine therapy: TNF inhibition from one pathogenic source. *Proceedings of the National Academy of Sciences of the United States of America*, *113*(11), 3006–3011.
<https://doi.org/10.1073/pnas.1520175113>
- Elstak, E. D., Neeft, M., Nehme, N. T., Voortman, J., Cheung, M., Goodarzifard, M., Gerritsen, H. C., Van Bergen En Henegouwen, P. M. P., Callebaut, I., De Saint Basile, G., & Van Der Sluijs, P. (2011). The munc13-4-rab27 complex is specifically required for tethering secretory lysosomes at the plasma membrane. *Blood*, *118*(6), 1570–1578. <https://doi.org/10.1182/blood-2011-02-339523>
- Fader, C. M., Sánchez, D. G., Mestre, M. B., & Colombo, M. I. (2009). TI-VAMP/VAMP7 and VAMP3/cellubrevin: two v-SNARE proteins involved in specific steps of the autophagy/multivesicular body pathways. *Biochimica et*

Biophysica Acta - Molecular Cell Research, 1793(12), 1901–1916.

<https://doi.org/10.1016/j.bbamcr.2009.09.011>

Fasshauer, D., Sutton, R. B., Brunger, A. T., & Jahn, R. (1998). Conserved structural features of the synaptic fusion complex: SNARE proteins reclassified as Q- and R-SNAREs (membrane fusion neurotransmission clostridial neurotoxins). *Neurobiology Communicated by Peter B. Moore*, 95(December), 15781–15786.

Fletcher, A. I., Shuang, R., Giovannucci, D. R., Zhang, L., Bittner, M. A., & Stuenkel, E. L. (1999). Regulation of exocytosis by cyclin-dependent kinase 5 via phosphorylation of Munc18. *Journal of Biological Chemistry*, 274(7), 4027–4035.
<https://doi.org/10.1074/jbc.274.7.4027>

Frank, S. P. C., Thon, K. P., Bischoff, S. C., & Lorentz, A. (2011). SNAP-23 and syntaxin-3 are required for chemokine release by mature human mast cells. *Molecular Immunology*, 49(1–2), 353–358.
<https://doi.org/10.1016/j.molimm.2011.09.011>

Frossi, B., Mion, F., Sibilano, R., Danelli, L., & Pucillo, C. E. M. (2018). Is it time for a new classification of mast cells? What do we know about mast cell heterogeneity? *Immunological Reviews*, 282(1), 35–46. <https://doi.org/10.1111/imr.12636>

Fukuishi, N., Murakami, S., Ohno, A., Yamanaka, N., Matsui, N., Fukutsuji, K., Yamada, S., Itoh, K., & Akagi, M. (2014). Does β -Hexosaminidase Function Only as a Degranulation Indicator in Mast Cells? The Primary Role of β -Hexosaminidase in Mast Cell Granules. *The Journal of Immunology*, 193(4), 1886–1894.
<https://doi.org/10.4049/jimmunol.1302520>

Galli, S. J., Gaudenzio, N., & Tsai, M. (2020). Mast Cells in Inflammation and Disease:

- Recent Progress and Ongoing Concerns. *Annual Review of Immunology*, 38, 49–77.
<https://doi.org/10.1146/annurev-immunol-071719-094903>
- Galli, S. J., & Tsai, M. (2010). Mast cells in allergy and infection: Versatile effector and regulatory cells in innate and adaptive immunity. *European Journal of Immunology*, 40(7), 1843–1851. <https://doi.org/10.1002/eji.201040559>
- Genç, Ö., Kochubey, O., Toonen, R. F., Verhage, M., & Schneggenburger, R. (2014). Munc18-1 is a dynamically regulated PKC target during short-term enhancement of transmitter release. *ELife*, 3, 1–19. <https://doi.org/10.7554/elife.01715>
- Gilfillan, A. M., & Beaven, M. A. (2011). Regulation of mast cell responses in health and disease. *Critical Reviews in Immunology*, 31(6), 475–529.
<https://doi.org/10.1615/critrevimmunol.v31.i6.30>
- Gilfillan, A. M., & Rivera, J. (2009). The tyrosine kinase network regulating mast cell activation. *Immunological Reviews*, 228(1), 149–169. <https://doi.org/10.1111/j.1600-065X.2008.00742.x>
- González-Deolano, D., & Álvarez-Twose, I. (2018). Mast cells as key players in allergy and inflammation. *Journal of Investigational Allergology and Clinical Immunology*, 28(6), 365–378. <https://doi.org/10.18176/jiaci.0327>
- Gordon, D. E., Bond, L. M., Sahlender, D. A., & Peden, A. A. (2010). A targeted siRNA screen to identify SNAREs required for constitutive secretion in mammalian cells. *Traffic (Copenhagen, Denmark)*, 11(9), 1191–1204. <https://doi.org/10.1111/j.1600-0854.2010.01087.x>
- Gordon, D. E., Chia, J., Jayawardena, K., Antrobus, R., Bard, F., & Peden, A. A. (2017). VAMP3/Syb and YKT6 are required for the fusion of constitutive secretory carriers

with the plasma membrane. *PLoS Genetics*, 13(4), 1–24.

<https://doi.org/10.1371/journal.pgen.1006698>

Gurish, M. F., & Austen, K. F. (2012). Developmental Origin and Functional Specialization of Mast Cell Subsets. *Immunity*, 37(1), 25–33.

<https://doi.org/10.1016/j.immuni.2012.07.003>

Gutierrez, B. A., Chavez, M. A., Rodarte, A. I., Ramos, M. A., Dominguez, A., Petrova, Y., Davalos, A. J., Costa, R. M., Elizondo, R., Tuvim, M. J., Dickey, B. F., Burns, A. R., Heidelberger, R., & Adachi, R. (2018). Munc18-2, but not Munc18-1 or Munc18-3, controls compound and single-vesicle-regulated exocytosis in mast cells. *Journal of Biological Chemistry*, 293(19), 7148–7159.

<https://doi.org/10.1074/jbc.RA118.002455>

Hata, Y., Slaughter, C. A., & Südhof, T. C. (1993). Synaptic vesicle fusion complex contains unc-18 homologue bound to syntaxin. *Nature*, 366(6453), 347–351.

<https://doi.org/10.1038/366347a0>

Hellman, L. T., Akula, S., Thorpe, M., & Fu, Z. (2017). Tracing the origins of IgE, mast cells, and allergies by studies of wild animals. *Frontiers in Immunology*, 8(DEC), 1–22. <https://doi.org/10.3389/fimmu.2017.01749>

Hepp, R., Puri, N., Hohenstein, A. C., Crawford, G. L., Whiteheart, S. W., & Roche, P. A. (2005). Phosphorylation of SNAP-23 regulates exocytosis from mast cells.

Journal of Biological Chemistry, 280(8), 6610–6620.

<https://doi.org/10.1074/jbc.M412126200>

Hessvik, N. P., & Llorente, A. (2018). Current knowledge on exosome biogenesis and release. *Cellular and Molecular Life Sciences*, 75(2), 193–208.

<https://doi.org/10.1007/s00018-017-2595-9>

Higashio, H., Satoh, Y. I., & Saino, T. (2017). Inhibitory role of Munc13-1 in antigen-induced mast cell degranulation. *Biomedical Research (Japan)*, *38*(6), 321–329.

<https://doi.org/10.2220/biomedres.38.321>

Hong W. (2005). SNAREs and traffic. *Biochimica et biophysica acta*, *1744*(2), 120–144.

<https://doi.org/10.1016/j.bbamcr.2005.03.014>

Hu, S. H., Christie, M. P., Saez, N. J., Latham, C. F., Jarrott, R., Lua, L. H. L., Collins, B.

M., & Martin, J. L. (2011). Possible roles for Munc18-1 domain 3a and Syntaxin1 N-peptide and C-terminal anchor in SNARE complex formation. *Proceedings of the National Academy of Sciences of the United States of America*, *108*(3), 1040–1045.

<https://doi.org/10.1073/pnas.0914906108>

Hutagalung, A. H., & Novick, P. J. (2011). Role of Rab GTPases in membrane traffic and cell physiology. *Physiological Reviews*, *91*(1), 119–149.

<https://doi.org/10.1152/physrev.00059.2009>

Ikeda, T., & Funaba, M. (2003). Altered function of murine mast cells in response to lipopolysaccharide and peptidoglycan. *Immunology Letters*, *88*(1), 21–26.

[https://doi.org/10.1016/S0165-2478\(03\)00031-2](https://doi.org/10.1016/S0165-2478(03)00031-2)

Jahn, R., & Fasshauer, D. (2012). Molecular machines governing exocytosis of synaptic vesicles. *Nature*, *490*(7419), 201–207. <https://doi.org/10.1038/nature11320>

Jahn, R., Lang, T., & Südhof, T. C. (2003). Membrane fusion. *Cell*, *112*(4), 519–533.

[https://doi.org/10.1016/S0092-8674\(03\)00112-0](https://doi.org/10.1016/S0092-8674(03)00112-0)

Jahn, R., & Scheller, R. H. (2006). SNAREs - Engines for membrane fusion. *Nature*

Reviews Molecular Cell Biology, *7*(9), 631–643. <https://doi.org/10.1038/nrm2002>

- Jang, D., Lee, A., Shin, H., Song, H., Park, J., Kang, T., Lee, S., & Yang, S. (2021). *The Role of Tumor Necrosis Factor Alpha (TNF- α) in Autoimmune Disease and Current TNF- α Inhibitors in Therapeutics.*
- Jemima, E. A., Prema, A., & Thangam, E. B. (2014). Functional characterization of histamine H4 receptor on human mast cells. *Molecular Immunology*, *62*(1), 19–28.
<https://doi.org/10.1016/j.molimm.2014.05.007>
- Jiménez, M., Cervantes-García, D., Córdova-Dávalos, L. E., Pérez-Rodríguez, M. J., Gonzalez-Espinosa, C., & Salinas, E. (2021). Responses of Mast Cells to Pathogens: Beneficial and Detrimental Roles. *Frontiers in Immunology*, *12*(June), 1–31.
<https://doi.org/10.3389/fimmu.2021.685865>
- Katsanos, G. S., Anogeianaki, A., Orso, C., Tetè, S., Salini, V., Antinolfi, P. L., & Sabatino, G. (2008). Mast cells and chemokines. In *Journal of biological regulators and homeostatic agents* (Vol. 22, Issue 3, pp. 145–151).
- Kawasaki, T., & Kawai, T. (2014). Toll-like receptor signaling pathways. *Frontiers in Immunology*, *5*(SEP), 1–8. <https://doi.org/10.3389/fimmu.2014.00461>
- Kioumourtzoglou, D., Gould, G. W., & Bryant, N. J. (2014). Insulin Stimulates Syntaxin4 SNARE Complex Assembly via a Novel Regulatory Mechanism. *Molecular and Cellular Biology*, *34*(7), 1271–1279.
<https://doi.org/10.1128/mcb.01203-13>
- Klein, O., & Sagi-Eisenberg, R. (2019). Anaphylactic degranulation of mast cells: Focus on compound exocytosis. *Journal of Immunology Research*, *2019*.
<https://doi.org/10.1155/2019/9542656>
- Koblan, L. W., Doman, J. L., Wilson, C., Levy, J. M., Tay, T., Newby, G. A., Maianti, J.

- P., Raguram, A., & Liu, D. R. (2018). Improving cytidine and adenine base editors by expression optimization and ancestral reconstruction. *Nature Biotechnology*, 36(9), 843–848. <https://doi.org/10.1038/nbt.4172>
- Komor, A. C., Kim, Y. B., Packer, M. S., Zuris, J. A., & Liu, D. R. (2016). Programmable editing of a target base in genomic DNA without double-stranded DNA cleavage. *Nature*, 533(7603), 420–424. <https://doi.org/10.1038/nature17946>
- Kritas, S. K., Saggini, A., Cerulli, G., Caraffa, A., Antinolfi, P., Pantalone, A., Rosati, M., Tei, M., Speziali, A., Saggini, R., & Conti, P. (2014). Relationship between serotonin and mast cells: Inhibitory effect of anti-serotonin. *Journal of Biological Regulators and Homeostatic Agents*, 28(3), 377–380.
- Krystel-Whittemore, M., Dileepan, K. N., & Wood, J. G. (2016). Mast cell: A multi-functional master cell. *Frontiers in Immunology*, 6(JAN), 1–12. <https://doi.org/10.3389/fimmu.2015.00620>
- Kuscu, C., Parlak, M., Tufan, T., Yang, J., Szlachta, K., Wei, X., Mammadov, R., & Adli, M. (2017). CRISPR-STOP: Gene silencing through base-editing-induced nonsense mutations. *Nature Methods*, 14(7), 710–712. <https://doi.org/10.1038/nmeth.4327>
- Kushnir-Sukhov, N. M., Brown, J. M., Wu, Y., Kirshenbaum, A., & Metcalfe, D. D. (2007). Human mast cells are capable of serotonin synthesis and release. *Journal of Allergy and Clinical Immunology*, 119(2), 498–499. <https://doi.org/10.1016/j.jaci.2006.09.003>
- Lazki-Hagenbach, P., Ali, H., & Sagi-Eisenberg, R. (2021). Authentic and Ectopically Expressed MRGPRX2 Elicit Similar Mechanisms to Stimulate Degranulation of

- Mast Cells. *Cells*, *10*(2), 1–20. <https://doi.org/10.3390/cells10020376>
- Lee, S., Shin, J., Jung, Y., Son, H., Shin, J., Jeong, C., Kweon, D. H., & Shin, Y. K. (2020). Munc18-1 induces conformational changes of syntaxin-1 in multiple intermediates for SNARE assembly. *Scientific Reports*, *10*(1), 1–8. <https://doi.org/10.1038/s41598-020-68476-3>
- Li, W., Ma, C., Guan, R., Xu, Y., Tomchick, D. R., & Rizo, J. (2011). The crystal structure of a Munc13 C-terminal module exhibits a remarkable similarity to vesicle tethering factors. *Structure*, *19*(10), 1443–1455. <https://doi.org/10.1016/j.str.2011.07.012>
- Liu, Y., Ding, X., Wang, D., Deng, H., Feng, M., Wang, M., Yu, X., Jiang, K., Ward, T., Aikhionbare, F., Guo, Z., Forte, J. G., & Yao, X. (2007). A mechanism of Munc18b-syntaxin 3-SANP25 complex assembly in regulated epithelial secretion. *FEBS Letters*, *581*(22), 4318–4324. <https://doi.org/10.1016/j.febslet.2007.07.083>
- Lorentz, A., Baumann, A., Vitte, J., & Blank, U. (2012). The SNARE Machinery in Mast Cell Secretion. *Frontiers in immunology*, *3*, 143. <https://doi.org/10.3389/fimmu.2012.00143>
- Lou, X., & Shin, Y. K. (2016). SNARE zippering. *Bioscience Reports*, *36*(3), 1–7. <https://doi.org/10.1042/BSR20160004>
- Lundquist, A., & Pejler, G. (2011). Biological implications of preformed mast cell mediators. *Cellular and Molecular Life Sciences*, *68*(6), 965–975. <https://doi.org/10.1007/s00018-010-0587-0>
- Ma, L., Rebane, A. A., Yang, G., Xi, Z., Kang, Y., Gao, Y., & Zhang, Y. (2015). Munc18-1-regulated stage-wise SNARE assembly underlying synaptic exocytosis.

ELife, 4, 1–30. <https://doi.org/10.7554/elife.09580>

Malmersjö, S., Di Palma, S., Diao, J., Lai, Y., Pfuetzner, R. A., Wang, A. L., McMahon, M. A., Hayer, A., Porteus, M., Bodenmiller, B., Brunger, A. T., & Meyer, T. (2016). Phosphorylation of residues inside the SNARE complex suppresses secretory vesicle fusion. *The EMBO Journal*, 35(16), 1810–1821.

<https://doi.org/10.15252/emj.201694071>

Matsushima, H., Yamada, N., Matsue, H., & Shimada, S. (2004). TLR3-, TLR7-, and TLR9-mediated production of proinflammatory cytokines and chemokines from murine connective tissue type skin-derived mast cells but not from bone marrow-derived mast cells. *Journal of Immunology (Baltimore, Md. : 1950)*, 173(1), 531–541. <https://doi.org/10.4049/jimmunol.173.1.531>

McNew, J. A. (2008). Regulation of SNARE-mediated membrane fusion during exocytosis. *Chemical Reviews*, 108(5), 1669–1686.

<https://doi.org/10.1021/cr0782325>

Melicoff, E., Sansores-Garcia, L., Gomez, A., Moreira, D. C., Datta, P., Thakur, P., Petrova, Y., Siddiqi, T., Murthy, J. N., Dickey, B. F., Heidelberger, R., & Adachi, R. (2009). Synaptotagmin-2 controls regulated exocytosis but not other secretory responses of mast cells. *Journal of Biological Chemistry*, 284(29), 19445–19451.

<https://doi.org/10.1074/jbc.M109.002550>

Meurer, S. K., Neß, M., Weiskirchen, S., Kim, P., Tag, C. G., Kauffmann, M., Huber, M., & Weiskirchen, R. (2016). Isolation of mature (Peritoneum-Derived) mast cells and immature (Bone Marrow-Derived) mast cell precursors from mice. *PLoS ONE*, 11(6), 1–16. <https://doi.org/10.1371/journal.pone.0158104>

- Moon, T. C., St Laurent, C. D., Morris, K. E., Marcet, C., Yoshimura, T., Sekar, Y., & Befus, A. D. (2010). Advances in mast cell biology: New understanding of heterogeneity and function. *Mucosal Immunology*, *3*(2), 111–128.
<https://doi.org/10.1038/mi.2009.136>
- Moon, T. C., Befus, A. D., & Kulka, M. (2014). Mast cell mediators: their differential release and the secretory pathways involved. *Frontiers in immunology*, *5*, 569.
<https://doi.org/10.3389/fimmu.2014.00569>
- Mukai, K., Tsai, M., Saito, H., & Galli, S. J. (2018). Mast cells as sources of cytokines, chemokines, and growth factors. *Immunological Reviews*, *282*(1), 121–150.
<https://doi.org/10.1111/imr.12634>
- Murray, R. Z., Kay, J. G., Sangermani, D. G., & Stow, J. L. (2005). Cell biology: A role for the phagosome in cytokine secretion. *Science*, *310*(5753), 1492–1495.
<https://doi.org/10.1126/science.1120225>
- Murray, R. Z., & Stow, J. L. (2014). Cytokine Secretion in Macrophages: SNAREs, Rabs, and Membrane Trafficking. *Frontiers in immunology*, *5*, 538.
<https://doi.org/10.3389/fimmu.2014.00538>
- Nigam, R., Sepulveda, J., Tuvim, M., Petrova, Y., Adachi, R., Dickey, B. F., & Agrawal, A. (2005). Expression and transcriptional regulation of Munc18 isoforms in mast cells. *Biochimica et Biophysica Acta - Gene Structure and Expression*, *1728*(1–2), 77–83. <https://doi.org/10.1016/j.bbaexp.2005.01.018>
- Noli, C., & Miolo, A. (2001). The mast cell in wound healing. *Veterinary Dermatology*, *12*(6), 303–313. <https://doi.org/10.1046/j.0959-4493.2001.00272.x>
- Noto, C. N., Hoft, S. G., & DiPaolo, R. J. (2021). Mast Cells as Important Regulators in

- Autoimmunity and Cancer Development. *Frontiers in Cell and Developmental Biology*, 9(October), 1–13. <https://doi.org/10.3389/fcell.2021.752350>
- Park, J. H., Jung, M. S., Kim, Y. S., Song, W. J., & Chung, S. H. (2012). Phosphorylation of Munc18-1 by Dyrk1A regulates its interaction with Syntaxin 1 and X11 α . *Journal of neurochemistry*, 122(5), 1081–1091. <https://doi.org/10.1111/j.1471-4159.2012.07861.x>
- Passante, E., & Frankish, N. (2010). Deficiencies in elements involved in TLR4-receptor signalling in RBL-2H3 cells. *Inflammation Research : Official Journal of the European Histamine Research Society ... [et Al.]*, 59 Suppl 2, S185-6. <https://doi.org/10.1007/s00011-009-0123-6>
- Passante, E., & Frankish, N. (2009). The RBL-2H3 cell line: its provenance and suitability as a model for the mast cell. *Inflammation research : official journal of the European Histamine Research Society ... [et al.]*, 58(11), 737–745. <https://doi.org/10.1007/s00011-009-0074-y>
- Paumet, F., Le Mao, J., Martin, S., Galli, T., David, B., Blank, U., & Roa, M. (2000). Soluble NSF Attachment Protein Receptors (SNAREs) in RBL-2H3 Mast Cells: Functional Role of Syntaxin 4 in Exocytosis and Identification of a Vesicle-Associated Membrane Protein 8-Containing Secretory Compartment. *The Journal of Immunology*, 164(11), 5850–5857. <https://doi.org/10.4049/jimmunol.164.11.5850>
- Prior, I. A., & Clague, M. J. (2000). Detection of thiol modification following generation of reactive nitrogen species: Analysis of synaptic vesicle proteins. *Biochimica et Biophysica Acta - General Subjects*, 1475(3), 281–286. [https://doi.org/10.1016/S0304-4165\(00\)00078-7](https://doi.org/10.1016/S0304-4165(00)00078-7)

- Puri, N., & Roche, P. A. (2008). Mast cells possess distinct secretory granule subsets whose exocytosis is regulated by different SNARE isoforms. *Proceedings of the National Academy of Sciences of the United States of America*, *105*(7), 2580–2585. <https://doi.org/10.1073/pnas.0707854105>
- Qiao, H., & Beaven, M. A. (2006). FcεR1 and Toll-Like Receptors Mediate Synergistic Signals to Markedly Augment Production of Inflammatory Cytokines in Murine Mast Cells. *Journal of Allergy and Clinical Immunology*, *117*(2), S317. <https://doi.org/10.1016/j.jaci.2005.12.1253>
- Ran, F. A., Hsu, P. D., Wright, J., Agarwala, V., Scott, D. A., & Zhang, F. (2013). Genome engineering using the CRISPR-Cas9 system. *Nature Protocols*, *8*(11), 2281–2308. <https://doi.org/10.1038/nprot.2013.143>
- Rao, K. N., & Brown, M. A. (2008). Mast cells: multifaceted immune cells with diverse roles in health and disease. *Annals of the New York Academy of Sciences*, *1143*, 83–104. <https://doi.org/10.1196/annals.1443.023>
- Raposo, G., Tenza, D., Mecheri, S., Peronet, R., Bonnerot, C., & Desaynard, C. (1997). Accumulation of major histocompatibility complex class II molecules in mast cell secretory granules and their release upon degranulation. *Molecular biology of the cell*, *8*(12), 2631–2645. <https://doi.org/10.1091/mbc.8.12.2631>
- Reber, L. L., Marichal, T., & Galli, S. J. (2012). New models for analyzing mast cell functions in vivo. *Trends in Immunology*, *33*(12), 613–625. <https://doi.org/10.1016/j.it.2012.09.008>
- Ribatti, D. (2018). The Staining of Mast Cells: A Historical Overview. *International Archives of Allergy and Immunology*, *176*(1), 55–60.

<https://doi.org/10.1159/000487538>

Richmond, J. E., Davis, W. S., & Jorgensen, E. M. (1999). UNC-13 is required for synaptic vesicle fusion in *C. elegans*. *Nature Neuroscience*, 2(11), 959–964.

<https://doi.org/10.1038/14755>

Rizo, J., Rosenmund, C., & Struct Mol Biol Author manuscript, N. (2008). Synaptic vesicle fusion HHS Public Access Author manuscript. *Nat Struct Mol Biol*, 15(7), 665–674. http://www.nature.com/authors/editorial_policies/license.html#terms

Rizo, J., & Xu, J. (2015). The Synaptic Vesicle Release Machinery. *Annual Review of Biophysics*, 44, 339–367. <https://doi.org/10.1146/annurev-biophys-060414-034057>

Rodarte, E. M., Ramos, M. A., Davalos, A. J., Moreira, D. C., Moreno, D. S., Cardenas, E. I., Rodarte, A. I., Petrova, Y., Molina, S., Rendon, L. E., Sanchez, E., Breaux, K., Tortoriello, A., Manllo, J., Gonzalez, E. A., Tuvim, M. J., Dickey, B. F., Burns, A. R., Heidelberger, R., & Adachi, R. (2018). Munc13 proteins control regulated exocytosis in mast cells. *Journal of Biological Chemistry*, 293(1), 345–358.

<https://doi.org/10.1074/jbc.M117.816884>

Roy, B., Zhao, J., Yang, C., Luo, W., Xiong, T., Li, Y., Fang, X., Gao, G., Singh, C. O., Madsen, L., Zhou, Y., & Kristiansen, K. (2018). CRISPR/Cascade 9-Mediated Genome Editing-Challenges and Opportunities. *Frontiers in genetics*, 9, 240.

<https://doi.org/10.3389/fgene.2018.00240>

Ruiz-Martinez, M., Navarro, A., Marrades, R. M., Viñolas, N., Santasusagna, S., Muñoz, C., Ramírez, J., Molins, L., & Monzo, M. (2016). YKT6 expression, exosome release, and survival in non-small cell lung cancer. *Oncotarget*, 7(32), 51515–51524. <https://doi.org/10.18632/oncotarget.9862>

- Saggini, A., Tripodi, D., Maccauro, G., Castellani, M. L., Anogeianaki, A., Teté, S., Felaco, P., De Lutiis, M. A., Galzio, R., Fulcheri, M., Theoharides, T. C., Caraffa, A., Antinolfi, P., Felaco, M., Conti, F., Neri, G., Pandolfi, F., Toniato, E., & Shaik-Dasthagirisaheb, Y. B. (2011). Tumor necrosis factor-alpha and mast cells: Revisited study. *European Journal of Inflammation*, 9(1), 17–22.
<https://doi.org/10.1177/1721727X1100900103>
- Saleeb, R. S., Kavanagh, D. M., Dun, A. R., Dalgarno, P. A., & Duncan, R. R. (2019). A VPS33A-binding motif on syntaxin 17 controls autophagy completion in mammalian cells. *Journal of Biological Chemistry*, 294(11), 4188–4201.
<https://doi.org/10.1074/jbc.RA118.005947>
- Sanchez, E., Gonzalez, E. A., Moreno, D. S., Cardenas, R. A., Ramos, M. A., Davalos, A. J., Manllo, J., Rodarte, A. I., Petrova, Y., Moreira, D. C., Chavez, M. A., Tortoriello, A., Lara, A., Gutierrez, B. A., Burns, A. R., Heidelberger, R., & Adachi, R. (2019). Syntaxin 3, but not syntaxin 4, is required for mast cell–regulated exocytosis, where it plays a primary role mediating compound exocytosis. *Journal of Biological Chemistry*, 294(9), 3012–3023. <https://doi.org/10.1074/jbc.RA118.005532>
- Sander, L. E., Frank, S. P. C., Bolat, S., Blank, U., Galli, T., Bigalke, H., Bischoff, S. C., & Lorenz, A. (2008). Vesicle associated membrane protein (VAMP)-7 and VAMP-8, but not VAMP-2 or VAMP-3, are required for activation-induced degranulation of mature human mast cells. *European Journal of Immunology*, 38(3), 855–863.
<https://doi.org/10.1002/eji.200737634>
- Sandig, H., & Bulfone-Paus, S. (2012). TLR signaling in mast cells: common and unique features. *Frontiers in immunology*, 3, 185.

<https://doi.org/10.3389/fimmu.2012.00185>

Sauvola, C. W., & Littleton, J. T. (2021). SNARE Regulatory Proteins in Synaptic Vesicle Fusion and Recycling. *Frontiers in molecular neuroscience*, *14*, 733138.

<https://doi.org/10.3389/fnmol.2021.733138>

Schraw, T. D., Lemons, P. P., Dean, W. L., & Whiteheart, S. W. (2003). A role for Sec1/Munc18 proteins in platelet exocytosis. *Biochemical Journal*, *374*(1), 207–217.

<https://doi.org/10.1042/BJ20030610>

Shelburne, C. P., & Abraham, S. N. (2011). The mast cell in innate and adaptive immunity. *Advances in Experimental Medicine and Biology*, *716*(1), 162–185.

https://doi.org/10.1007/978-1-4419-9533-9_10

Shen, B., Zhang, W., Zhang, J., Zhou, J., Wang, J., Chen, L., Wang, L., Hodgkins, A., Iyer, V., Huang, X., & Skarnes, W. C. (2014). Efficient genome modification by CRISPR-Cas9 nickase with minimal off-target effects. *Nature methods*, *11*(4), 399–402.

<https://doi.org/10.1038/nmeth.2857>

Shen, H. H., Lithgow, T., & Martin, L. L. (2013). Reconstitution of membrane proteins into model membranes: Seeking better ways to retain protein activities.

International Journal of Molecular Sciences, *14*(1), 1589–1607.

<https://doi.org/10.3390/ijms14011589>

Shen, J., Tareste, D. C., Paumet, F., Rothman, J. E., & Melia, T. J. (2007). Selective Activation of Cognate SNAREpins by Sec1/Munc18 Proteins. *Cell*, *128*(1), 183–195.

<https://doi.org/10.1016/j.cell.2006.12.016>

Shu, T., Jin, H., Rothman, J. E., & Zhang, Y. (2020). Munc13-1 MUN domain and Munc18-1 cooperatively chaperone SNARE assembly through a tetrameric

- complex. *Proceedings of the National Academy of Sciences of the United States of America*, 117(2), 1036–1041. <https://doi.org/10.1073/pnas.1914361117>
- Singh, R. K., Mizuno, K., Wasmeier, C., Wavre-Shapton, S. T., Recchi, C., Catz, S. D., Futter, C., Tolmachova, T., Hume, A. N., & Seabra, M. C. (2013). Distinct and opposing roles for Rab27a/Mlph/MyoVa and Rab27b/Munc13-4 in mast cell secretion. *FEBS Journal*, 280(3), 892–903. <https://doi.org/10.1111/febs.12081>
- Snyder, D. A., Kelly, M. L., & Woodbury, D. J. (2006). SNARE complex regulation by phosphorylation. *Cell Biochemistry and Biophysics*, 45(1), 111–123. <https://doi.org/10.1385/cbb:45:1:111>
- St. John, A. L., & Abraham, S. N. (2013). Innate Immunity and Its Regulation by Mast Cells. *The Journal of Immunology*, 190(9), 4458–4463. <https://doi.org/10.4049/jimmunol.1203420>
- Stow, J. L., Manderson, A. P., & Murray, R. Z. (2006). SNAREing immunity: The role of SNAREs in the immune system. *Nature Reviews Immunology*, 6(12), 919–929. <https://doi.org/10.1038/nri1980>
- Supajatura, V., Ushio, H., Nakao, A., Akira, S., Okumura, K., Ra, C., & Ogawa, H. (2002). Differential responses of mast cell Toll-like receptors 2 and 4 in allergy and innate immunity. *Journal of Clinical Investigation*, 109(10), 1351–1359. <https://doi.org/10.1172/JCI0214704>
- Sutton, R. B., Davletov, B. A., Berghuis, A. M., Sudhof, T. C., & Sprang, S. R. (1995). Structure of the first C2 domain of synaptotagmin I: A novel Ca²⁺/phospholipid-binding fold. *Cell*, 80(6), 929–938. [https://doi.org/10.1016/0092-8674\(95\)90296-1](https://doi.org/10.1016/0092-8674(95)90296-1)
- Suzuki, K., & Verma, I. M. (2008). Phosphorylation of SNAP-23 by IκB Kinase 2

- Regulates Mast Cell Degranulation. *Cell*, *134*(3), 485–495.
<https://doi.org/10.1016/j.cell.2008.05.050>
- Tadokoro, S., Kurimoto, T., Nakanishi, M., & Hirashima, N. (2007). Munc18-2 regulates exocytotic membrane fusion positively interacting with syntaxin-3 in RBL-2H3 cells. *Molecular Immunology*, *44*(13), 3427–3433.
<https://doi.org/10.1016/j.molimm.2007.02.013>
- Tadokoro, S., Nakanishi, M., & Hirashima, N. (2010). Complexin II regulates degranulation in RBL-2H3 cells by interacting with SNARE complex containing syntaxin-3. *Cellular Immunology*, *261*(1), 51–56.
<https://doi.org/10.1016/j.cellimm.2009.10.011>
- Tadokoro, S., Shibata, T., Inoh, Y., Amano, T., Nakanishi, M., Hirashima, N., & Utsunomiya-Tate, N. (2016). Phosphorylation of syntaxin-3 at Thr 14 negatively regulates exocytosis in RBL-2H3 mast cells. *Cell Biology International*, *40*(5), 589–596. <https://doi.org/https://doi.org/10.1002/cbin.10600>
- Thangam, E. B., Jemima, E. A., Singh, H., Baig, M. S., Khan, M., Mathias, C. B., Church, M. K., & Saluja, R. (2018). The Role of Histamine and Histamine Receptors in Mast Cell-Mediated Allergy and Inflammation: The Hunt for New Therapeutic Targets. *Frontiers in immunology*, *9*, 1873.
<https://doi.org/10.3389/fimmu.2018.01873>
- Theoharides, T. C., Bondy, P. K., Tsakalos, N. D., & Askenase, P. W. (1982). Differential release of serotonin and histamine from mast cells. *Nature*, *297*(5863), 229–231. <https://doi.org/10.1038/297229a0>
- Tiwari, N., Wang, C. C., Brochetta, C., Scanduzzi, L., Hong, W., & Blank, U. (2009).

- Increased formation of VAMP-3-containing SNARE complexes in mast cells from VAMP-8 deficient cells. *Inflammation Research*, 58(SUPPL. 1), 13–14.
<https://doi.org/10.1007/s00011-009-0645-y>
- Tiwari, N., Wang, C. C., Brochetta, C., Ke, G., Vita, F., Qi, Z., Rivera, J., Soranzo, M. R., Zabucchi, G., Hong, W., & Blank, U. (2008). VAMP-8 segregates mast cell-preformed mediator exocytosis from cytokine trafficking pathways. *Blood*, 111(7), 3665–3674. <https://doi.org/10.1182/blood-2007-07-103309>
- Travis, E. R., Wang, Y. M., Michael, D. J., Caron, M. G., & Wightman, R. M. (2000). Differential quantal release of histamine and 5-hydroxytryptamine from mast cells of vesicular monoamine transporter 2 knockout mice. *Proceedings of the National Academy of Sciences of the United States of America*, 97(1), 162–167.
<https://doi.org/10.1073/pnas.97.1.162>
- Urb, M., & Sheppard, D. C. (2012). The role of mast cells in the defence against pathogens. *PLoS Pathogens*, 8(4), 2–4. <https://doi.org/10.1371/journal.ppat.1002619>
- Vaidyanathan, V. V., Puri, N., & Roche, P. A. (2001). The Last Exon of SNAP-23 Regulates Granule Exocytosis from Mast Cells. *Journal of Biological Chemistry*, 276(27), 25101–25106. <https://doi.org/10.1074/jbc.M103536200>
- Varadaradjalou, S., Féger, F., Thieblemont, N., Hamouda, N. B., Pleau, J. M., Dy, M., & Arock, M. (2003). Toll-like receptor 2 (TLR2) and TLR4 differentially activate human mast cells. *European journal of immunology*, 33(4), 899–906.
<https://doi.org/10.1002/eji.200323830>
- Veit, M. (2004). The human SNARE protein Ykt6 mediates its own palmitoylation at C-terminal cysteine residues. *The Biochemical Journal*, 384(Pt 2), 233–237.

<https://doi.org/10.1042/BJ20041474>

Verhage, M., Maia, A. S., Plomp, J. J., Brussaard, A. B., Heeroma, J. H., Vermeer, H., Toonen, R. F., Hammer, R. E., van den Berg, T. K., Missler, M., Geuze, H. J., & Südhof, T. C. (2000). Synaptic assembly of the brain in the absence of neurotransmitter secretion. *Science (New York, N.Y.)*, 287(5454), 864–869.

<https://doi.org/10.1126/science.287.5454.864>

Vivona, S., Liu, C. W., Strop, P., Rossi, V., Filippini, F., & Brunger, A. T. (2010). The longin SNARE VAMP7/TI-VAMP adopts a closed conformation. *Journal of Biological Chemistry*, 285(23), 17965–17973.

<https://doi.org/10.1074/jbc.M110.120972>

Voehringer, D. (2013). Protective and pathological roles of mast cells and basophils.

Nature Reviews Immunology, 13(5), 362–375. <https://doi.org/10.1038/nri3427>

Vrljic, M., Strop, P., Hill, R. C., Hansen, K. C., Chu, S., & Brunger, A. T. (2011). Post-translational modifications and lipid binding profile of insect cell-expressed full-length mammalian synaptotagmin 1. *Biochemistry*, 50(46), 9998–10012.

<https://doi.org/10.1021/bi200998y>

Vukman, K., Metz, M., Maurer, M., & O'Neill, S. (2014). Isolation and Culture of Bone Marrow-derived Mast Cells. *Bio-Protocol*, 4(4), 2–6.

<https://doi.org/10.21769/bioprotoc.1053>

Weber, T., Zemelman, B. V., McNew, J. A., Westermann, B., Gmachl, M., Parlati, F., Söllner, T. H., & Rothman, J. E. (1998). SNAREpins: Minimal machinery for membrane fusion. *Cell*, 92(6), 759–772. [https://doi.org/10.1016/S0092-8674\(00\)81404-X](https://doi.org/10.1016/S0092-8674(00)81404-X)

- Wernersson, S., & Pejler, G. (2014). Mast cell secretory granules: Armed for battle. *Nature Reviews Immunology*, *14*(7), 478–494. <https://doi.org/10.1038/nri3690>
- Wierzbicki, M., & Brzezińska-Błaszczyk, E. (2009). Diverse effects of bacterial cell wall components on mast cell degranulation, cysteinyl leukotriene generation and migration. *Microbiology and Immunology*, *53*(12), 694–703. <https://doi.org/10.1111/j.1348-0421.2009.00174.x>
- Woo, S. S., James, D. J., & Martin, T. F. J. (2017). Munc13-4 functions as a Ca²⁺ sensor for homotypic secretory granule fusion to generate endosomal exocytic vacuoles. *Molecular Biology of the Cell*, *28*(6), 792–808. <https://doi.org/10.1091/mbc.E16-08-0617>
- Woska, J. R., & Gillespie, M. E. (2011). Small-Interfering RNA-Mediated Identification and Regulation of the Ternary SNARE Complex Mediating RBL-2H3 Mast Cell Degranulation. *Scandinavian Journal of Immunology*, *73*(1), 8–17. <https://doi.org/10.1111/j.1365-3083.2010.02471.x>
- Xu, H., Arnold, M. G., & Kumar, S. V. (2015). Differential effects of munc18s on multiple degranulation-relevant trans-SNARE complexes. *PLoS ONE*, *10*(9), 1–16. <https://doi.org/10.1371/journal.pone.0138683>
- Xu, H., Bin, N. R., & Sugita, S. (2018). Diverse exocytic pathways for mast cell mediators. *Biochemical Society transactions*, *46*(2), 235–247. <https://doi.org/10.1042/BST20170450>
- Xu, J., Brewer, K. D., Perez-Castillejos, R., & Rizo, J. (2013). Subtle interplay between synaptotagmin and complexin binding to the SNARE complex. *Journal of Molecular Biology*, *425*(18), 3461–3475. <https://doi.org/10.1016/j.jmb.2013.07.001>

- Yang, S., Wang, J., Brand, D. D., & Zheng, S. G. (2018). Role of TNF-TNF receptor 2 signal in regulatory T cells and its therapeutic implications. *Frontiers in Immunology*, 9(APR). <https://doi.org/10.3389/fimmu.2018.00784>
- Yang, Y., Kong, B., Jung, Y., Park, J. B., Oh, J. M., Hwang, J., Cho, J. Y., & Kweon, D. H. (2018). Soluble N-ethylmaleimide-sensitive factor attachment protein receptor-derived peptides for regulation of mast cell degranulation. *Frontiers in Immunology*, 9(APR). <https://doi.org/10.3389/fimmu.2018.00725>
- Yoon, T. Y., & Munson, M. (2018). SNARE complex assembly and disassembly. *Current Biology*, 28(8), R397–R401. <https://doi.org/10.1016/j.cub.2018.01.005>
- Yu, H., Rathore, S. S., Lopez, J. A., Davis, E. M., James, D. E., Martin, J. L., & Shen, J. (2013). Comparative studies of Munc18c and Munc18-1 reveal conserved and divergent mechanisms of Sec1/Munc18 proteins. *Proceedings of the National Academy of Sciences of the United States of America*, 110(35). <https://doi.org/10.1073/pnas.1311232110>
- Yu, H., Rathore, S. S., Shen, C., Liu, Y., Ouyang, Y., Stowell, M. H., & Shen, J. (2015). Reconstituting Intracellular Vesicle Fusion Reactions: The Essential Role of Macromolecular Crowding. *Journal of the American Chemical Society*, 137(40), 12873–12883. <https://doi.org/10.1021/jacs.5b08306>
- Zhang, B., Alysandratos, K. D., Angelidou, A., Asadi, S., Sismanopoulos, N., Delivanis, D. A., Weng, Z., Miniati, A., Vasiadi, M., Katsarou-Katsari, A., Miao, B., Leeman, S. E., Kalogeromitros, D., & Theoharides, T. C. (2011). Human mast cell degranulation and preformed TNF secretion require mitochondrial translocation to exocytosis sites: Relevance to atopic dermatitis. *Journal of Allergy and Clinical*

Immunology, 127(6), 1522-1531.e8. <https://doi.org/10.1016/j.jaci.2011.02.005>

Zhang, X., Jiang, S., Mitok, K. A., Li, L., Attie, A. D., & Martin, T. F. J. (2017). BAI AP3, a C2 domain-containing Munc 13 protein, controls the fate of dense-core vesicles in neuroendocrine cells. *Journal of Cell Biology*, 216(7), 2151–2166. <https://doi.org/10.1083/jcb.201702099>

Zhang, X., Rebane, A. A., Ma, L., Li, F., Jiao, J., Qu, H., Pincet, F., Rothman, J. E., Zhang, Y., & Brunger, A. T. (2016). Stability, folding dynamics, and long-range conformational transition of the synaptic t-SNARE complex. *Proceedings of the National Academy of Sciences of the United States of America*, 113(50), E8031–E8040. <https://doi.org/10.1073/pnas.1605748113>